



TRIBHUVAN UNIVERSITY
INSTITUTE OF ENGINEERING
PULCHOWK CAMPUS

THESIS NO.: G020/073

**Design of Support System for Headrace Tunnel of Upper Balephi 'A'
Hydropower Project Using Three-Dimensional and Conventional Approach**

by

Nishkarsha Dawadi

A THESIS

SUBMITTED TO THE DEPARTMENT OF CIVIL ENGINEERING
IN PARTIAL FULFILLMENT OF THE REQUIREMENTS FOR THE
DEGREE OF MASTER OF SCIENCE IN GEOTECHNICAL ENGINEERING

DEPARTMENT OF CIVIL ENGINEERING

LALITPUR, NEPAL

SEPTEMBER, 2020

COPYRIGHT

The author has agreed that the library, Department of Civil Engineering, Pulchowk Campus, Institute of Engineering may make this thesis freely available for inspection. Moreover, the author has agreed that permission for extensive copying of this thesis for scholarly purpose may be granted by the professor(s) who supervised the work recorded herein or, in their absence, by the Head of the Department wherein the thesis was done. It is understood that the recognition will be given to the author of this thesis and to the Department of Civil Engineering, Pulchowk Campus, Institute of Engineering in any use of the material of this thesis. Copying, publication, or the other use of this thesis for financial gain without approval of the Department of Department of Civil Engineering, Pulchowk Campus, Institute of Engineering and author's written permission is prohibited. Request for permission to copy or to make any other use of the material in this thesis in whole or in part should be addressed to:

Head of the Department

Department of Civil Engineering,

Institute of Engineering, Pulchowk Campus,

Pulchowk, Lalitpur, Nepal

TRIBHUVAN UNIVERSITY
INSTITUTE OF ENGINEERING
PULCHOWK CAMPUS

The under signed certify that they have read, and recommended to the Institute of Engineering for acceptance, a thesis entitled **“DESIGN OF SUPPORT SYSTEM FOR HEADRACE TUNNEL OF UPPER BALEPHI ‘A’ HYDROPOWER PROJECT USING THREE-DIMENSIONAL AND CONVENTIONAL APPROACH”** submitted by Mr. Nishkarsha Dawadi (073/MSGT/820) in partial fulfillment of the requirements for the degree of Master of Science in Geotechnical Engineering.

.....

Supervisor, Prof. Dr. Akkal Bahadur Singh

Department of Civil Engineering
Institute of Engineering
Pulchowk Campus

.....

External Examiner, Dr. Pawan Kumar Shrestha

Senior Hydropower Engineer
Hydro Tunneling and research Pvt. Ltd.

.....

Program Coordinator, Dr. Indra Prasad Acharya

Associate Professor
M.Sc. in Geotechnical Engineering
Department of Civil Engineering
Pulchowk Campus, Lalitpur, Nepal

September,2020

ABSTRACT

Tunnel Construction is one of the most complicated tasks among various Civil Engineering works. In Hydropower Tunnels, the work becomes even more complicated because we have to deal with huge water pressure when water is conveyed from intake to power station and ultimately back to the river. When a tunnel is dug the then prevalent in-situ condition of the surroundings is disturbed and new set of stresses are induced. This may lead to failure of the rock mass around the tunnel if not properly assessed. The risks and hazards involved are life threatening, so stabilizing the excavation with support system is of utmost importance. When resistance is developed against the impending failure, then permanency can be achieved. Conventionally, Tunnel is considered as a continuous two-dimensional structure and the stresses in the longitudinal direction are not assessed with. But in case of discrete features like bends in the Tunnel, Adit connections and underground surge shaft, the stresses are significantly disturbed in all three directions and only three-dimensional analysis can recommend the best support system in such case.

In this thesis, using the actual project information of Balephi Hydropower project, support system is designed using the Empirical, Analytical and Numerical modelling approaches. Support system is designed with conventional two-dimensional methods at five different chainages with varying overburden and rock mass parameters. Three-Dimensional approach is taken at a bent, the adit connectional and the underground vertical surge shaft. The typical geological data of the site formed the input parameters for the aforementioned approaches. All these methods independently suggest support system for various sections based on their scientific principles which are compared and the one which gives the most economical support design with highest factor of safety is recommended.

ACKNOWLEDGEMENT

I am immensely grateful to my thesis supervisor Prof. Dr. Akkal Bahadur Singh for his continuous support and guidance throughout this thesis. His persistent encouragement and intellect supervision have made me attempt this thesis work.

I wish to express my gratitude to the respected program coordinator Associate Prof. Dr. Indra Prasad Acharya, for his valuable suggestions and support in different stages of this research work.

I would like to thank all staffs of M. Sc. in Geotechnical Engineering program. I am equally thankful to my friends MSG/073 batch for their cooperation and intellect suggestions. My sincere thanks also go to all those who helped and gave valuable suggestions to me during the course of this research work. I am very grateful to different governmental and private organizations for providing the drawings and data.

Last but not the least, I would like to express my sincere thanks to my friends, whose support, critical comments and suggestions on different stages of my research work actually motivated me to overcome the difficulties and led to this stage of my thesis.

Nishkarsha Dawadi

073/MSGT/820

TABLE OF CONTENTS

COPYRIGHT.....	i
ABSTRACT.....	iii
ACKNOWLEDGEMENT.....	iv
TABLE OF CONTENTS.....	v
LIST OF FIGURES.....	viii
LIST OF TABLES.....	xii
ABBREVIATIONS.....	xiv
1 INTRODUCTION.....	1
1.1 Background.....	1
1.2 Three-Dimensional approach and its importance.....	2
1.3 Problem Statement.....	5
1.4 Objectives of the study.....	5
1.4.1 General Objectives.....	5
1.4.2 Specific Objectives.....	5
1.5 Scope and Limitations of the study.....	6
1.6 Upper Balephi ‘A’ Hydropower Project.....	6
1.6.1 Location of the Project area.....	6
1.6.2 Geological overview of the Project area.....	7
1.6.3 Rock Mass Classification for Tunnel Alignment.....	9
1.6.4 Rock Mass Classification at Surge Shaft.....	10
1.6.5 Rock Mass Classification around Adit.....	11
2 LITERATURE REVIEW.....	12
2.1 Basic concept on Tunnel.....	12
2.2 Rock Mechanics and Rock Mass Properties.....	12
2.3 Parameters and Properties of Rock.....	13
2.4 Stress.....	13
2.4.1 Basic concept on stress.....	13
2.4.2 In-situ and Induced stress in underground opening.....	15

2.4.3	Stress around a circular excavation boundary	18
2.4.4	Rock stress redistribution around a tunnel in isostatic condition	22
2.4.5	Stresses remote from the excavation boundary	23
2.4.6	Stresses: independent of size of excavation.....	23
2.4.7	Influence of excavation shape and orientation	24
2.5	Squeezing in Rock.....	24
2.5.1	Empirical Approach to squeezing.....	25
2.5.2	Semi-Empirical approach	27
2.6	Rock Burst.....	32
2.7	Empirical Method of support system design.....	33
2.7.1	Rock Mass Rating Method	34
2.7.2	Q-Value Method	34
2.8	Analytical method of support system design	35
2.8.1	Assumptions of rock support interaction analysis	35
2.8.2	Convergence Confinement Method.....	36
2.9	Numerical modelling.....	43
2.9.1	Finite Element Modeling and Modeling Issues	43
2.9.2	Three-Dimensional Modeling.....	45
2.9.3	Software used in this research	46
2.10	Rock Support Interaction	48
2.10.1	Assumptions of Rock Support Interaction Analysis.....	49
2.10.2	Steps wise procedure for the mechanism of Rock Support Interaction	50
3	METHODOLOGY	52
3.1	General Flowchart.....	52
3.2	Preliminary Study	53
3.3	Data Collection.....	53
3.4	Determination of rock mass parameters.....	53
3.5	Assessment of Potential Squeezing.....	54
3.6	Assessment of Potential Rock Burst	54
3.7	Support System Design.....	54
3.7.1	Empirical Method (RMR and Q-value).....	55
3.7.2	Analytical Method	56
3.7.3	Two-Dimensional Numerical Modelling.....	56

3.7.4	Three-Dimensional Numerical Modelling.....	59
3.8	Recommendation of the support system	59
4	RESULTS AND DISCUSSIONS	60
4.1	Determination of Overburden	60
4.2	Calculation of Rock Mass Parameters	60
4.3	Assessment of Potential Squeezing.....	61
4.3.1	Empirical approach to squeezing.....	61
4.3.2	Semi Empirical Approach for Squeezing	62
4.4	Assessment of Rock Burst	63
4.5	Empirical Method.....	66
4.6	Analytical Method.....	68
4.7	Numerical Modeling	82
4.8	Three-Dimensional Numerical Modelling.....	97
4.8.1	3D Adit Connection	98
4.8.2	3D Surge Shaft and Ventilation Tunnel.....	104
4.8.3	3D bend in the tunnel.....	110
4.9	Discussions.....	117
5	CONCLUSIONS AND RECOMMENDATIONS.....	120
5.1	Conclusions	120
5.2	Recommendations:.....	121
6	REFERENCES	123
7	ANNEX A: DETAILS OF CALCULATION	126
8	ANNEX B: NUMERICAL MODELLING RESULTS	140
9	ANNEX C: STANDARD CHARTS AND FIGURES	149
10	ANNEX D: PROJECT RELATED DATA AND DOCUMENTS	156

LIST OF FIGURES

Figure 1-1: Projection of a T-intersection showing tunnel span (created in ANSYS)	2
Figure 1-2: Graph showing stand up time vs unsupported span (Rehman et al, 2018)....	3
Figure 1-3: Model of an Intersection showing orientation of joints (created in ANSYS)	4
Figure 1-4: Wedge formation in jointed rock at intersections (created in ANSYS).....	4
Figure 1-5: Location of the project area	6
Figure 1-6: Geological overview of the project area (Report on Rock Support Analysis of Underground Excavation, 2017)	8
Figure 1-7: Various Rock Support Classes defined based on Q-value.....	9
Figure 2-1: Cartesian components of stress at a point (Goodier, 1951)	14
Figure 2-2: Ratio of horizontal to vertical stress for different deformation moduli based upon Sheorey's equation (P.R.Sheorey, 1994).....	17
Figure 2-3: Variation of ratio of average horizontal to vertical stress with depth below surface (Hoek & Brown, Underground Excavation in rock, 1980)	18
Figure 2-4: A circular hole in an infinite plate (Kirsch, 1898).....	19
Figure 2-5: Stress around circular opening for $K=0.25$ (Terzaghi and Richart, 1952) ..	21
Figure 2-6: Influence of K on stresses at the circumference of an underground circular opening (Terzaghi and Richart, 1952)	21
Figure 2-7: Stress trajectories in rock mass surrounding a circular opening (left) and tangential and radial stress distribution in elastic and non-elastic conditions (right). (Hoek & Brown, Underground Excavation in rock, 1980).....	22
Figure 2-8: Criteria for predicting squeezing of ground (Singh & Goel, 2006).....	26
Figure 2-9: Criteria for squeezing (Goel, 1994)	27
Figure 2-10: Plot of tunnel convergence against the ratio of rock mass strength to in situ stress in case of unsupported tunnel (Hoek & Marinos, Predicting tunnel squeezing problems in weak heterogeneous rock masses, 2000)	29
Figure 2-11: Approximate relationship and the degree of difficulty associated with tunneling through squeezing in rock in case of unsupported tunnel (Hoek & Marinos, Predicting tunnel squeezing problems in weak heterogeneous rock masses, 2000).....	30

Figure 2-12: Schematic representation of Longitudinal Displacement Profile (LDP), Ground Reaction Curve (GRC) and Support Characteristic Curve (SCC) (Carrazza-Torres & Fairhurst, 2000)	37
Figure 2-13 : Characteristics Curve of Rock Support Interaction (Hoek & Brown, Underground Excavation in rock, 1980).....	50
Figure 3-1: L-section of headrace tunnel showing 2D and 3D numerical modeling sections.....	54
Figure 3-2: Response of support system to tunnel wall displacement, resulting in establishment of equilibrium (Hoek, Kaiser, & Bawden, Support of underground excavation in hard rock, 1995)	56
Figure 3-3: Longitudinal Displacement Profile (Vlachopoulos & Diederichs, 2009)....	58
Figure 4-1: Plot showing Singh's approach to assessment of squeezing	62
Figure 4-2: GRC and LDP of section 0+600	69
Figure 4-3: GRC and LDP of section 1+400	70
Figure 4-4: GRC and SCC for section 1+400.....	71
Figure 4-5: GRC and LDP of section 2+000	72
Figure 4-6: SCC for section 2+000.....	74
Figure 4-7: GRC and SCC of section 2+000	74
Figure 4-8: GRC and LDP of section 2+500	75
Figure 4-9: SCC for section 2+500.....	77
Figure 4-10: GRC and SCC of section 2+500	78
Figure 4-11: GRC and LDP of section 3+200	79
Figure 4-12: SCC of section 3+200	81
Figure 4-13: GRC and SCC of section 3+200	82
Figure 4-14: Plastic zone and tunnel closure for section 0+600.....	83
Figure 4-15: Axial force on bolts and BM in liners for section 0+600	84
Figure 4-16: Safety envelope for section 0+600.....	84
Figure 4-17: Plastic zone and tunnel closure for section 1+400.....	86
Figure 4-18: Axial force and BM in supports for section 1+400	86
Figure 4-19: Safety envelope for section 1+400.....	87
Figure 4-20: Plastic displacement and tunnel closure for section 2+000	88
Figure 4-21: Axial force and BM on supports in section 2+000	89

Figure 4-22: Safety envelope for section 2+000 with 100mm shotcrete.....	90
Figure 4-23: Safety envelope for section 2+000 with 120mm shotcrete.....	90
Figure 4-24: Safety envelope for section 2+000 with 200mm shotcrete.....	91
Figure 4-25: Plastic zone and Tunnel Closure for section 2+500	92
Figure 4-26: Axial force and BM on supports in section 2+500	93
Figure 4-27: Safety envelope for section 2+500.....	93
Figure 4-28: Plastic zone and Tunnel Closure in section 3+200	95
Figure 4-29: Axial force and BM at section 3+200	96
Figure 4-30: Safety envelope for section 3+200.....	96
Figure 4-31: Location of Adit.....	98
Figure 4-32: 3D Geometric modeling of Adit connection.....	99
Figure 4-33: 3D Material modeling of Adit connection.....	99
Figure 4-34: 3D presence of Concrete panel, Shotcrete and Rock Bolt in adit connection	100
Figure 4-35: Construction stages in analysis of Adit connection	101
Figure 4-36: Displacement around adit connection	102
Figure 4-37: Maximum shear stress in shotcrete lining and concrete panel.....	103
Figure 4-38: Axial force in rock bolts around adit	104
Figure 4-39: Location of Surge Shaft in HRT	105
Figure 4-40: 3D geometric model of surge shaft.....	106
Figure 4-41: 3D meshing, loading and boundary conditions of Surge Shaft	106
Figure 4-42: 3D presence of shotcrete lining and rock bolts in Surge Shaft, main tunnel and ventilation tunnel.....	107
Figure 4-43: Displacement around the Surge Shaft.....	108
Figure 4-44: Maximum shear stress around the Surge Shaft.....	109
Figure 4-45: Axial force imposed on rock bolts around the Surge Shaft	110
Figure 4-46: Location of a bend in the tunnel	111
Figure 4-47: 3D geometric model of a tunnel bend.....	112
Figure 4-48: Meshing, Loading and boundary conditions around the tunnel bend.....	112
Figure 4-49: 3D presence of shotcrete and rock bolts around the bend	113
Figure 4-50: Displacement around the tunnel bend.....	115
Figure 4-51: Maximum shear stress around the tunnel bend.....	115

Figure 4-52: Axial force in the rock bolts around the tunnel bend.....	116
Figure 8-1: Mean stress around tunnel without support at section 0+600.....	140
Figure 8-2: Mean stress around tunnel with support at section 0+600.....	140
Figure 8-3: Mean stress around tunnel without support at section 1+400.....	141
Figure 8-4: Mean stress around tunnel with support at section 1+400.....	141
Figure 8-5: Mean stress around tunnel without support at section 2+000.....	142
Figure 8-6: Mean stress around tunnel with support at section 2+000.....	142
Figure 8-7: Mean stress around tunnel without support at section 2+500.....	143
Figure 8-8: Mean stress around tunnel with support at section 2+500.....	143
Figure 8-9: Mean stress around tunnel without support at section 3+200.....	144
Figure 8-10: Mean stress around tunnel with support at section 3+200.....	144
Figure 8-11: Mean stress around 3D Adit connection.....	145
Figure 8-12: Displacement around Adit Connection, Stage 1.....	145
Figure 8-13: Displacement around Adit Connection, Stage 6.....	146
Figure 8-14: Displacement around Adit Connection, Stage 23.....	146
Figure 8-15: Displacement around Adit Connection, Stage 28.....	147
Figure 8-16: Mean stress around Surge Shaft.....	147
Figure 8-17: Mean stress around Tunnel bend.....	148
Figure 9-1: Q-support chart published by Grimstad in 2007 (Barton & Grimstad, 2014)	152
Figure 9-2: Guidelines for estimating disturbance factor D.....	155

LIST OF TABLES

Table 1-1: Rock Mass Properties around selected sections at different chainages (Report on Rock Support Analysis of Underground Excavation, 2017)	10
Table 1-2: Rock mass classification at Surge Shaft.....	10
Table 1-3: Rock mass classification around adit connection.....	11
Table 2-1: Material properties influencing the discontinuous rock parameters.	13
Table 2-2: Squeezing behavior (Jethwa, 1984)	28
Table 2-3: Geotechnical issues associated with the squeezing severity classes and appropriate support types (Hoek & Marinos, Predicting tunnel squeezing problems in weak heterogeneous rock masses, 2000)	31
Table 2-4: Criteria defined by different methods for prediction of Rock Burst	33
Table 4-1 Overburden and uniaxial compressive strength of rock mass at selected sections	60
Table 4-2: Estimation of rock mass deformation modulus.....	61
Table 4-3: Calculation for empirical method of estimation of squeezing	61
Table 4-4: Calculations for semi-empirical method of assessment of squeezing using Jethwa et al. approach (1984) approach.....	62
Table 4-5: Calculations for semi-empirical method of assessment of squeezing using Hoek and Marinos (2000) approach.	63
Table 4-6: Calculations for prediction of rock burst.....	64
Table 4-7: Results of Rock Burst assessment using Hoek and Brown’s approach	64
Table 4-8: Results of Rock Burst assessment using Grimstad and Barton’s approach ..	64
Table 4-9: Support system design on the basis of RMR rock mass classification	66
Table 4-10: Support system design on the basis of Q-system (Annex C, Figure 9-1) ...	67
Table 4-11: Calculation of GRC of section 0+600	68
Table 4-12: Calculation of GRC of section 1+400	69
Table 4-13: Calculation of SCC for section 1+400	70
Table 4-14: Calculation of GRC for section 2+000.....	71
Table 4-15: Calculation of SCC for section 2+000	72
Table 4-16: Calculation of GRC of section 2+500	74
Table 4-17: Calculation of SCC for section 2+500	75

Table 4-18: Calculation of GRC for section 3+200.....	78
Table 4-19: Calculation of SCC for section 3+200	79
Table 4-20: Support system suggested by Numerical Modeling for section 0+600.....	85
Table 4-21: Supports suggested by numerical modeling for section 1+400.....	87
Table 4-22: Supports suggested by Numerical Modeling for section 2+000	91
Table 4-23: Supports suggested by numerical modeling for section 2+500.....	94
Table 4-24: Supports suggested by Numerical Modeling for section 3+200	97
Table 4-25: Supports suggested by 3D numerical analysis of adit connection	101
Table 4-26: Supports suggested by 3D numerical analysis of Surge Shaft	108
Table 4-27: Supports suggested on the tunnel bend by 3D numerical modeling	114
Table 7-1: Detail calculation of GRC for section 0+600.....	126
Table 7-2: Detail calculation of LDP for section 0+600	127
Table 7-3: Detail calculation for GRC in section 1+400	129
Table 7-4: Detail Calculation for LDP pf section 1+400	130
Table 7-5: Detail calculation for GRC in section 2+000.....	131
Table 7-6: Detail calculation of LDP for section 2+000	133
Table 7-7: Detail calculations for GRC in section 2+500	134
Table 7-8: Detail calculation of LDP at section 2+500	135
Table 7-9: Detail calculation for LDP in chainage 3+200.....	136
Table 7-10: Detail calculations for LDP in section 3+200	138
Table 9-1: Guidelines for excavation support by RMR system (After Bienawski, 1989)	149
Table 9-2: Rock Mass Classification using Q value.....	150
Table 9-3: Table for ESR.....	151
Table 9-4: Values of constant m_i given by intact rock (Hoek & Brown, 1997).....	153
Table 9-5 : General chart for GSI estimates from the geological observations.....	154
Table 10-1: Summary of geological classification of the rock mass along the tunnel alignment based on Q-chart published by Barton in 2007 (Barton & Grimstad, 2014) taken from (Report on Rock Support Analysis of Underground Excavation, 2017)....	156

ABBREVIATIONS

CCM	Convergence Confinement Method
E_b	Modulus of Elasticity of bolt
E_c	Modulus of Elasticity of concrete/shotcrete
E_{rm}	Modulus of Elasticity of rock mass
E_s	Modulus of Elasticity of steel
FEM	Finite Element Method
FoS	Factor of Safety
G_{rm}	Shear modulus of rock mass
GPa	Giga Pascal
GRC	Ground Reaction Curve
GSI	Geological Strength Index
h	Height of overburden
ISRM	International Society of Rock Mechanics
LDP	Load Displacement Curve
m	Meters
MPa	Mega Pascal
MW	Mega Watt
P_o	In-situ stress
r_i	Internal radius of tunnel
RMR	Rock Mass Rating
RQD	Rock Quality Designation
SCC	Support Characteristics Curve
S/C	Shotcrete
UCS	Uniaxial Compressive Strength
γ	Unit Weight
σ_r	Radial stress
σ_θ	Tangential Stress
ν	Poisson's ratio

1 INTRODUCTION

1.1 Background

Today, production of energy is one of the main sources of our country's economy. Hydropower comprises almost all of the Energy production in Nepal. While the majority of the running Hydropower project are low to medium capacity, most of the proposed projects are of medium to large capacity. For large projects, the discharge will be higher which means the water pressure to be handles will be large as well. Also, steep topography is the main reason it has been possible to produce large amount of energy within short stretches of fast flowing, steep rivers. Due to this steep topography, the use of canals or pipes to convey water is not feasible in most of the cases, hence Tunnel conveyance is the most appropriate solution. But with it, it brings the high risk and uncertainty that comes along with underground excavations.

The geology of Nepal Himalayas is very young and fragile which has proved to be the most challenging factor in underground works. Only properly designed support can attenuate the risk associated with such excavations. Tunnel is considered to be a two-dimensional problem because of the homogeneity of the stress distribution around it in the longitudinal direction. By this consideration, it is considered to be in plane strain condition and analysis is usually done using simpler cross-sectional plain strain approximation, i.e. the strain occurring in the longitudinal direction is considered negligible. This approach is also helped by the fact that the length of the tunnel is always very much larger than its cross-sectional dimensions. The changes in cross sectional periphery, geological and mechanical properties of the surrounding medium are assumed to be non-significant along the axis of the tunnel.

While this is true 99% of the time, there may be some discrete features like Adit connections, bends, or even underground Surge Shafts where the stress distribution is not homogeneous in longitudinal direction either. In these cases, the induced stress becomes three dimensional as the effect of one opening has to be considered in the design of the other openings. Therefore, only three-dimensional methods can provide a complete analysis of stress occurring in the vicinity of the opening.

Generally, these features are treated as salient features and some additional factor of safety is provided but even upon doing so, we don't know where we stand in terms of safety privileges precisely, or the support system might unknowingly turn out to be uneconomical. Considering this, a modern Three-Dimensional approach has been taken in this thesis and using actual project data of the Upper Balephi A hydropower project, the support system for the Adit connection, underground Surge shaft and a bent in the tunnel has been designed using the GTS-NX (MIDAS IT Co., 2020) software along with the conventional empirical and analytical methods for other parts of the tunnel. The importance of Three-Dimensional approach in Tunneling is presented in the following section.

1.2 Three-Dimensional approach and its importance

Underground excavations are made frequently in many subsurface civil engineering constructions, e.g. subway systems, power stations complexes, sewer, water-supply networks, etc. Intersections involving galleries and shaft are commonly excavated in underground mining operations. Especially, in mining works where room and pillar method is employed, intersections become a major part of the system as entries and crosscuts are made in different directions forming intersections.

However, the structural instability in intersections are magnified in comparison to an isolated excavation. This is mainly due to following major reason (Gercek, 1986):

- a) At the intersection the span to be supported is larger than the span of the individual openings involved. This larger unsupported span corresponds to a shorter stand up time. This is shown in Figure 1-1 and 1-2 below.

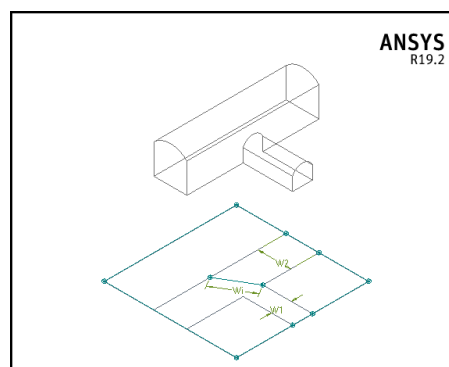


Figure 1-1: Projection of a T-intersection showing tunnel span (created in ANSYS)

$$W_i > W_2 > W_1$$

Where,

W_1 = Span of Tunnel 1

W_2 = Span of Tunnel 2

W_i = Span of Intersection

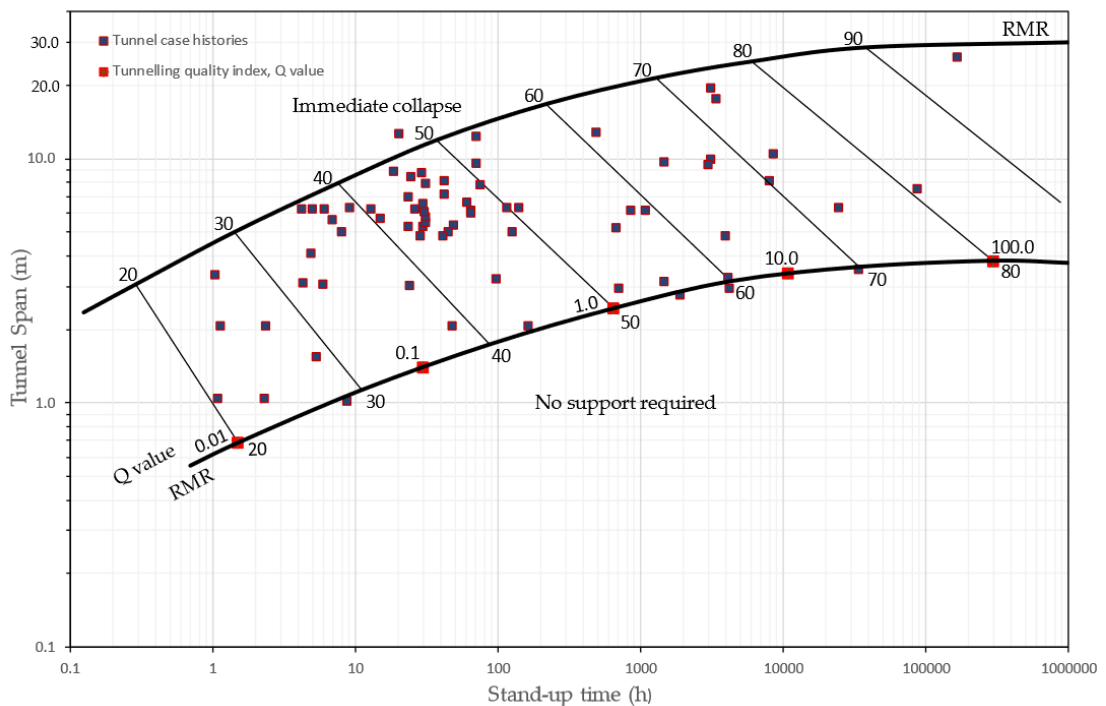


Figure 1-2: Graph showing stand up time vs unsupported span (Rehman et al, 2018)

b) A favorable orientation of joints for one opening may become less favorable for other openings. Hence, it can be a very difficult task to create an intersection establishment that is equally suitable for all the openings forming the intersection. An example of such possibility is illustrated in figure 1-3 below. In tunnel I, the tunnel axis is perpendicular to strike of joints drive with dip $> 45^\circ$ which is a very favorable condition while in case of tunnel II, the axis is parallel to strike of joints which is very unfavorable condition.

The cross-sectional geometry along the longitudinal axis of an opening changes as it approaches an intersection. As result of it, the stress distribution gets superimposed and the state of induced stress becomes three dimensional.

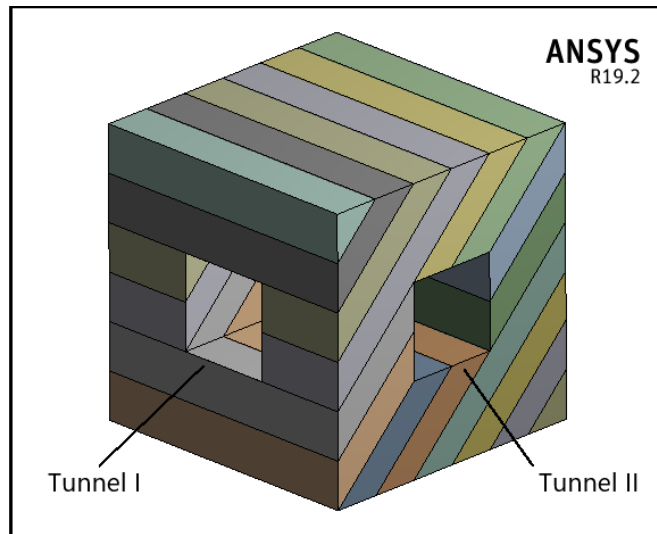


Figure 1-3: Model of an Intersection showing orientation of joints (created in ANSYS)

- c) At an intersection, the side walls of an opening are removed. This removes the support that was initially available for the individual opening and additional free spaces are created exposing some unstable rock blocks or wedges in case of a jointed or blocky rock mass as shown in Figure 1-4 below.

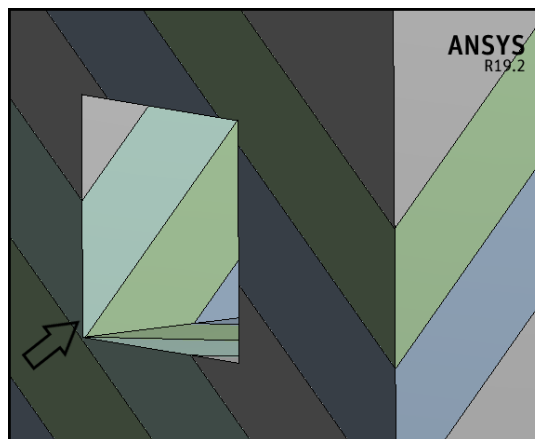


Figure 1-4: Wedge formation in jointed rock at intersections (created in ANSYS)

Therefore, intersection zone is not only characterized by the combination of properties of individual openings but some additional adverse conditions are created by new geometry and superimposition of boundary stresses.

1.3 Problem Statement

Fifty-three percent of global tunnel failures are related to ground conditions (Lance, Anderson, & Lamont, 2007). Therefore, correctness of geotechnical and geological ground conditions, herein after referred to as the ground, is critical to minimize risk imposed by instability. Problematic ground comprises abrasive, weak, squeezing and swelling material, rock bursts and discontinuities such as faults, fissures and jointing. These problems can be seen when the tunnel is excavated. Rock is naturally very diverse and impossible to generalize its properties, behavior, design and suitable construction methods. The support required for a tunnel in rock is a complex function of the properties and condition of the rock, the geometry and orientation of the tunnel, and the construction procedures. In majority of tunnel in the design phase, decision in selecting tunnel alignment and predicting the rock mass quality and rock support requirement has direct influence on the overall cost and time requirement. Furthermore, at regions in tunnel alignment where the longitudinal homogeneity of stress distribution is disturbed, three-dimensional analysis has to be done for designing support as the stress varies in longitudinal direction too and plane strain condition cannot be assumed.

1.4 Objectives of the study

1.4.1 General Objectives

- To design the support system of Upper Balephi ‘A’ hydropower project using conventional approaches and Three-Dimensional approach.
- To compare the support system suggested by various approaches and recommend the most economic and safe one.

1.4.2 Specific Objectives

- To clarify how factors like discontinuities and their orientation affect the stability of tunnel in junctions and intersections.
- To predict potential squeezing and rock burst in tunnel sections.
- To compare convergence confinement method with numerical modelling approach.
- To conduct a Three-Dimensional numerical modeling for support design in region where stress varies in longitudinal direction along the axis of the tunnel.

1.5 Scope and Limitations of the study

- It is based on literatures available in tunneling principle of rock mechanics and geotechnical engineering.
- Only geotechnical engineering factors influencing the tunnel stability were considered. Other factors like seismic forces are not considered.
- Other aspects to design of tunnel support such as structural integrity of the rock bolts, shotcrete and concrete lining is outside the scope of study.
- The strength parameters of the support materials are not verified using laboratory tests.

1.6 Upper Balephi 'A' Hydropower Project

1.6.1 Location of the Project area

Upper Balephi 'A' Hydroelectric Project is a run-of-river hydropower project proposed along the Balephi khola in Sindhupalchowk District, of Bagmati Zone (Figure 1). The project area lies in Gumba and Golche Village Development Committees (VDC). The project has the gross head of 203 m, installed capacity of 36 MW which will generate 212.8 GWh of annual energy.



Figure 1-5: Location of the project area

1.6.2 Geological overview of the Project area

The continuous convergence of two tectonic plate boundaries (Indian plate and Euro-Asian plate) has resulted in complex thrusting of the northern edge of the Indian plate. The Indus-Tsangpo Suture (ITS) is thought to have been the initial thrusting plate boundary. Subsequently, the plate boundary moved southwards to the MCT and later to the MBT where the main seismic activity is currently concentrated. It is assumed that, the active boundary is moving progressively towards the HFT. Active movement can be traced along the MBT where pressure ridges can be found uninterrupted in excess of 100 km. Equally, recent movement is also apparent on the Himalayan Frontal Thrust (HFT). Upper Balephi 'A' Hydroelectric Project lies predominantly in the higher Himalayan physiographic province. However, the project area is very close to one of the major tectonic boundary (thrust) i.e. Main Central Thrust (MCT), which is known to be an inactive thrust. The MCT is within 1-3 km distance from the powerhouse location. As a result, the valley slope between Baramchi Bazaar and Kartike Bazaar are highly disturbed with respect to valley slope stability along the left bank of the Balephi river. However, upstream valley from Kartike Bazaar where the project area is located is sound and stable, especially the right bank of the Balephi River, where all engineering structures are located. The Balephi River has cut through the major discontinuity trending north-east-north southwest-south in the higher Himalayan crystalline rocks of Paleozoic to Precambrian age and extended through the valley cutting the rocks of the lesser Himalayan meta-sedimentary sequence and joins with Sunkoshi River at Balephi Bazaar.

this process, this river crosses the MCT zone that lies between Kartike bazaar and Baramchi Bazaar.

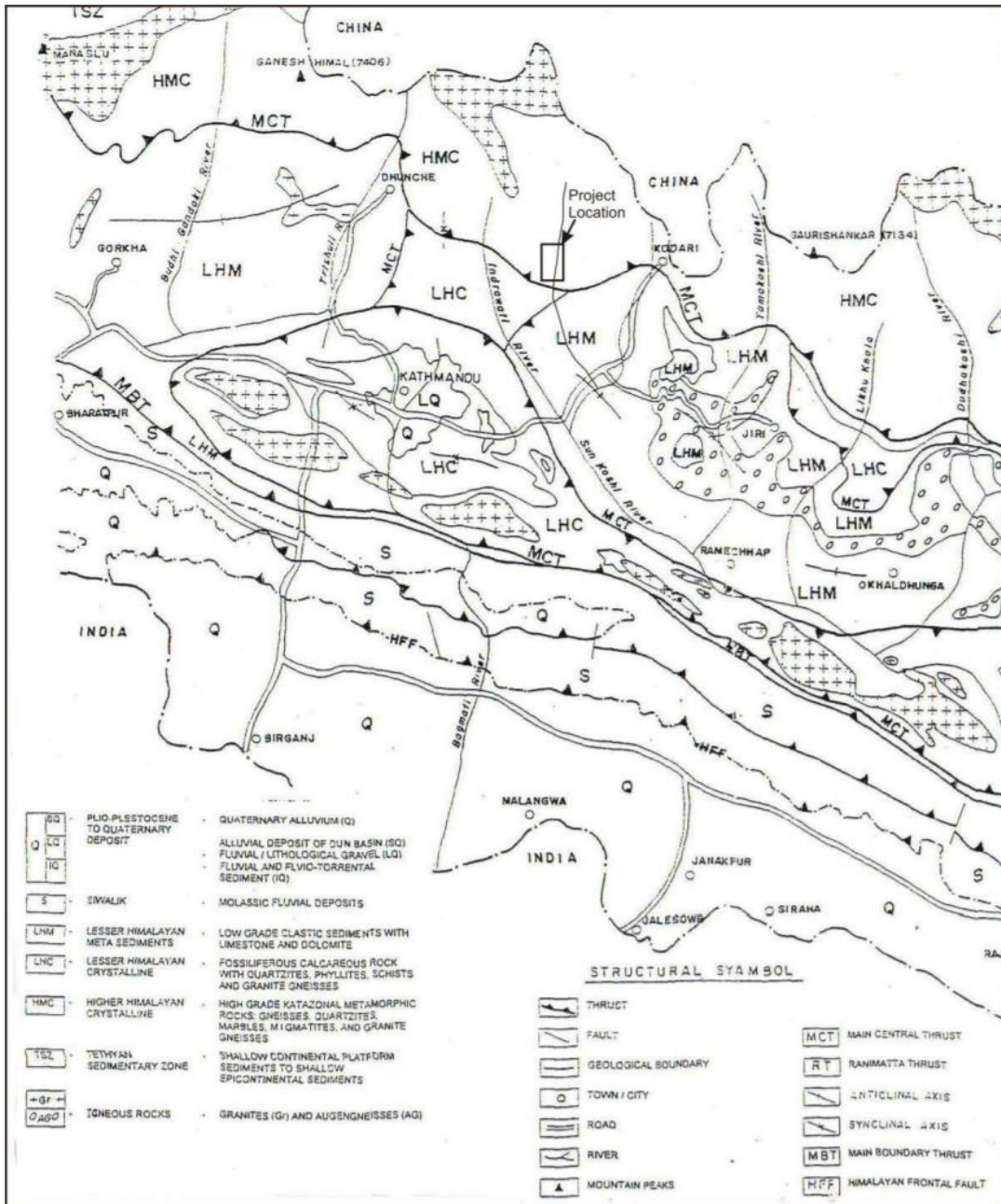


Figure 1-6: Geological overview of the project area (Report on Rock Support Analysis of Underground Excavation, 2017)

The geological overview around the project area are shown in a schematic sketch shown in Figure 1-6 above. As shown in Figure 1-6, the project area lies in the Higher Himalayan Crystalline Group. The rock mass in the project area are of Paleozoic to Precambrian age

that mainly consists of garnet bearing gneiss, kyanite, bearing biotite gneiss, garnetiferous mica schist, mica gneiss, micaceous quartzite, thin bands of marbles and highly sheared and schistose phyllite. The area is characterized by varied topography. The landform is controlled mainly by tectonic processes, subordinately by mass wasting and deep shear failures. Rugged hills, numerous deep gorges, steep slopes and some of unstable surface failure caused by deep shear failure, and active gullies represent the erosional landform of the area. River terrace alluvial fans along the Balephi River, sizable boulders carried by the river and talus deposit mass of various landslides are the main depositional landform of the project area. Balephi River is one of major tributaries of Sunkoshi River and it consists of small tributaries with sub-dendritic drainage pattern.

1.6.3 Rock Mass Classification for Tunnel Alignment

For Upper Balephi ‘A’ Hydroelectric Project, Barton’s Q-method of rock mass classification method has been used as a basis for quality assessment of the rock mass and design of rock support. The strength of this method is that it gives quantitative assessment of the different parameters of the rock mass and also suggests the rock support requirement for the respective rock mass class.

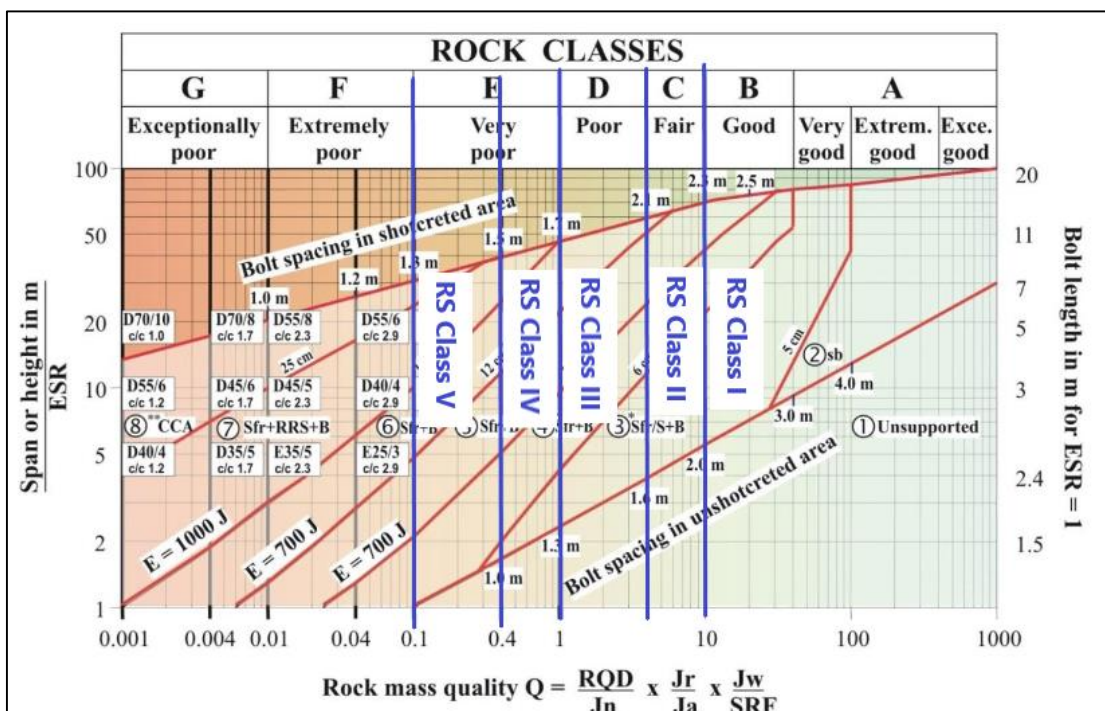


Figure 1-7: Various Rock Support Classes defined based on Q-value

The maximum Q-value along the tunnel alignment is 15 while minimum is 0.1. Keeping this in mind, five sections in the tunnel alignment are taken for study that best represents different strength of Rock. The minimum value of each sections shown in Figure 1-7 is taken and supports are designed as Rock Support I-V. The five chainages shown in table below represent the five Rock Support Classes with highest value of overburden and therefore, the design of support system in this study focuses in these five chainages. The Rock mass properties at five sections selected for two-dimensional analysis, that has been extracted from the geological summary of the project report, are given below:

Table 1-1: Rock Mass Properties around selected sections at different chainages (Report on Rock Support Analysis of Underground Excavation, 2017)

Rock Support Class	Chainage (m)	Q-value	GSI	Unit weight	UCS (MPa)	Maximum Overburden (m)
RS Class I	0+600	10	65	26.923	50	155
RS Class II	1+400	4	50	27.053	50	205
RS Class III	2+000	1	35	26.936	40	590
RS Class IV	2+500	0.4	25	27.014	40	345
RS Class V	3+200	0.1	20	26.613	30	145

More details of rock mass classification of the project are discussed in the geological report. The summary of rock mass classification is discussed in Annex D, Table 10-1.

1.6.4 Rock Mass Classification at Surge Shaft

The rock mass quality assessment for ventilation tunnel and surge shaft has been made based on the same concept as for headrace tunnel. The summary of the rock mass class that is likely to be met along these two underground structures are given in Table 1-2.

Table 1-2: Rock mass classification at Surge Shaft

Chainage (m)	Q (RMR)	Rock Mass Quality	Rock Type Description
Top to Bottom	1 to 3 (45 to 62)	Poor Rock Mass (Class IV)	Thinly foliated moderately weathered garnetiferous schist intercalated with occasional bands of mica gneiss.

1.6.5 Rock Mass Classification around Adit

The rock mass classification around the adit connection is shown below. The chainages in this table are measured from the point of intersection of Adit with the main tunnel. Starting chainage, face chainage and advance shows the real time excavation stages.

Table 1-3: Rock mass classification around adit connection

Adit						
Starting Chainage m		Face Chainage m		Advance (m)	Rock Class	Q-Value
0+	175.20	0+	177.2	2.0	IIIA	0.125
0+	177.20	0+	179.3	2.1	IIIA	0.141
0+	179.30	0+	181.3	2.0	IIIA	0.156
0+	181.30	0+	183.9	2.6	IIIA	0.156
0+	183.90	0+	186.4	2.5	IIIA	0.141
0+	186.40	0+	188.2	1.8	IIIA	0.125
0+	188.20	0+	190.2	2.0	IV	0.073
0+	190.20	0+	192.1	1.9	IV	0.073
0+	192.10	0+	193.9	1.8	IV	0.073
0+	193.90	0+	195.6	1.7	IV	0.073
0+	195.60	0+	197.3	1.7	IV	0.073
0+	197.30	0+	198.5	1.2	IV	0.073
Downstream Face						
Starting Chainage m		Face Chainage m		Advance (m)	Rock Class	Q-Value
0+	0.00	0+	1.7	1.7	V	0.009
0+	1.70	0+	3.6	1.9	V	0.009
0+	3.60	0+	5.4	1.8	V	0.009
0+	5.40	0+	7.3	1.9	V	0.007
0+	7.30	0+	9.2	1.9	V	0.007
0+	9.10	0+	11.1	2.0	V	0.003
0+	11.10	0+	13.0	1.9	V	0.003
0+	13.00	0+	14.8	1.8	V	0.004
0+	14.80	0+	16.6	1.8	V	0.004
0+	16.60	0+	18.5	1.9	V	0.006
0+	18.50	0+	20.3	1.8	V	0.006
0+	20.30	0+	22.1	1.8	IV	0.083
0+	22.10	0+	24.0	1.9	IV	0.096
0+	24.00	0+	25.7	1.7	IV	0.096
0+	25.70	0+	27.5	1.8	IV	0.092

2 LITERATURE REVIEW

2.1 Basic concept on Tunnel

Tunnel is an artificially constructed underground passage to by- pass obstacles safely without disturbing the over burden. Tunnels are created by the process of excavation. (Balasubramanian, 2017). There are various stages in construction of a tunnel, supporting is one among the various activities. The selection of efficient support methods for tunneling is very important to reduce problems during construction and minimize project cost and time within the project budget and the planned schedule. Tunnel construction is generally characterized by uncertainties. Rock tunneling, in general, depend on largely on the rock mass locking up as joints and interlocking blocks of rock interact and dilate during the process of convergence towards the excavation. Good quality rock often forms a natural arch and no or little support is needed. However, in weaker ground, such as in fault zones, the rock mass cannot support itself, even with reinforcement, and requires artificial support in the form of steel arch ribs, typically encased in shotcrete. Optimizing support requirements in weaker ground requires prediction of likely convergence rates, making observations as excavation is undertaken, i.e. observational methods, and then applying support such as rock bolts and/or shotcrete and/or steel arch ribs to control the movement and prevent excessive loosening (Powderham, 1994). In stronger, blocky rock masses, rock movement will be much less, and the purpose of the support is then to prevent loss of loose blocks and wedges, which would destabilize the arch and maybe lead to raveling failure.

2.2 Rock Mechanics and Rock Mass Properties

The theoretical and applied science of mechanical behavior of rock is rock mechanics. It is the branch of mechanics concerned with the response of rock to the force field of the physical environment. Rock mechanics in broader field is concerned with investigation, testing, analysis, design, construction and monitoring the performance of engineering structures built on, in or off rock (Ramamurthy, 2011). The rock mass is discontinuous, anisotropic and homogenous naturally occurring pre stressed medium. The discontinuous nature of rock mass due to the action of tectonic forces play a decisive role in the rock mass behavior and the displacement take primarily along these planes of weakness. The mode of failure of rock mass is dictated by the joint 7 system. The combined influence

of the joints, their configuration and the strength along them will have to be considered in the analysis and design.

2.3 Parameters and Properties of Rock

Although rock is naturally stable or slowly changes its chemical composition only under extreme conditions, its material properties influence strength, deformability, permeability and stability of rock masses. Material properties of a rock determines whether it is suitable for construction or not and the precautions required when using it. It is therefore important to understand rock mineralogy, structure, discontinuity sets, hydrogeology, squeezing and swelling problematic material behavior (Panthi, 2006). Table 2-1 shows the specific material properties which influence discontinuous rock parameters.

Table 2-1: Material properties influencing the discontinuous rock parameters.

Parameter	Specific Material Property
Rock Mass Structure	Type, strength, degree of weathering of rock, in-situ stress magnitude and direction
Discontinuities	Interlocking/ wedge spacing, block size and shape, discontinuity sets and persistence
Construction	Excavation method and support sequence
Hydrogeology and Voids	Groundwater, Seepage/ permeability, pore pressures

2.4 Stress

2.4.1 Basic concept on stress

A body tends to oppose the deformation due to the applied external forces. While the applied forces have a deforming or straining action on the body, internal forces are developed to oppose such deforming action and the body thus remains in equilibrium in a strained state. This internal resistance developed by the body over unit area of its cross

section is called stress. The quantification of stress is very important in order to understand the response shown by the body against deformation and hence make appropriate designs in order to improve the strength of the body against the loadings.

For the exact quantification of stress in Cartesian system of co-ordinates, we need six components of stress and they are expressed in vector form as shown in figure below (Goodier, 1951):

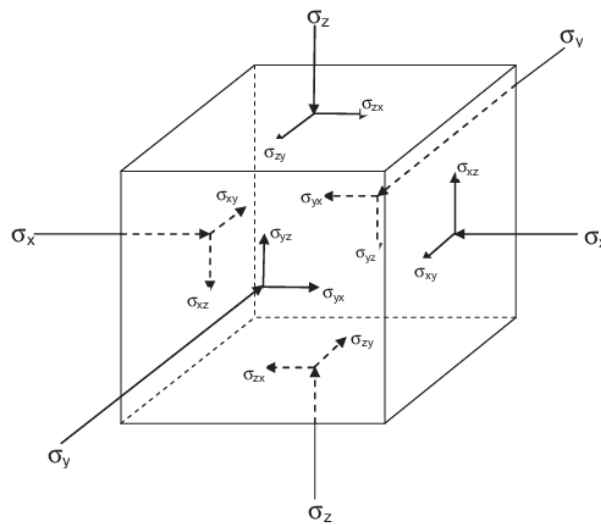


Figure 2-1: Cartesian components of stress at a point (Goodier, 1951)

Where, the term σ indicates the normal force and the suffix in it indicate the direction in which it is acting. In the similar way, the term τ represents the surface traction of shear force, the first suffix in it represents the plane that is perpendicular to it and the second suffix represents the direction in which it is acting.

Whatever be the state of stress at a point, it is always possible to find out a particular orientation of coordinate axes for which all shear stress components vanish. These axes are called principal axes and the corresponding plane parallel to the face of the volume element is called principal planes. The stress on the face of the plane are purely normal and are called principal stresses denoted by σ_1 , σ_2 , and σ_3 .

This is a basic concept regarding stress and readers are suggested to refer the books in references in case detail knowledge is required.

2.4.2 In-situ and Induced stress in underground opening

Rock at depth is subjected to stresses resulting from the weight of the overlying strata and from locked in stresses of tectonic origin. When an opening is excavated in this rock, the stress field is locally disrupted and a new set of stresses are induced in the rock surrounding the opening. A knowledge of the magnitudes and directions of these in situ and induced stresses is an essential component of underground excavation design since, in many cases, the strength of the rock is exceeded and the resulting instability can have serious consequences on the behavior of the excavations.

In a region situated at a depth, the rock mass is subjected to stresses resulting from the weight of the overlying strata and from the locked in stress of tectonic origins. When an opening is excavated in this rock, the stress field is locally disrupted and a new set of stress are induced in the rock surrounding the opening. Knowledge of the magnitudes and directions of these in situ and induced stresses is an essential component of underground excavation design since, in many cases, the strength of the rock is exceeded and the resulting instability can have serious consequences on the behavior of the excavations.

The estimation of vertical stresses in the element at certain depth can be obtained as:

$$\sigma_v = \gamma Z \quad 2-1$$

Where σ_v is the vertical stress, γ is the unit weight of the overlying rock and z is the depth below surface.

In elastic rock mass with a Poisson's ratio of ν , the horizontal stresses are induced by gravity.

$$\sigma_h = \sigma_x = \sigma_y = \frac{\nu}{1-\nu} \gamma Z \quad 2-2$$

where γ is the unit weight of the overlying rock, and Z is the depth below surface. The horizontal stresses acting on an element of rock at depth a Z below the surface are much more difficult to estimate than the vertical stresses. Normally, the ratio of the average horizontal stress to the vertical stress is denoted by the letter k such that:

$$\sigma_h = k\sigma_v = k\gamma Z \quad 2-3$$

Terzaghi and Richart (1952) suggested that, for a gravitationally loaded rock mass in which no lateral strain was permitted during formation of the overlying strata, the value of k is independent of depth and is given by $k = \nu/(1-\nu)$, where ν is the Poisson's ratio of the rock mass. This relationship was widely used in the early days of rock mechanics but, as discussed below, it proved to be inaccurate and is seldom used today. Measurements of horizontal stresses at civil and mining sites around the world show that the ratio k tends to be high at shallow depth and that it decreases at depth (R.C.Firth, 1990). In order to understand the reason for these horizontal stress variations it is necessary to consider the problem on a much larger scale than that of a single site. Sheorey developed an elastostatic thermal stress model of the earth (P.R.Sheorey, 1994). This model considers curvature of the crust and variation of elastic constants, density and thermal expansion coefficients through the crust and mantle. A detailed discussion on Sheorey's model is beyond the scope of this chapter, but he did provide a simplified equation which can be used for estimating the horizontal to vertical stress ratio k . This equation is:

$$k = 0.25 + 7E_h \left(0.001 + \frac{1}{Z} \right) \quad 2.4$$

Where Z in meter is the depth below surface and E_h in GPa is the average deformation modulus of the upper part of the earth's crust measured in a horizontal direction. This direction of measurement is important particularly in layered sedimentary rocks, in which the deformation modulus may be significantly different in different directions.

A plot of this equation is given in figure below for a range of deformation moduli. The curves relating k with depth below surface Z are similar to those published by (Hoek & Brown, Underground Excavation in rock, 1980).

Hence equation 2.4 is considered to provide a reasonable basis for estimating the value of k .

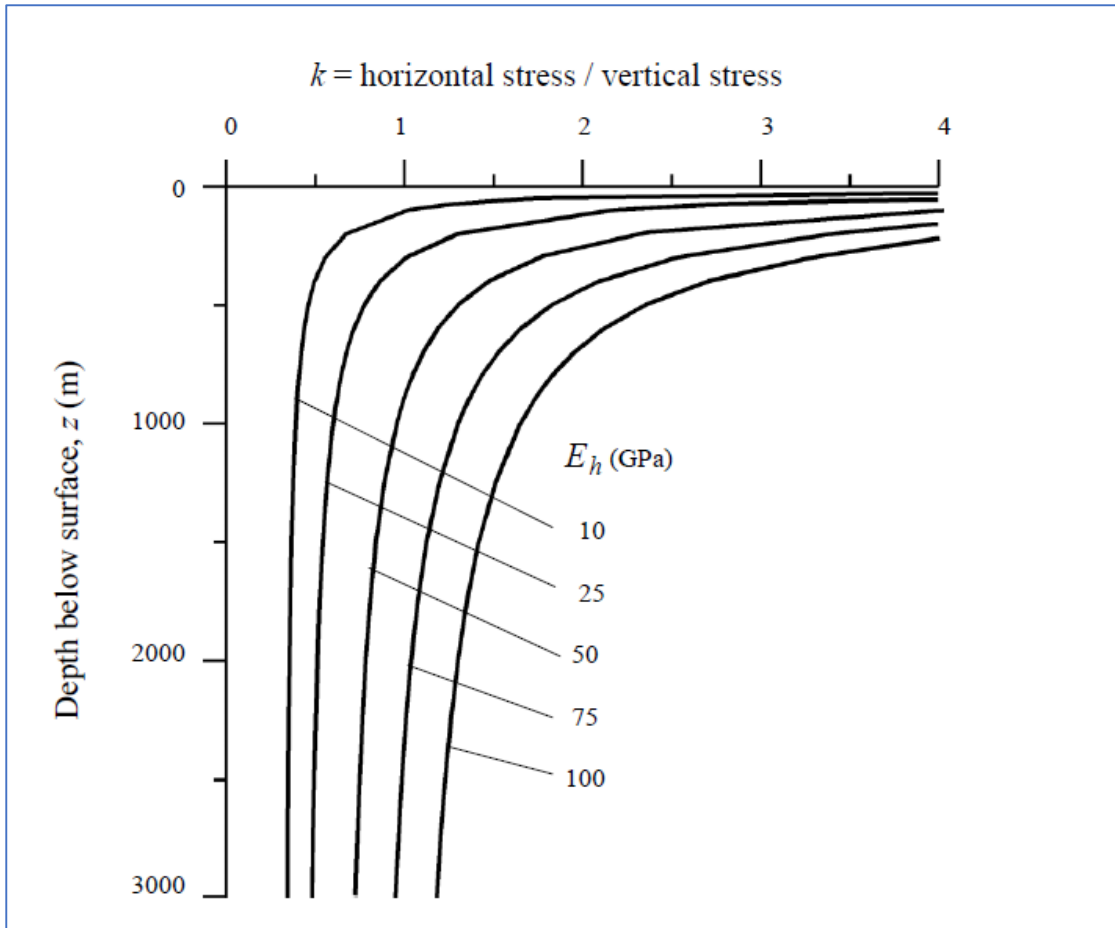


Figure 2-2: Ratio of horizontal to vertical stress for different deformation moduli based upon Sheorey's equation (P.R.Sheorey, 1994)

Hoek and Brown (1980) have found that the ratio (k) between horizontal and vertical in-situ stresses vary greatly and that the average horizontal stress near the surface is in most cases greater than the vertical stress. While the ratio k is greater than one at shallow depths, it is less than one and approaches a constant value at great depth. This means that the magnitude of average horizontal stress (σ_h) is to a great extent influenced by plate tectonic movements.

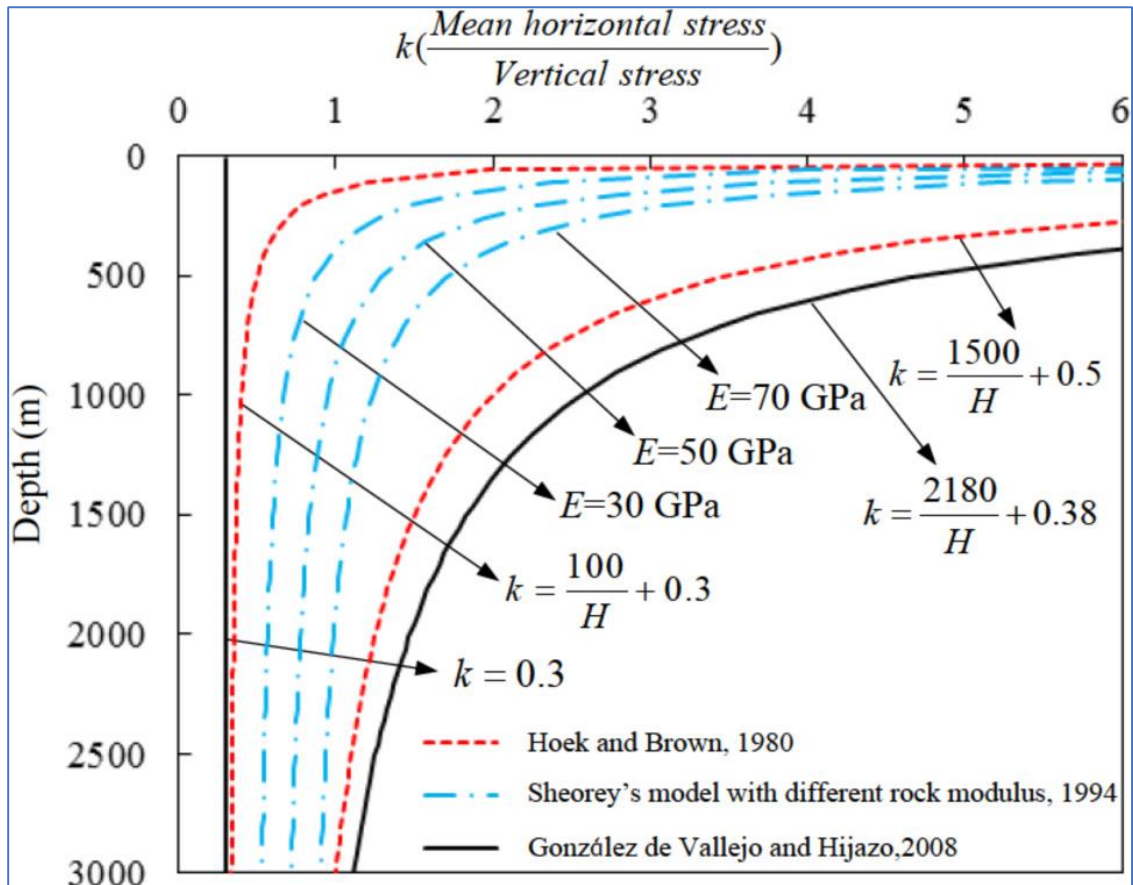


Figure 2-3: Variation of ratio of average horizontal to vertical stress with depth below surface (Hoek & Brown, Underground Excavation in rock, 1980)

Due to the convergence of the Indian and the Asian tectonic plates, the Himalayan region has been undergoing persistent compression for more than 50 million years. As a result, the Himalaya is one of the most seismically active regions of the world. Other tectonic activities like faulting, folding, thrusting and shearing are also responsible for the buildup of tectonic stresses. Here, total horizontal stress is higher than can be attributed to gravity alone.

2.4.3 Stress around a circular excavation boundary

When an underground excavation is made in a rock mass, the stresses which previously existed in the rock are disturbed and new stresses are induced in the rock in the immediate vicinity of the opening. One method of representing this new stress field is by means of principal stress trajectories which are imaginary lines in a stressed elastic body along which principal stresses act.

In order to calculate the stresses, strains and displacements induced around excavations in elastic materials, it is necessary to turn to the mathematical theory of elasticity. This requires that a set of equilibrium and displacement compatibility equations be solved for given boundary conditions and constitutive equations for the material. One of the earliest solutions for the two-dimensional distribution of stresses around an opening in an elastic body was published in 1898 by Kirsch for the simplest cross-sectional shape, the circular hole (Kirsch, 1898). A full discussion on the derivation of the Kirsch equations, as they are now known, is given by Jaeger and Cook (Jaeger and Cook, 1976). Many of the interesting and important facts about stresses around openings are illustrated by this example and some of them which are important in determining the size of the control volume of this research paper are discussed in subsequent sections.

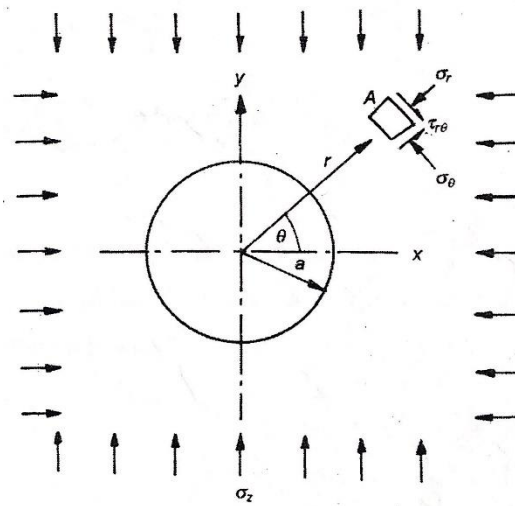


Figure 2-4: A circular hole in an infinite plate (Kirsch, 1898)

A long horizontal tunnel at a depth in a uniform rock formation is represented as a circular hole of radius, a , located at the origin, as shown in Figure 2-4 above, in an infinite plate of finite thickness. For the applied stresses (as in-situ) far away from the origin in x and z directions, σ_x and σ_z , respectively, and using Airy stress function, the expressions for radial, tangential and shear stresses are given at the element A as (Kirsch, 1898):

$$\sigma_r = \frac{1}{2} (\sigma_x + \sigma_z) \left(1 - \frac{a^2}{r^2}\right) + \frac{1}{2} (\sigma_x - \sigma_z) \left(1 + \frac{3a^4}{r^4} - \frac{4a^2}{r^2}\right) \cos 2\theta \quad 2.5$$

$$\sigma_{\theta} = \frac{1}{2} (\sigma_x + \sigma_z) \left(1 + \frac{a^2}{r^2}\right) - \frac{1}{2} (\sigma_x - \sigma_z) \left(1 + \frac{3a^4}{r^4}\right) \cos 2\theta \quad 2.6$$

$$\tau_{r\theta} = -\frac{1}{2} (\sigma_x - \sigma_z) \left(1 - \frac{3a^4}{r^4} + \frac{2a^2}{r^2}\right) \sin 2\theta \quad 2.7$$

Where,

σ_r = radial stress

σ_{θ} = tangential stress

$\tau_{r\theta}$ = shear stress

$\sigma_z = \gamma h$ = geostatic overburden pressure, in situ

$\sigma_x = k \cdot \sigma_z$ = horizontal pressure, in situ

K = stress ratio (horizontal stress / vertical stress)

γ = density of rock mass

h = depth of overburden

a = radius of circular opening

θ = central angle with x-axis

r = radial distance from center of the opening

Terzaghi and Richart, in 1952 used Kirsch's solutions to study the stress distribution around circular openings (Terzaghi and Richart, 1952). The horizontal and vertical stresses are transformed from radial and tangential stresses at the crown and the springing levels with the help of the following equations:

$$\sigma_h = \frac{\sigma_{\theta} + \sigma_r}{2} + \frac{\sigma_{\theta} - \sigma_r}{2} \cos 2\theta + \tau_r \sin 2\theta \quad 2.8$$

$$\sigma_v = \frac{\sigma_{\theta} + \sigma_r}{2} - \frac{\sigma_{\theta} - \sigma_r}{2} \cos 2\theta - \tau_r \sin 2\theta \quad 2.9$$

$$\sigma_v = -\frac{\sigma_{\theta} - \sigma_r}{2} - \sin 2\theta - \tau_r \cos 2\theta \quad 2.10$$

The stress distribution around a circular tunnel is shown in Figure 2-5. They also considered the influence of ratio $K = \sigma_h/\sigma_v$ on the circumferential principal stress which is shown in Figure 2-6.

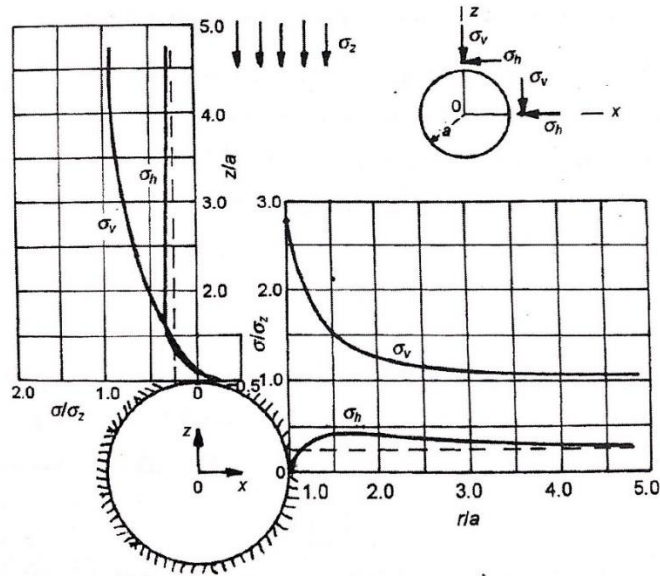


Figure 2-5: Stress around circular opening for $K=0.25$ (Terzaghi and Richart, 1952)

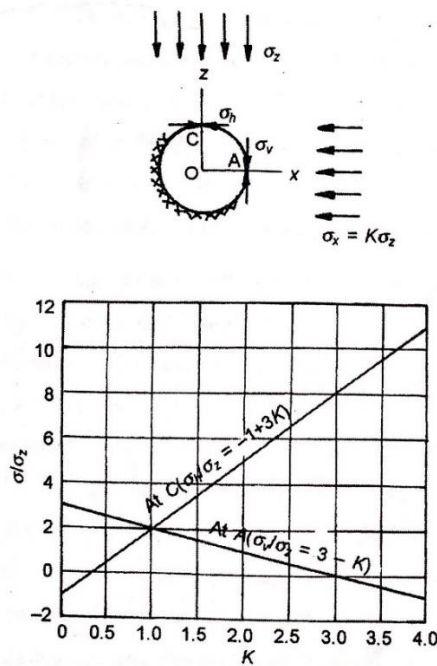


Figure 2-6: Influence of K on stresses at the circumference of an underground circular opening (Terzaghi and Richart, 1952)

2.4.4 Rock stress redistribution around a tunnel in isostatic condition

After excavation of an underground opening, the in-situ stresses in the rock mass are disturbed. Stresses are redistributed along the periphery of the excavation. According to Kirsch solution, the redistribution of stresses around a circular opening in an elastic material in isostatic stress conditions ($\sigma_h = \sigma_v = \sigma_z$) may be expressed as shown in Figure 2-7.

As shown the tangential stresses (σ_θ) and the radial stress (σ_r) at the periphery of a circular opening in fully isostatic stress condition and for elastic rock material will be twice and zero times the isostatic stress respectively. Stresses become normalized as the ratio between radial distance (R) and opening radius (r) increases. The magnitudes of σ_θ and σ_r are:

$$\text{Radial Stress: } \sigma_r = \sigma \left(1 - \frac{r_i^2}{r^2}\right) \quad 2-11$$

$$\text{Tangential Stress: } \sigma_\theta = \sigma \left(1 + \frac{r_i^2}{r^2}\right) \quad 2-12$$

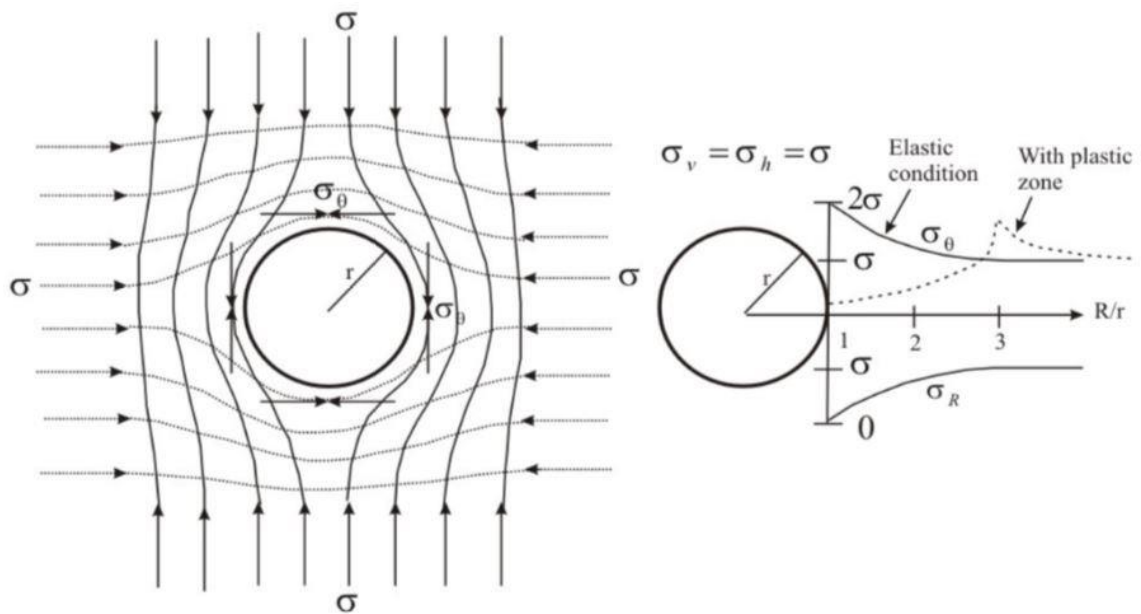


Figure 2-7: Stress trajectories in rock mass surrounding a circular opening (left) and tangential and radial stress distribution in elastic and non-elastic conditions (right).

(Hoek & Brown, Underground Excavation in rock, 1980)

2.4.5 Stresses remote from the excavation boundary

As the distance r from the hole increases, the influence of the opening upon the stresses in the rock decreases. A plot of the ratio of σ/σ_z against the distance r along the horizontal axis of the stressed model shows that the stress concentrating effect of the hole dies away fairly rapidly and that, at $r = 3a$, the ratio of induced to applied stress is very close to unity. This means that, at this distance from the excavation boundary, the stresses in the rock do not 'see' the influence of the opening. This fact has been utilized by those concerned with model studies of stresses around underground excavations. The general rule is that the minimum size of the model should be 3 to 4 times the maximum dimension of the excavation in the model. (Brady and Brown, 2004)

But in this research work, considering the plastic nature of the rock mass, and the shape of the tunnel, control volume is taken as 10-20 times the diameter of the excavation.

2.4.6 Stresses: independent of size of excavation

It is important to note that the equations for the stresses around a circular hole in an infinite rock mass given for Figure 2-5 do not include terms in the radius of the tunnel a , but rather, include terms in the dimensionless parameter a/r . This means that the calculated stress levels at the boundaries of the excavation, for example, are independent of the absolute value of the radius. The same stress levels will be induced in the walls of a 1 m diameter circular tunnel as in the walls of a 10 m tunnel in the same elastic rock.

This fact has led to considerable confusion in the past. Some underground excavation designers have concluded that, because the stresses induced in the rock around an excavation are independent of the size of the excavation, the stability of the excavation is also independent of its size. If the rock mass is perfectly elastic and completely free of defects, this conclusion would be reasonably correct, but it is not valid for real rock masses which are already fractured. Even if the stresses are the same, the stability of an excavation in a fractured and jointed rock mass will be controlled by the ratio of excavation size to the size of the blocks in the rock mass. Consequently, increasing the size of an excavation in a typical jointed rock mass may not cause an increase in stress but it will almost certainly give rise to a decrease in stability.

But from the experiences in mines where difficulties have been encountered when small scraper drifts have been enlarged to accommodate trackless mining equipment. The assumption was made that the stability of the excavations was independent of size and that a doubling of the span of the tunnels would have no significant influence upon their stability. This assumption has proved to be incorrect and serious stability problems have been encountered as a result of roof falls caused by the release of joints which had not been disturbed by the smaller scraper drifts.

2.4.7 Influence of excavation shape and orientation

Some of the main design principles which emerge from a consideration of the distribution of elastic stresses around excavations of various shapes and orientations in biaxial stress fields are:

- Critical stress concentrations increase as the relative radius of curvature of the boundary decreases. Openings with sharp corners should therefore be avoided.
- Since the lowest stresses on the boundary of the opening occur for the largest radius of curvature of that boundary, the optimum shape for an opening in a hydrostatic stress field ($k = 1$) is a circle.
- For stress fields other than hydrostatic ($k \neq 1$), the lowest boundary stresses will be associated with an opening of ovaloid shape. Hence, if a cavern with a height to width ratio of 1:2 has to be excavated in a stress field in which the horizontal stress is equal to half the vertical stress, the opening shape which will give the lowest boundary stresses is the ovaloid illustrated in the upper margin sketch.
- Boundary stresses in an elliptical opening can be reduced to a minimum if the axis ratio of the opening can be matched to the ratio between the in-situ stresses.

Under applied stress conditions in which the value of k is very low, tensile stresses occur on the boundaries of all excavation shapes. These tensile stresses are replaced by compressive stresses as the value of k increases above a value of approximately $1/3$, for a circular excavation.

2.5 Squeezing in Rock

According to ISRM squeezing of rock is the time dependent large deformation which occurs around a tunnel and other underground openings and is essentially associated with

creep caused by exceeding shear strength (limiting shear stress). Deformation may terminate or continue over a long period of time.

Squeezing depends upon (Singh & Goel, 2006)

- The rate of deformation
- Geological condition
- In-situ stress relative to rock mass
- Ground water flow
- Pore water pressure
- Rock mass properties

2.5.1 Empirical Approach to squeezing

Empirical method is firmly based on or concerned with observation or experience rather than theory. Empirical methods are based on overburden height, dimension of tunnel and UCS of rock mass. For the tunnel squeezing assessment, Singh's approach (1992) and Goel's approach (1994) are used.

Singh's approach

Singh's approach (1992) this method of analysis is based on the rock mass classification approach. Singh et al. (1992) developed an empirical relationship from the log-log plot between the tunnel depth (H) and the logarithmic mean of the rock mass quality, Q Figure 3-1. Forty-one tunnel sections data were used to plot this figure. A clear line of demarcation can be seen on the figure, which is in between the elastic and squeezing condition. The equation of this line is given as:

$$H = 350 Q^{1/3} \qquad 2-13$$

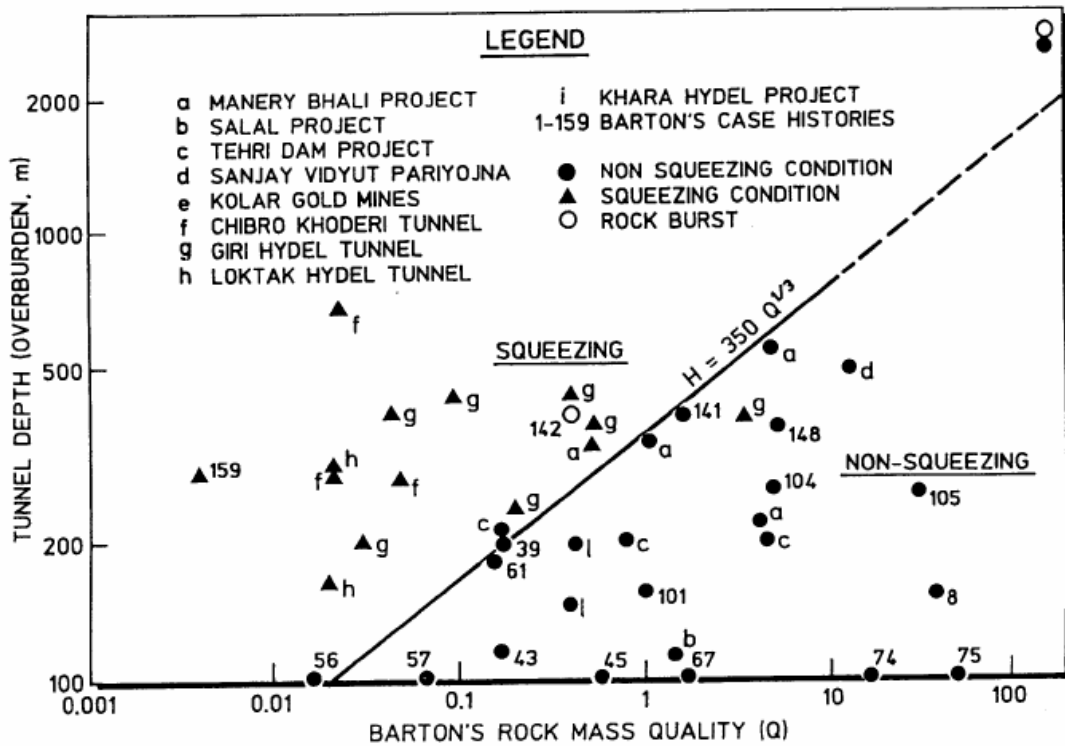


Figure 2-8: Criteria for predicting squeezing of ground (Singh & Goel, 2006)

If the value of overburden exceeds $350 Q^{1/3}$ then squeezing is likely to occur but if overburden is less than $350 Q^{1/3}$ then squeezing is not likely to occur. Alternatively, the point on the graph lying above the line represents squeezing condition and point lying below represents non-squeezing condition. The relation presented by Singh is very easy and simple to use.

Goel's Approach

Goel developed an empirical approach based on the rock mass number N (Goel, 1994). Rock mass number N is equal to Q -value with $SRF = 1$. ' N ' was used to avoid the problems and uncertainties in obtaining the correct rating of parameter SRF in Q method. Considering the overburden depth H , the tunnel span or diameter B , and the rock mass number N from 99 tunnel sections, Goel (1994) plotted the available data on log-log diagram (figure 8) between N and $HB^{0.1}$. Out of 99 tunnel section data, 39 data were taken from Barton's case histories and 60 from projects in India. Out of those 60 data 38 data were from five projects in Himalayan region. All the 27 squeezing tunnel sections were observed in those five projects in Himalayan region. Other 72 data sets were from

non-squeezing sections. As shown in the Figure 3-2 a line distinguishes the squeezing and non-squeezing cases.

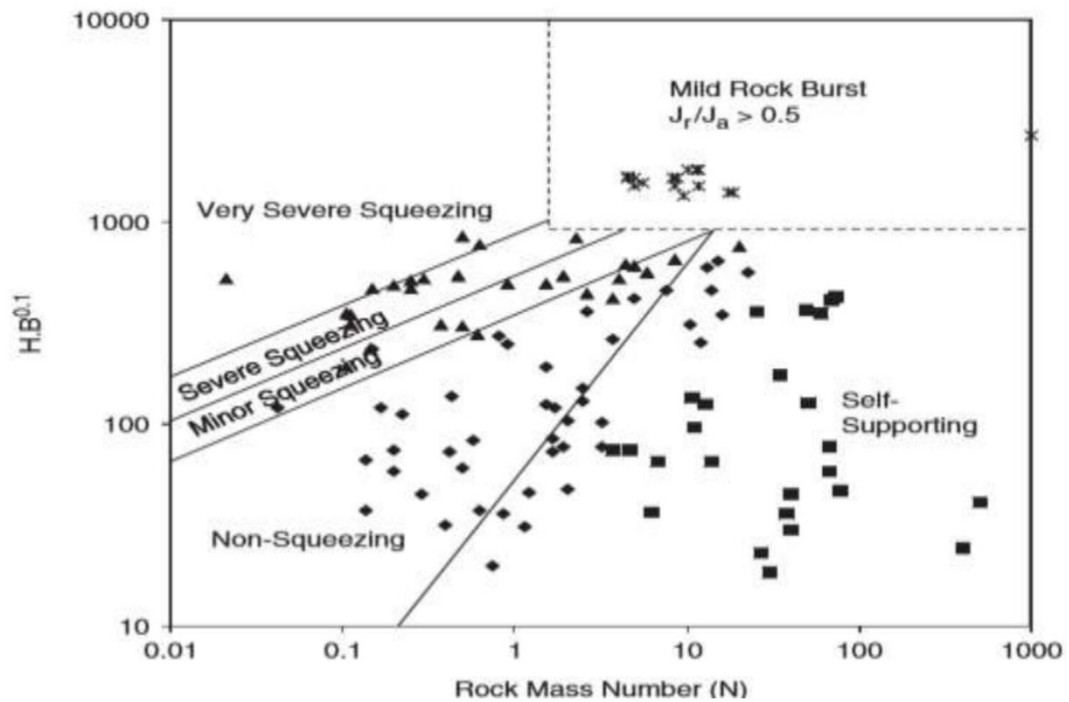


Figure 2-9: Criteria for squeezing (Goel, 1994)

The equation of the line is:

$$H > (275 N^{0.33}) B^{-0.1} \text{ meters} \quad 2-14$$

Where H = tunnel depth or overburden in meters and B = tunnel span or diameter in meter. The data point lying above the line AB Figure 2-9 represents squeezing condition whereas points lying below the line represent non-squeezing condition.

2.5.2 Semi-Empirical approach

Among various approaches Jethwa et al. approach (1984) and Hoek and Marinos (2000) approach has been discussed here:

Jethwa et al. approach (1984)

The degree of squeezing in this approach is described using coefficient N_c which is equal to the ratio of rock mass uniaxial compressive strength (UCS) to in-situ stress. Based on

this value, type of behavior of tunnel can be estimated. Jethwa et al. (1984) define the degree of squeezing based on following relation

$$N_c = \frac{\sigma_{cm}}{P_o} \quad 2-15$$

Where, σ_{cm} = rock mass uniaxial compressive strength, P_o = in-situ stress, γ = Unit weight of rock mass and H = tunnel depth below surface.

Table 2-2: Squeezing behavior (Jethwa, 1984)

Nc	Type of Behavior
<0.4	Highly squeezing
0.4-0.8	Moderately squeezing
0.8-2.0	Mildly squeezing
>2.0	Non squeezing

Hoek and Marinos approach

According to Hoek and Marinos, the ratio of uniaxial compressive strength (σ_{cm}) of the rock mass to the in-situ stress (p_o) can be used as the indicator of the potential tunnel squeezing problems (Hoek & Marinos, Predicting tunnel squeezing problems in weak heterogeneous rock masses, 2000), They used (Sakurai, 1983) approach to determine the relationship between σ_{cm}/p_o and the percentage strain of the tunnel. The result of study based on the closed form analytical solutions for the circular tunnel in a hydrostatic stress field presented by (Duncan Fama, 1993) and (Carranza-Torres & Fairhurst, 1999) is shown in the Figure 2-11. Hoek and Marinos (2000) used Monte Carlo simulations to determine the strain in the tunnels for a wide range of conditions. For this, they used 2000 iterations with assumed uniform distributions for the following ranges of parameters: In situ stress 2 to 20 MPa (80 to 800m depth), tunnel diameter 4 to 16 m, uniaxial strength of intact rock 1 to 30 MPa, Hoek and Brown constant m_i of 5 to 12, GSI of 10 to 35 and a dilation angle of 0 to 10. The simulation indicated that all tunnels follow a clearly

defined pattern, which is well predicted by means of the equation included in Figure 2-10.

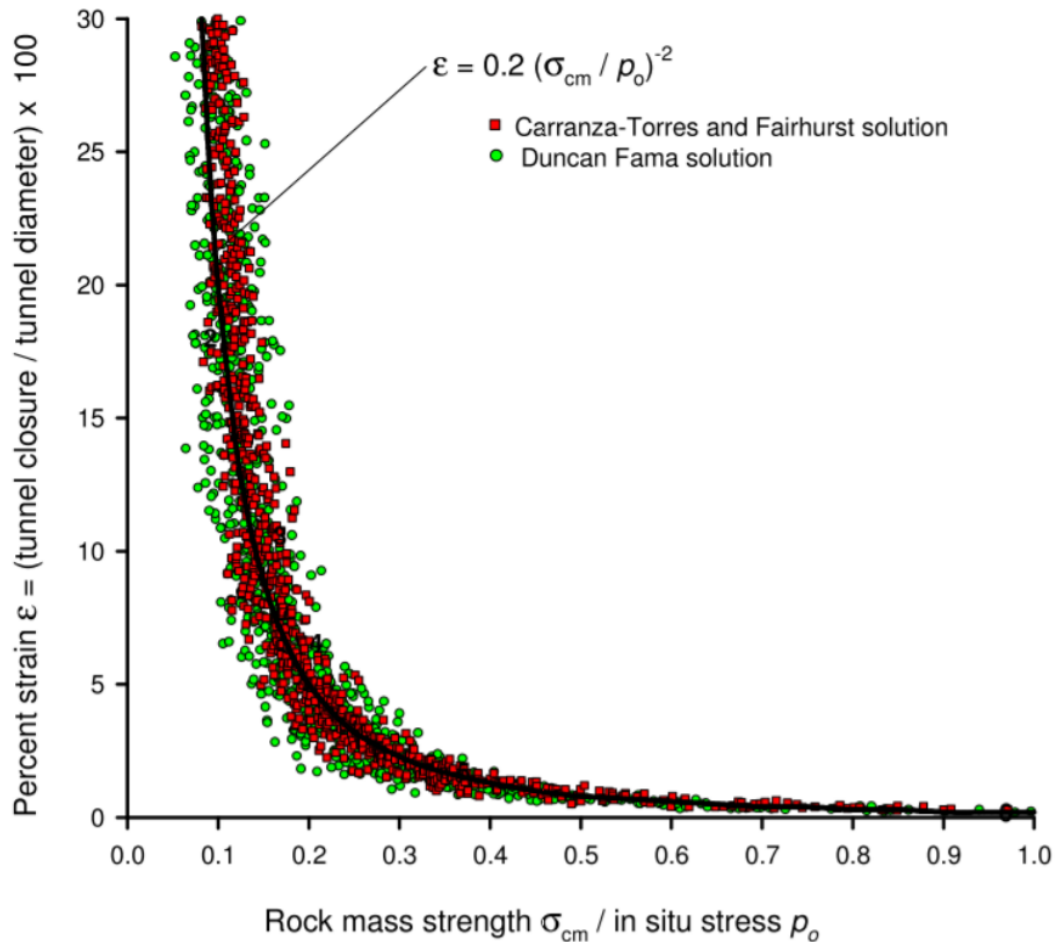


Figure 2-10: Plot of tunnel convergence against the ratio of rock mass strength to in situ stress in case of unsupported tunnel (Hoek & Marinos, Predicting tunnel squeezing problems in weak heterogeneous rock masses, 2000)

Hoek and Brown failure criteria proposed by (Hoek et al.) 2000, used for estimating strength and deformation characteristics of rock masses, assumes that the rock mass behaves isotropically. However, even if the rock mass is heavily fractured, continuity of the bedding surfaces will have been disrupted and the rock may behave as an isotropic mass. Thus, this criterion can be adapted to weak heterogeneous rock masses too.

The analysis presented above can be extended to cover tunnels in which an internal pressure is used to simulate the effects of support. Using a curve fitting process, Hoek

and Marinos (2000) proposed following equations to determine size of the plastic zone and deformation of a tunnel in squeezing ground.

$$\frac{d_p}{d_o} = \left(1.25 - 0.625 \frac{p_i}{p_o} \right) \frac{\sigma_{cm}}{p_o} \left(\frac{p_i}{p_o} \right)^{-0.57} \quad 2-16$$

$$\frac{\delta_i}{d_o} = \left(0.002 - 0.025 \frac{p_i}{p_o} \right) \frac{\sigma_{cm}}{p_o} \left(2.4 \frac{p_i}{p_o} - 2 \right) \quad 2-17$$

Where, d_p = Plastic zone diameter, d_o = Original tunnel diameter in meters, δ_i = Tunnel sidewall deformation, p_i = internal support pressure, p_o = In situ stress = depth x unit weight and σ_{cm} = Rock mass strength.

Hoek and Marinos (2000) also suggested the classifications of squeezing severity based on the strain percentage. There are five classes of squeezing problems from few support problems to extreme squeezing problems i.e.; from A to E. The ranges of these classes and their description are shown in Figure 2-11 and Table 2-2.

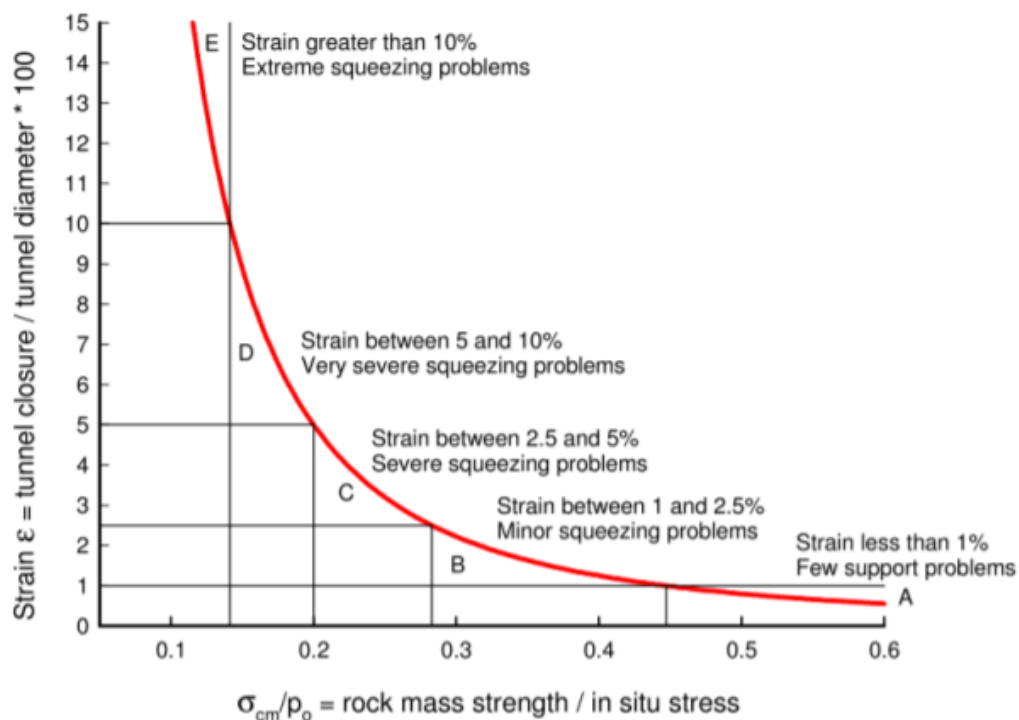


Figure 2-11: Approximate relationship and the degree of difficulty associated with tunneling through squeezing in rock in case of unsupported tunnel (Hoek & Marinos, Predicting tunnel squeezing problems in weak heterogeneous rock masses, 2000)

Table 2-3: Geotechnical issues associated with the squeezing severity classes and appropriate support types (Hoek & Marinos, Predicting tunnel squeezing problems in weak heterogeneous rock masses, 2000)

	Strain	Geotechnical Issues	Support types
A	Less than 1	Few stability problems and very simple tunnel support design methods can be used. Tunnel support recommendations based upon rock mass classification provide an adequate basis for design.	Very simple tunneling conditions, with rock bolts and shotcrete typically used for support.
B	1 to 2.5	Convergence confinement methods are used to predict the formation of a plastic zone in the rock mass surrounding a tunnel and of the interaction between the progressive development of this zone and different types of support.	Minor squeezing problems which are generally dealt with by rock bolts and shotcrete; sometimes with light steel sets or lattice girders are added for additional security.
C	2.5 to 5	Two-dimensional finite element analysis, incorporating support elements and excavation sequence, are normally used for this type of problem. Face stability is generally not a major problem.	Severe squeezing problems requiring rapid installation of support and careful control of construction quality. Heavy steel sets embedded in shotcrete are generally required
D	5 to 10	The design of the tunnel is dominated by face stability issues and, while two-dimensional finite analyses are generally carried out, some estimates of the effects of fore poling and face reinforcement are required.	Very severe squeezing and face stability problems. Fore poling and face reinforcement with steel sets embedded in shotcrete are usually necessary.
E	More than 10	Severe face instability as well as squeezing of the tunnel make this an extremely difficult three-dimensional problem for which no effective design methods are currently available. Most solutions are based on experience.	Extreme squeezing problems. Fore poling and face reinforcement are usually applied and yielding support may be required in extreme cases

Although this approach can give useful indication of potential squeezing and support requirements for tunnels in weak ground, the solutions cannot be considered adequate for the final design purpose. The basic assumptions of this method is that the analysis is based on a simple closed-form solution for a circular tunnel in a hydrostatic stress field and support is assumed to act uniformly on entire perimeter of tunnel. These conditions

are seldom met in the field, and tunnel shape and in situ stress conditions are seldom as simple as those assumed. Therefore, Hoek and Marinos (2000) recommended that, where there are significant potential squeezing problems, numerical analysis should be used in such cases.

2.6 Rock Burst

Rock Bursting is a common and serious form of disaster that can happen in deep underground excavation. When deep excavations are made, it passes through variable rock cover, this variation can induce instabilities like spalling, raveling, squeezing and rock bursting. In weak strata squeezing of rock can take place whereas in unjointed massive strata, rock bursting can occur where rock mass strength is less than induced stress. The estimation of rock squeezing, bursting and deformation modulus of rock mass before excavation is one of the most important parameters of the rock mass to subside the chances of rock bursting in the tunnel by applying safest and economical support. In this study, the prediction of rock burst is made using field stress parameters.

Hoek and Browns' and Grimstad and Barton's' approach has been used in this research for the assessment of rock bursting. Hoek and Brown have made detail studies for the stability analysis in different tunnels in south Africa. The ratio of uniaxial compressive strength (σ_c) and tangential stress (σ_θ) is compared in this study to assess the rock bursting condition (Hoek & Brown, Underground Excavation in rock, 1980). Grimstad and Barton made a relation by using stress measurements, the strength of the rocks and arrived at relationships which also support the findings of Hoek and Brown. They also described the bursting potential by using the ratio of compressive stress and tangential stress (σ_c/σ_θ) which is mentioned in the table below (Grimstad & Barton, 1993).

Hoek and Brown proposed a method to estimate the tangential stresses for roof ($\sigma_{\theta r}$) and walls ($\sigma_{\theta w}$) in massive rocks according to the excavation shapes.

$$\sigma_{\theta r} = (A \times k - 1)\sigma_z \quad 2-18$$

$$\sigma_{\theta w} = (B - k)\sigma_z \quad 2-19$$

where σ_θ is for tangential stress ($\sigma_{\theta r}$ for roof and $\sigma_{\theta w}$ for wall), k is the horizontal/vertical stress ratio, σ_z is the vertical stress and A , B are the excavation geometry factors.

Table 2-4: Criteria defined by different methods for prediction of Rock Burst

<i>Hoek and Brown</i>		<i>Grimstad and Barton</i>	
Ratio(σ_c/σ_θ)	Description	Ratio(σ_c/σ_θ)	Description
$\sigma_c/\sigma_\theta > 7$	Stable	$\sigma_c/\sigma_\theta > 100$	Low stress, near surface, open joints
$\sigma_c/\sigma_\theta = 3.5$	Minor sidewall spalling	$\sigma_c/\sigma_\theta = 3-100$	Medium stress, favorable stress conditions
$\sigma_c/\sigma_\theta = 2$	Severe spalling	$\sigma_c/\sigma_\theta = 2-3$	High stress, usually favorable to stability, maybe unfavorable to wall stability
$\sigma_c/\sigma_\theta = 1.7$	Heavy support required	$\sigma_c/\sigma_\theta = 1.5-2$	Moderate slabbing after one hour
$\sigma_c/\sigma_\theta < 1.4$	Severe rock burst problem	$\sigma_c/\sigma_\theta = 1-1.5$	Slabbing and rock burst after minutes in massive rocks
		$\sigma_c/\sigma_\theta < 1$	Heavy rock burst and immediate rock deformation

2.7 Empirical Method of support system design

The various methods to predict tunnel support and excavation requirement have either empirical, analytical character or finite element modeling approach. The empirical method is based on prototype observations, and the analytical methods are based on first principle. A feature that both empirical and analytical method share is the characterization of the rock mass. This is accomplished by describing the rock mass in terms of parameters which are either empirical characterization or theoretical property. The various physical parameters are determined in the empirical method. The empirically derived relationship between rock mass parameters and supports are then utilized to predict the support types and quantities and possibly the excavation procedure. Empirical method is generally applied during two circumstances when there might be limited geological information

but relatively unlimited time and during construction when there is ample geological information but time is critical.

2.7.1 Rock Mass Rating Method

The geomechanics classification or the rock mass rating (RMR) system was initially developed at the South African Council of Scientific and Industrial Research (CSIR) by Bieniawski (1973) on the basis of his experiences in shallow tunnels in sedimentary rocks (Kaiser, 1986). The following six parameters are determined for each of the structural unit:

- Uniaxial compressive strength of intact rock material,
- Rock quality designation RQD,
- Joint or discontinuity spacing
- Joint condition
- Ground water condition

Joint orientation in applying the classification system, the rock mass is divided into a number of structural regions and each region is classified separately. The boundaries of the structural region must coincide with a major structural feature such as a fault or with a change in rock type. In some cases, a significant change in discontinuity spacing or characteristics, within the same rock type, may necessitate the division of the rock mass into a number of small structural units.

2.7.2 Q-Value Method

Barton et al. (1974) of Norwegian Geotechnical Institute (NGI) originally proposed the Q-system of rock mass classification on the basis of about 200 case histories of tunnels and caverns.

$$Q = RQD J_n \times J_r J_a \times J_w \times SRF \quad (0.001 \leq Q \leq 1000) \quad 2-20$$

Where, RQD = Deere's Rock Quality Designation

J_n = Joint set number, J_r = Joint roughness number for critically oriented joint set, J_a = Joint alteration number for critically oriented joint set, J_w = Joint water reduction factor, SRF = Stress reduction factor to consider in situ stresses and J_v = Volumetric joint count.

The relation between Q and RMR system as proposed by Barton (1995) is:

$$\text{RMR} = 15 \times \log Q + 50 \quad 2-21$$

2.8 Analytical method of support system design

The Analytical solution is divided on the basis of in situ stress conditions. In low stress conditions, the support is designed to resist deformation induced by dead weight of loosened rock blocks or wedges locally. Limit equilibrium method is applicable to design the support for wedges or blocks or beams for local stability. On the other hand, in high stress condition, the deformation is induced by a redistribution of the stress field in the rock mass surrounding the excavation and the corresponding rock support is usually carried out in a systematic pattern. The development of the concept of interaction of load deformation characteristics of rock mass and support system, results in the convergence confinement method (CCM), which is often used in design of support based on idealized uniform stress field and circular opening. Similarly, in terms of Mohr-Coulomb criteria, tangential stress σ_{θ} acts as the major principal stress σ_1 and radial stress σ_r acts as the minor principal stress σ_3 . At the tunnel contour, σ_r is zero so σ_3 indicates the required tunnel support pressure p_i (Duncan, 1993). Thus, these two types of analytical solutions discussed in the following sections are for general tunnel stability analysis.

2.8.1 Assumptions of rock support interaction analysis

The Basic Assumptions considered (Hoek & Brown, Underground Excavation in rock, 1980) are:

- Tunnel geometry: The analysis assumes a circular tunnel of initial radius r_i . The length of the tunnel is such that the problem can be treated two-dimensional.
- In situ stress Field: The horizontal and vertical in situ stresses are assumed to be equal and to have a magnitude p_0 .
- Support pressure: The installed support is assumed to exert a uniform radial support pressure p_i in the Walls of the tunnel.
- Material properties of original rock mass: The original rock mass is assumed to be linear-elastic and to be characterized by a Young's modulus (E) and a Poisson's ratio (ν).

2.8.2 Convergence Confinement Method

This analysis method is based on the concept of a Ground reaction curve or Characteristic line, obtained from the analytical solution for a circular tunnel in an elasto-plastic rock mass under a hydrostatic stress field. The ground pressure acting on tunnel lining depends upon:

- Rock mass property
- Natural stress field
- Type and rigidity of the lining
- Time of installation of support

Fenner carried out the first major attempt to use elasto-plastic stress analysis for determining tunnel support pressure by using the Mohr-Coulomb yield criterion. He attempted to prove theoretically that any cylindrical opening can stand on its own without supports, provided that the plastic zone is allowed unhindered expansion. He demonstrated, through numerical examples, that the extent of plastic zone required to ensure tunnel stability without supports was several times larger than the tunnel radius and concluded that it was desirable to install flexible supports rather than remove large volume of crushed zone. Goel was the first to recognize that the failed rock mass has low cohesion and friction as compared to an intact rock mass (Goel, 1994). He concluded that supports were necessary for tunnel stability. He suggested further that radial displacements may continue even after the broken zone has stabilized.

The Convergence-Confinement method is based on the analytical solution for the elastoplastic response of a circular cylindrical opening in isotropic material when subjected to isotropic or hydrostatic in-situ stresses, and supported around the opening. CCM is the procedure that allows the load imposed on support installed behind the face of tunnel to be estimated. If the support is installed immediately in the vicinity of face, it does not carry out full load to which it is supposed to. The part of load is carried by face itself. As tunnel and face advance away from the support, face effect decreases and support must carry more loads. When the tunnel moves well away from face, the support will be subjected to full design load.

CCM has three basic components viz. the Longitudinal Displacement Profile (LDP), the Ground Reaction Curve (GRC) and the Support Characteristics Curve (SCC) (Carrazza-Torres & Fairhurst, 2000).

Longitudinal Displacement Profile (LDP)

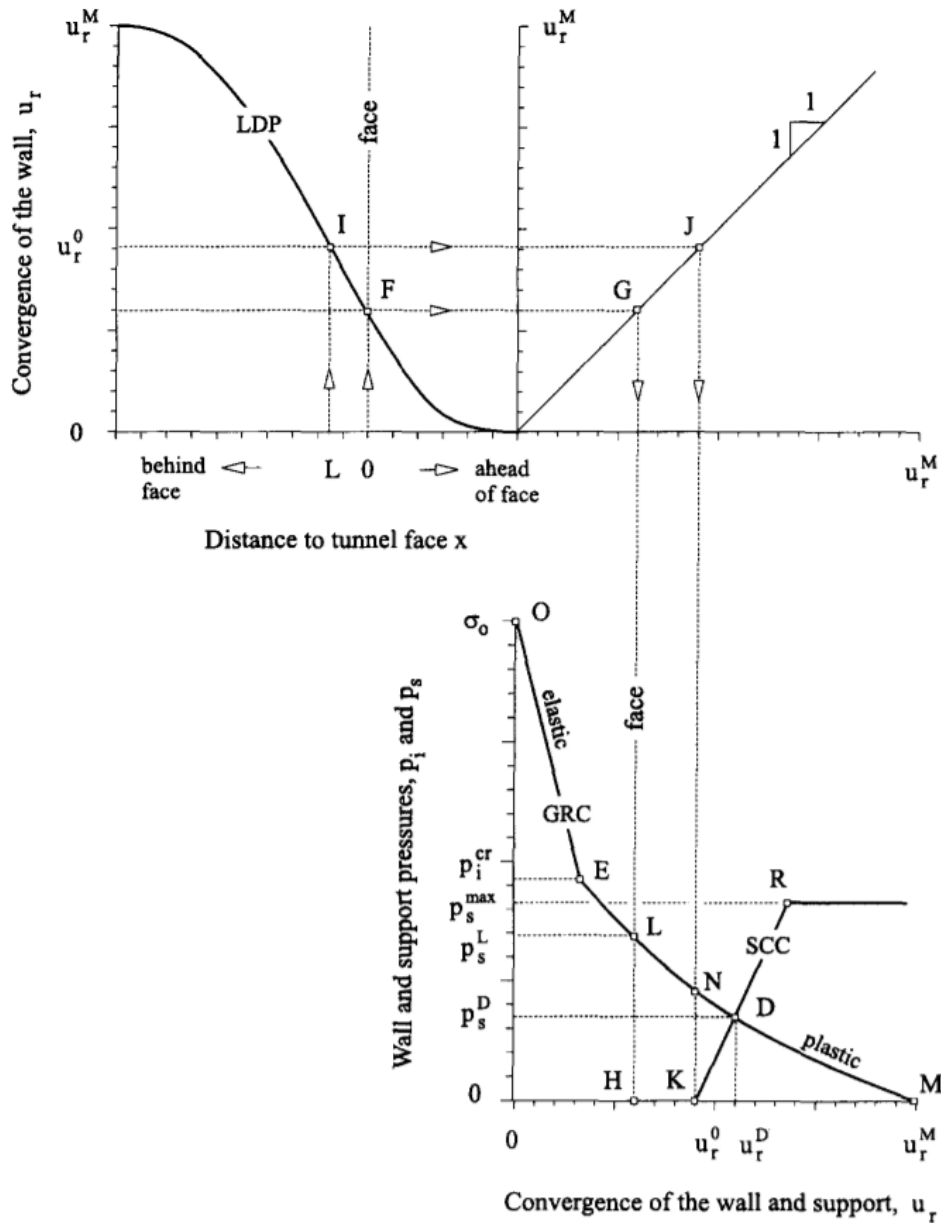


Figure 2-12: Schematic representation of Longitudinal Displacement Profile (LDP), Ground Reaction Curve (GRC) and Support Characteristic Curve (SCC) (Carrazza-Torres & Fairhurst, 2000)

LDP is the graphical representation of radial displacement that occurs along the axis of unsupported cylindrical excavation i.e. for the sections located ahead of and behind tunnel face. The upper diagram in Figure 2-10 represents the typical LDP. The diagram indicates that at some distance behind tunnel face the effect of face is small so that beyond this distance the tunnel has converged by final value i.e. u_r^M . At some distance ahead of face, the tunnel excavation has no effect on the rock mass and the radial displacement is zero. Hence, it provides insight into how quickly the support.

The construction of LDP is very important task in CCM. According to Vlachopoulos and Diederichs (2009), in order to facilitate to construct the LDP, Panet (1995) derived the following equation based on plastic analysis.

$$u^* = \frac{u_r}{u_{max}} = \frac{1}{4} + \frac{3}{4} \left(1 - \left(\frac{3}{3+4X^*} \right)^2 \right) \quad 2-22$$

Where, $X^* = X/R_t$, u_r is the radial displacement and u_{max} is the maximum short-term radial displacement from distance from face. This formula is only used for positive value of x .

Similarly, based on the measured value of the convergence in the vicinity of the face for the tunnel in Mingtam power canal project by Chern et. al (1998), an empirical best fit relationship to these actual measured data was proposed by (Vlachopoulos & Diederichs, 2009).

$$u^* = \frac{u_r}{u_{max}} = \left(1 + e^{\left(\frac{-X^*}{11} \right)} \right)^{-1.7} \quad 2-23$$

Both the relationship given above is responsible for plastic analysis provided that the radius of plastic zone does not exceed 2 tunnel radii. However, there is possibility of developing the plastic zone radius exceeding 2 tunnel radii. In order to account for the influence of increased overall yielding on the shape of the normalized LDP, the term normalized plastic zone radius, $R^* = R_p/R_T$ (where, R_p is plastic zone radius and R_T is the tunnel radius), is logical to use. Based on analysis using Phase² in plain strain cross section and axisymmetric models, Vlachopoulos and Diederichs (2009) proposed a new set of best fit relationships which are shown in the following equations.

$$u_o^* = \frac{u_o}{u_{max}} = \frac{1}{3} e^{-0.15R^*} \quad 2-24$$

For $X^* \leq 0$ (in rock mass):

$$u_o = \frac{u_o}{u_{max}} = u_o^* e^{X^*} \quad 2-25$$

For $X^* \geq 0$ (in rock mass):

$$u^* = \frac{u}{u_{max}} = 1 - (1 - u_o^*) e^{\frac{-3X^*}{2R^*}} \quad 2-26$$

The relationships in the equations 2-22, 2-23 and 2-24 can be used to correlate the displacement to position to construct LDP. For 2D analysis, u_{max} and R_p need to be calculated prior to the sequenced analysis. (Vlachopoulos & Diederichs, 2009).

Ground Reaction Curve (GRC)

GRC is a relationship between decreasing internal pressure P_i and increasing radial displacement of the tunnel wall u_r . The relationship depends upon mechanical properties of rock mass and can be obtained from the elasto-plastic solution of rock deformation around an excavation (Carranza-Torres & Fairhurst, 2000). The curve OEM in Figure 2-10 is the typical diagram of GRC.

According to Carranza-Torres and Fairhurst (2000), the uniform internal pressure P_i and far field stress σ_o can be scaled to give the scaled internal pressure P_i and scaled far field stress S_o respectively. Assuming that the rock mass satisfies Hoek-Brown failure criteria, P_i will be

$$P_i = \frac{p_i}{m_b \sigma_{ci}} + \frac{s}{m_b^2} \quad 2-27$$

$$S_o = \frac{\sigma_o}{m_b \sigma_{ci}} + \frac{s}{m_b^2} \quad 2-28$$

The pressure p_{cr}^i defined by the point E in the GRC of the Figure 2-10, marks the transition from elastic to plastic behavior of the rock mass i.e for an internal pressure $p_i \geq p_{cr}^i$, a plastic region of radius R_{pl} develops around a tunnel. The scaled critical pressure P_{cr}^i for which the elastic limit is achieved is given by the following expression:

$$P_{cr}^i = \frac{1}{16} [1 - \sqrt{1 + 16S_o}] \quad 2-29$$

The actual critical pressure is found from inverse of the equation

$$p_{cr}^i = [P_{cr}^i - \frac{s}{m_b^2}] m_b \sigma_{ci} \quad 2-30$$

In case of $p_i \geq p_i^{cr}$, the relationship between radial displacement u_r^{el} and internal pressure p_i elastic part of GRC is given by:

$$u_r^{el} = \frac{\sigma_o - p_i}{2G_{rm}} \quad 2-31$$

For the values of internal pressure $p_i \leq p_i^{cr}$, the extend of the plastic region R_{pl} that develops around the tunnel is :

$$R_{pl} = R \exp \left[2 \left(\sqrt{P_{cr}^i} - \sqrt{P_i} \right) \right] \quad 2-32$$

Where R is the radius of tunnel.

Hoek and Brown (1997) suggest that in some cases the assumption of no plastic volume-change for the rock mass may be more appropriate. For the case of non-dilating rock masses is:

$$\frac{u_{pl}^r}{R} = \frac{2G_{rm}}{\sigma_o - p_i^{cr}} = \left[\frac{1-2\nu}{2} - \frac{\sqrt{P_i^{cr}}}{S_o - P_i^{cr}} + 1 \right] \left(\frac{R_{pl}}{R} \right)^2 + \frac{1-2\nu}{4(S_o - P_i^{cr})} - \frac{1-2\nu}{2} \frac{\sqrt{P_i^{cr}}}{S_o - P_i^{cr}} \left[2 \ln \left(\frac{R_{pl}}{R} \right) + 1 \right] \quad 2-33$$

Support Characteristics Curve (SCC)

Support characteristic Curve is the plot between increasing pressure P_s on the support and increasing radial displacement u_r of the support (Figure 2-10). If the elastic stiffness of the support is denoted by K_s , the elastic part of the SCC - i.e., segment KR in Figure 2-10 can be computed from the expression:

$$P_s = K_s u_r \quad 2-$$

The plastic part of the SCC i.e. horizontal segment starting at point R in Figure 5-1, is defined by the maximum pressure p_s^{\max} that support can accept before collapse. For different support system such as; concrete or shotcrete linings, ungrouted bolts and cables, steel ribs, lattice girders etc., the main task is to find the maximum pressure and elastic stiffness for the construction of SCC.

a. Available support for Concrete or Shotcrete Linings

Influence of light reinforcement is considered to have little effect on the stiffness of the lining. If heavy reinforcement is used the available support be evaluated taking into consideration the effect of reinforcement. The maximum support pressure developed by concrete or shotcrete lining can be calculated from the following relationship which is based on the theory of hollow cylinders.

The maximum support pressure developed by concrete or shotcrete lining can be calculated from the following relationship which is based on the theory of hollow cylinders.

$$p_s^{\max} = \frac{\sigma_{cc}}{2} \left[1 - \frac{(R-t_c)^2}{R^2} \right] \tag{2-35}$$

The stiffness constant K_s is as follows:

$$K_s = \frac{E_c}{(1-\nu_c)R} \frac{R^2 - (R-t_c)^2}{(1-2\nu_c)R^2 + (R-t_c)^2} \tag{2-36}$$

Where, E_c is elastic modulus of concrete

ν_c is Poisson's ratio

R is external radius of tunnel (m)

t_c is thickness of the concrete or shotcrete

σ_{cc} is unconfined compressive strength of the shotcrete or concrete

b. Available support for ungrouted bolts and cables

The maximum pressure provided by the support system, assuming that the bolts are equally space in the circumferential direction, is given by:

$$p_s^{\max} = \frac{T_{bf}}{s_c s_l} \tag{2-37}$$

And the stiffness is given by:

$$\frac{1}{K_s} = S_c S_l \left[\frac{4l}{\pi d_b E_s} + Q \right] \quad 2-38$$

Where,

d_b is the bolt or cable diameter (m)

l is the free length of bolt or cable (m)

T_{bf} is the ultimate load obtained from a pullout test (MN)

Q is a deformation load constant for the anchor and head (m/MN)

E_s is Young's modulus of bolt or cable (MPa)

S_c is the circumferential bolt spacing (m)

S_l is the longitudinal bolt spacing (m)

c. Available support for steel set support

The maximum support pressure of the set is:

$$p_s^{\max} = \frac{A_s \sigma_{ys}}{S_l R} \quad 2-39$$

And the stiffness is:

$$K = \frac{E}{S_l R^2} \quad 2-40$$

Where,

σ_{ys} is yield strength of steel (MPa)

E_s is the Young 's modulus of the steel (MPa)

A_s is the cross-sectional area of the section (m)

S_l is the set spacing along the tunnel axis(m)

R is the radius of the tunnel (m)

d. Combined effect of support system

In this case, the stiffness of the combined system is determined as the sum of the stiffness of the individual components.

$$K = K_1 + K_2 \quad 2-41$$

Where K_1 = stiffness of the first system and K_2 = stiffness of the individual components.

2.9 Numerical modelling

In geotechnical engineering practices, design and analysis of any problem is done by any of the three types of modeling procedures: Physical/Empirical Modeling, Mathematical/Analytical Modeling and Numerical Modeling.

Physical modeling incorporates laboratory and in situ model tests gives some information to Engineers to achieve some empirical solution of problem. But these are costlier and time consuming.

Mathematical modeling uses differential or algebraic equation which cannot solve most of the engineering problems analytically. It is because of the complexity in geometry, non-homogeneity of material and non-linear constitutive behavior of the medium.

Numerical models are mathematical models that use some sort of numerical time-stepping procedure to obtain the models behavior over time. Numerical models in combination with mathematical models, calibrating and validating against pre-existing data and analytical results, iterative calculation of the results in step with error analysis is done until the required numerical results are obtained. The generated table and/or graph represent the mathematical solution.

Numerical methods are techniques to approximate the governing equations in the mathematical models.

Numerical methods available for problem solving in geotechnical engineering are Finite Element Method (FEM), Spectral Element Method (SEM), Finite Difference Method (FDM), Finite Volume Method (FVM), Discrete Element Method (DEM).

2.9.1 Finite Element Modeling and Modeling Issues

These Finite Element Method (FEM) is a technique which approximates the solution of governing differential equations in the mathematical model by dividing the domain into

meshes or grids and applying simpler equations to individual elements or nodes in the mesh to approximate the solution by minimizing the associated error function (Ismail-Zadeh & Tackley, 2010) (Atkinson, 2007) (Abel & Desai, 1987)

Finite element is the most widely employed numerical method for rock mechanics and rock engineering. It does not require detailed programming experience to make efficient use of the finite element approach to problem solving in rock mechanics. However, familiarity with the fundamentals of the technique and with practical guidelines for generating reliable results is essential not only for the preparation of the program input, but also for recognition of faulty output.

FEM analysis constitutes three steps mainly, domain discretization, local approximation and assemblage and solution of global matrix equation. This method involves the representation of continuum as an assembly of elements which are connected at discrete points called nodes. The problem domain is divided into discrete elements of various shapes, e.g. triangles and quadrilaterals in two-dimension cases and tetrahedrons and bricks in three dimensions. All forces are assumed to be transmitted through the body by the forces that are set up at the nodes. Expressions for these nodal forces, which are essentially equivalent to forces acting between elements, are required to be established. Continuum problem is analyzed in terms of sets of nodal forces and displacements for the problem domain.

The displacement components within the finite elements are expressed in terms of nodal displacements. Derivation of these displacements describes strain in the element. The stiffness of the medium to this induced strain determines stress in the element. Total stress within an element can be found out by superimposition of initial and induced stresses. The matrix of each element describes the response characteristics of the elements. These coefficient matrices are of total potential energy. The elemental based on minimization stiffness matrices are assembled to give the global stiffness matrix which is related to global force and displacement. As the number of elements in a problem domain tends to infinity, this is equivalent to solving differential equation.

It is only rarely that analytical solutions can be found to rock mechanics problems of practical concern. This may be due to the problem in describing the boundary conditions

by simple mathematical functions, heterogeneity of the problem domain, non-linear nature of the governing partial differential equations, or the constitutive relation for the rock mass are non-linear or otherwise insufficiently simple mathematically (E. T. Brown, 1987). In all these cases, approximate solutions may be found by using computer-based numerical methods.

These days, due to the economy and increase in computational technology, numerical methods are used for rock-support interaction analysis. There are three categories of software widely used for geotechnical purposes:

- Large multifunctional general-purpose packages. In the main, such software is designed for supercomputers and is supplied as part of the systems support to the latter.
- There are also versions for personal computers. The packages provide a high level of service and graphics but have a very high price. They are somewhat cumbersome to use and do not have all the facilities specifically required for geotechnical jobs. Familiar examples are the ANSYS software, and other clones from the American SAP package (finite element method)
- Geotechnical dedicated software written at university centers. This provides a high-level scientific approach with moderate service and graphics and moderate prices. Of the best-known examples in this category are PHASES, PLAXIS and FLACs. Phase has been used in this research for two-dimensional modeling.
- GTS-NX is a multi-functional Numerical analysis software with user-friendly tools and user interface, which has been used in this research for three-dimensional modeling.

2.9.2 Three-Dimensional Modeling

Like any numerical modeling, three-dimensional modeling requires a control volume in which analysis is to be made. But in case of 3D-modeling a control volume with all three dimensions has to be selected. Keeping in mind the solution of a circular hole on a metal plate given by Kirsch, it is known that in case of elastic bodies the stress due to excavation dies out at a distance of 3-5 from the center of excavation (Kirsch, 1898). But the rock masses in which the tunnel under consideration is being excavated shows elasto-plastic nature so, plastic zone has to be considered. Hence, geometric model with control volume

of dimensions ten to twenty times that of tunnel diameter is created for analysis in this research work.

2.9.3 Software used in this research

Phase²

The Phase² is a 2-dimensional windows-based program and is very popular for the analysis of underground/surface excavation in rock mass or soil. The program code is used for a wide range of geotechnical engineering projects including complex tunneling problems in weak rock, stress analysis, tunnel design, slope stability, support design and ground water seepage analysis etc. Complex multistage models can be created and analyzed quickly. This program is user friendly, easy to operate and easy to understand. Some of the basic features of the program are:

- Elasto-plastic analysis
- Constant or gravity field stress
- Staged model
- Plain strain or Axisymmetric analysis
- Support analysis (Bolts, concrete or shotcrete liners, steel sets etc.)
- Multiple material
- Load splitting
- Core replacement technique
- Slope stability analysis
- Ground water seepage analysis

There are three basic components of the program i.e. model, compute and interpret. Model is the pre-processing module used for entering and editing the model boundaries, support, in-situ stresses, boundary conditions, material properties and creating finite element mesh. Model, compute and interpret will run as standalone programs.

In Phase², field stress can be constant or gravity stress. The gravity field stress option is used to define a gravity stress field which varies linearly with depth from a user-specified ground surface elevation. Gravity field stress is typically used for surface or near surface at shallow depth elevations and the areas where the effect of topography stress magnitudes and directions. Stress ratio is calculated with the help of Poisson's ratio. In

addition, the material parameters such as unconfined compressive strength of intact rock (σ_{ci}), Hoek-Brown constant (m_i), Geological Strength Index (GSI), Young's Modulus of Intact Rock (E_i), Poisson's ratio (ν), density of rock mass are the inputs to the material property.

GTS NX

GTS NX incorporates a hybrid mesh generation function that creates mesh set that use an optimal combination of hexahedron and tetrahedral elements. The main advantage of using hexahedron elements is that they generate comparatively more accurate stress results than tetrahedral elements; and the advantage of using tetrahedral elements is that they are more effective for modeling sharper curves and corners of complex geometry. GTS NX is capable of utilizing both tetrahedral and hexahedron elements without any significant loss in modeling or analysis speed.

The use of multiple geotechnical programs creates the need to learn the unique interface of each program. Even more inefficiencies arise when there is a need to perform various analyses for the same project. For example, dam and levee projects often require seepage, settlement, slope stability, and seismic analyses to be calculated. The same also applies to foundation and retaining wall projects that require soil structure interaction as well as stress deformation analyses to be performed. Most geotechnical programs can only perform one analysis type, which creates the need to tediously create the same project model for several programs. With GTS NX we no longer need to rely on several different geotechnical programs to perform various analyses. Instead we can be able to use GTS NX to perform any type of geotechnical analysis application.

In case of tunneling, construction stage has to be considered. When performing construction stage analysis, it is often necessary to create multiple models to compare the effects of a variation of design considerations. This process is made particularly cumbersome by the need to open a separate model file for each analysis case. GTS NX overcomes this limitation by its unique ability to have multiple construction stage analysis cases modeled in a single file. This feature makes it possible to directly compare the results of various construction stage analysis cases and determine the optimal design for the project.

GTS NX can perform complex tunnel analysis in either 2D or 3D. Linear static analysis, seepage, soil structure interaction, SRM slope stability analysis and a wide range of dynamic analysis applications can be done as well. Moreover, the efficiency will be greatly increased by the ability to run multiple analysis types on a single model file. In this research, GTS NX has been used for 3D numerical modeling of the tunnel excavation and A common inefficiency of using finite element analysis software is having to painstakingly sort through extensive amounts of output data to extract the desired results.

In most cases, creating the report can take just as long as the design and analysis process. To overcome this inefficiency, GTS NX features a state-of-the-art edge post-processing engine that makes it possible to quickly sort through extensive finite element analysis outputs and create beautifully detailed and high-quality reports. The post-processor renders richly colored 3D contour plots that provide detailed visual representations of the results. The post-processor also includes fully customizable filters so that we can easily extract our desired results based on construction stages, time history analysis, coordinates, and various other criteria. All results are neatly and clearly organized in both graph and spreadsheet formats. The result data can then be organized in a PDF file through an advanced report generator that enables us to directly create our report through the post-processing window. With the report generation functions, we will be able to create high quality reports with unprecedented levels of convenience quality and efficiency, thus freeing up more time for us to devote to other high priority tasks.

2.10 Rock Support Interaction

The principal objective in the design of underground excavation support is to help the rock mass to support itself. For this purpose, we must have a clear idea about the rock support interaction mechanism.

This is based on the concept of a Ground reaction curve or Characteristic line, obtained from the analytical solution for a circular tunnel in an elasto-plastic rock mass under a hydrostatic stress field. The ground pressure acting on tunnel lining depends upon

- Rock mass property
- Natural stress field
- Type and rigidity of the lining

- Time of installation of support

Fenner carried out the first major attempt to use elasto-plastic stress analysis for determining tunnel support pressure by using the Mohr-Coulomb yield criterion. He attempted to prove theoretically that any cylindrical opening can stand on its own without supports, provided that the plastic zone is allowed unhindered expansion (Goel, 1994) . He demonstrated, through numerical examples, that the extent of plastic zone required to ensure tunnel stability without supports was several times larger than the tunnel radius and concluded that it was desirable to install flexible supports rather than remove large volume of crushed zone. Goel was the first to recognize that the failed rock mass has low cohesion and friction as compared to an intact rock mass (Goel, 1994). He concluded that supports were necessary for tunnel stability. He suggested further that radial displacements may continue even after the broken zone has stabilized.

2.10.1 Assumptions of Rock Support Interaction Analysis

The Basic Assumptions considered (Hoek & Brown, Underground Excavation in rock, 1980) are:

- Tunnel geometry: The analysis assumes a circular tunnel of initial radius r_i . The length of the tunnel is such that the problem can be treated two-dimensional.
- In situ stress Field: The horizontal and vertical in situ stresses are assumed to be equal and to have a magnitude p_o .
- Support pressure: The installed support is assumed to exert a uniform radial support pressure p_i in the Walls of the tunnel.
- Material properties of original rock mass: The original rock mass is assumed to be linear-elastic and to be characterized by a Young's modulus (E) and a Poisson's ratio (ν).

2.10.2 Steps wise procedure for the mechanism of Rock Support Interaction

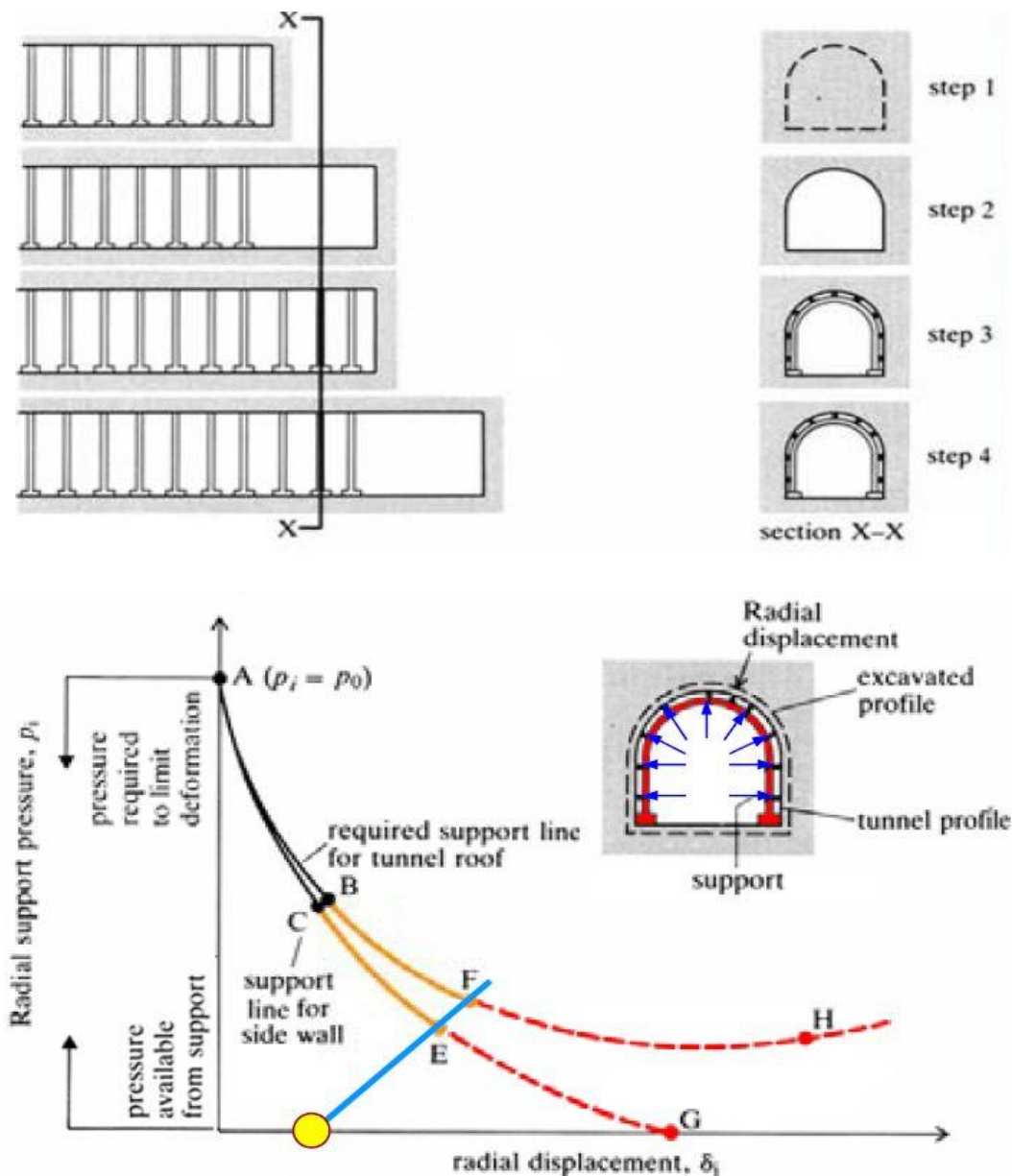


Figure 2-13 : Characteristics Curve of Rock Support Interaction (Hoek & Brown, Underground Excavation in rock, 1980)

Step 1: The heading has not reached section X-X and the rock mass on the periphery of the future tunnel profile is in equilibrium with the internal pressure P_i acting equal and opposite to hydrostatic pressure.

Step 2: The face has advanced beyond section X-X and the support pressure (P_i) provided by the rock inside the tunnel has been reduced to zero. Given that the blasted rock must

be mucked out before the steel sets can be installed, deformation of the excavation boundary occurs.

Step 3 : The heading has been mucked out and steel sets is installed close to the face. At this stage the sets carry no load, but from this point on any deformation of the tunnel roof or walls will result in loading of steel sets

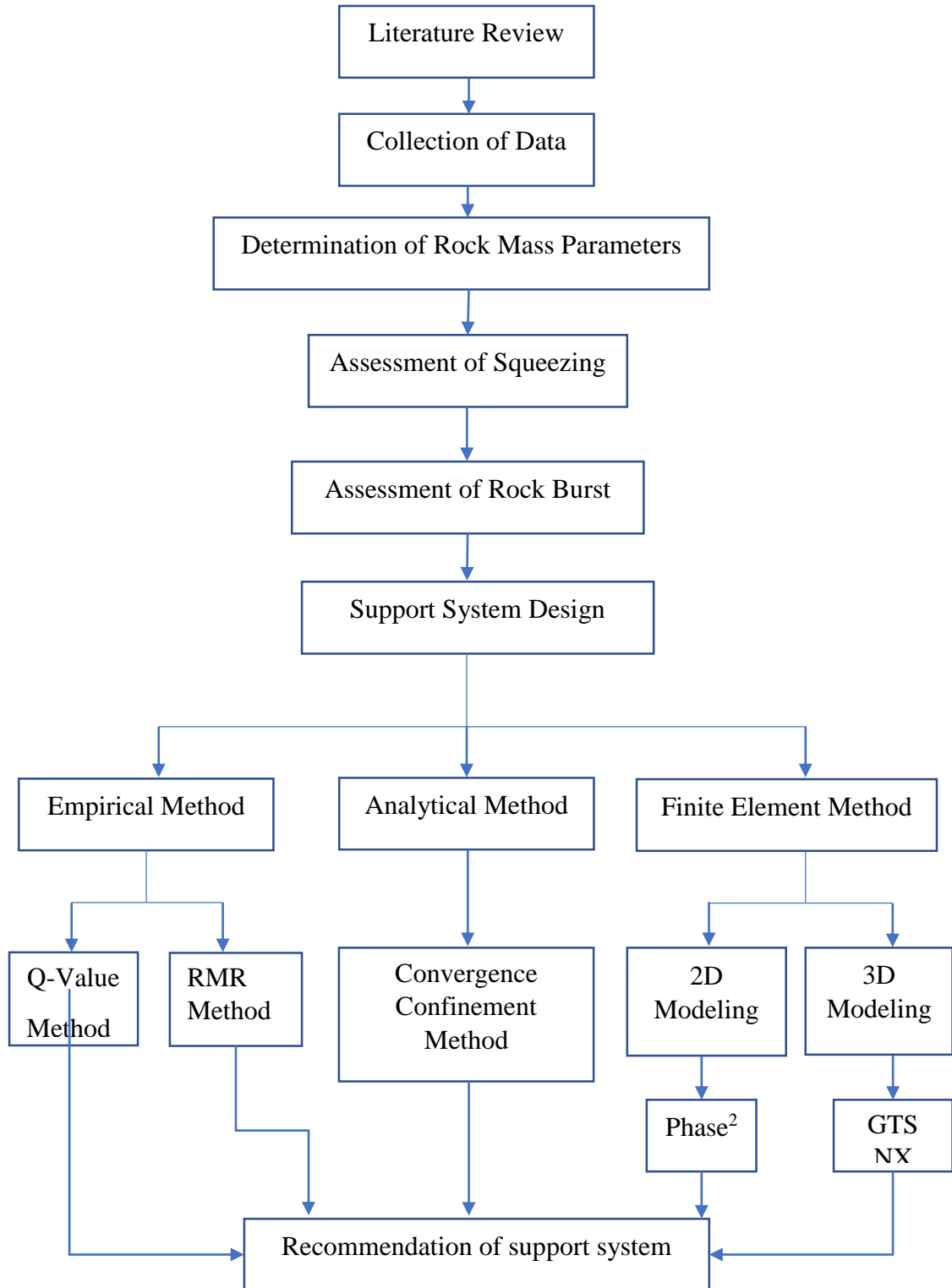
Step 4 : The Heading is advanced one and a half tunnel diameter beyond section X-X by another blast. The restraint offered by the proximity of the face is now negligible and the further convergence of the tunnel boundaries occurs.

Step 5 : If the Steel sets have not been installed the radial displacement at section X-X would continue increasing along the dashed lines EG and FH. In this case, the side walls would reach equilibrium at point G. However, the roof would continue deforming until it failed. But with the steel installed the tunnel convergence will begin to load the Support.

The rock support interaction mechanism deals with the elasto-plastic response of a circular cylindrical opening in isotropic material when subjected to isotropic or hydrostatic in- situ stresses, and supported around the opening. CCM is the procedure that allows the load imposed on support installed behind the face of tunnel to be estimated. If the support is installed immediately in the vicinity of face, it does not carry out full load to which it is supposed to. The part of load is carried by face itself. As tunnel and face advance away from the support, face effect decreases and support must carry more loads. When the tunnel moves well away from face, the support will be subjected to full design load.

3 METHODOLOGY

3.1 General Flowchart



3.2 Preliminary Study

Preliminary study consists of studying literatures, publications, research papers, journals, articles with similar scope and field of studies. Tutorials from the Internet were used to practice the software involved. Manuals that came along with the software were also used for reference.

3.3 Data Collection

General data like acceleration due to gravity, water pressure, weight, Poisson's ratio, etc. were taken from respective literatures. The specific data of the tunnel, viz. dimensions, length, cross section shape, Rock mass parameters, Overburden, longitudinal profile, disturbance factor, earth pressure coefficients, etc. were obtained from project report of the Upper Balephi 'A' Hydropower project.

3.4 Determination of rock mass parameters

The modulus of deformation of rock mass (E_m) may be defined as the ratio of stress to corresponding strain during loading of rock mass, including elastic and inelastic behavior whereas the modulus of elasticity of intact rock (E_i) is the ratio of applied stress and corresponding strain within the elasticity limit. The jointed rock mass does not behave elastically. Hence, the term modulus of deformation is used instead of modulus of elasticity. The deformation modulus of jointed rock mass is very low compared to the elasticity modulus of intact rock.

Rock mass deformation modulus was determined using the relationships below:

$$\text{Sarafim and Perera (2002)} \quad E_m = 10 \left(\frac{\text{RMR}-10}{40} \right) \quad 3-1$$

$$\text{Hoek et. al (2002)} \quad E_m = \left(1 - \frac{D}{2} \right) \sqrt{\frac{\sigma_{ci}}{100}} 10 \left(\frac{\text{GSI}-10}{40} \right) \quad 3-2$$

$$\text{Barton (2002)} \quad E_m = 10 \times \left(\frac{Q \times \sigma_{ci}}{100} \right)^{1/3} \quad 3-3$$

$$\text{Panthi (2006)} \quad E_m = \frac{1}{60} \times E_{ci} \times \sigma_{ci} \quad 3-4$$

$$\text{Hoek and Diederichs (2006)} \quad E_m = E_{ci} \times \left(0.02 + \frac{1-D/2}{1+e^{((60+15D-GSI)/11)}} \right) \quad 3-5$$

3.5 Assessment of Potential Squeezing

At selected regions on the longitudinal alignment of the tunnel, the input rock mass properties like RMR, Q-value, SRF, N-value and strain (ϵ) are determined and calculations are done to obtain the output of the equations suggested by Empirical and Semi-Empirical methods as stated in section 2.5.

3.6 Assessment of Potential Rock Burst

At selected regions on the longitudinal alignment of the tunnel, the input rock mass properties like σ_v , σ_θ , k are determined and calculations are done to obtain the output of the equations suggested by the methods as explained in section 2.6.

3.7 Support System Design

Five random chainages on the longitudinal section of the tunnel are so chosen that they comprise of all kinds of rock types with varying strength and overburden pressure. For those chainages, the support system is designed based on Empirical, Analytical and Numerical Modelling approaches. The most demanding support system suggested is selected among the empirical and analytical method and tested against numerical modeling. If the support gives a satisfactory factor of safety greater than two, then it is selected. The figure below just gives a general idea of the sections under consideration. The detailed L-section of the tunnel is attached in Annex D.

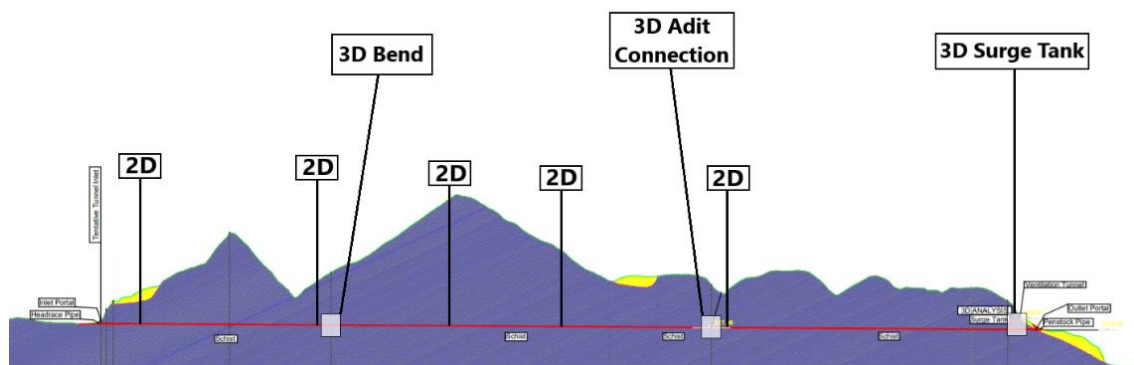


Figure 3-1: L-section of headrace tunnel showing 2D and 3D numerical modeling sections

3D Numerical Modelling

Three regions in the longitudinal alignment of tunnel has been selected for three-dimensional analysis and support system design. They are:

- The region where the adit meets the tunnel
- Underground Surge Shaft
- A bend in the tunnel

The displacement induced in and around the zone and the safety factor for the shotcrete lining and rock bolts is presented in the result.

3.7.1 Empirical Method (RMR and Q-value)

Among the various empirical methods for the design of a tunnel, Q and RMR system were used for the design purpose. For RMR value, guidelines are given in Annex C, Table 9-1.

Similarly, tunneling index Q is used to determine support system. For using Q-value to design support system, it was necessary to determine Excavation Support Ratio (ESR) and equivalent diameter (D_e). ESR is the value used to express factor of safety of underground excavation. The value of ESR for different condition of excavation is given in Annex C, Table 9-3. Whereas, equivalent diameter can be calculated by dividing excavation span, diameter or height by ESR. The equivalent diameter (D_e) is given by:

$$\text{Equivalent Dimension } (D_e) = \frac{\text{Excavation span, diameter or height(m)}}{\text{Excavation Support Ratio, ESR}}$$

The length L of rock bolts can be estimated from the excavation width B and Excavation support ratio ESR:

$$L = 2 + \frac{0.1 B}{\text{ESR}} \quad 3-6$$

The maximum unsupported span can be estimated from:

$$\text{Maximum span (unsupported)} = 2 \text{ ESR } Q^{0.4} \quad 3-7$$

3.7.2 Analytical Method

The analytical method has been used in rock support interaction analysis developed by (Hoek & Brown, 1980). The ground reaction curve and support reaction curve are determined using (Carrazza-Torres & Fairhurst, 2000). Support was designed to limit radial deformation inside the tunnel within permissible limit. GRC and SCC had been used to design support. A unique Factor of safety is calculated in a deterministic analysis. A factor of safety greater than 1 is calculated as shown in Figure 11 below. In this case factor of safety is simply ratio of the maximum support pressure P_{sm} to the equilibrium pressure P_{eq} (the pressure at the intersection point of the ground reaction curve and support reaction curve).

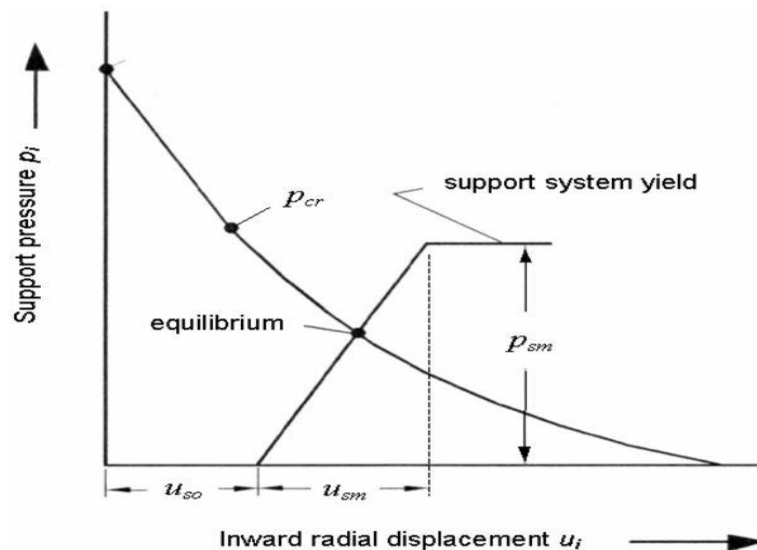


Figure 3-2: Response of support system to tunnel wall displacement, resulting in establishment of equilibrium (Hoek, Kaiser, & Bawden, Support of underground excavation in hard rock, 1995)

3.7.3 Two-Dimensional Numerical Modelling

Phase² has been used in this research for two-dimensional numerical modeling. There are two method of modeling under Phase² i.e. Core Replacement Method and Load Factor Method. Stress, deformation and stability of tunnel was determined using Phase². The tunnel alignment was divided into five sections on the basis of change of rock type pattern and overburden. Field stress can be entered as gravity or constant value in the software. In this study, field stress is in the form of gravitational stress and calculated as product of

unit weight of rock mass and overburden depth for σ_1 and σ_1 times active pressure coefficient of rock mass to estimate σ_3 . The head race tunnel of Upper Balephi 'A' Hydropower Project was designed using load factor method. Load factor method was used for analysis so internal pressure was applied in the model. Internal pressure is applied normal to the boundary and varies with stage with maximum value equal to in-situ stress and minimum value equals to zero. Maximum iteration is kept 500 with tolerance level of 0.01 which is expected to give significantly reliable results. Analysis of failure was performed using Generalized Hoek-Brown criterion.

The finite element analysis is carried out in three stages using Phase². The first stage is a consolidation stage in which the model, with no excavation present, is allowed to deform while being loaded by the in-situ stress field. In the second stage, after excavation of the tunnel of radius (R_i) of 2m, a uniform support pressure is applied to the tunnel boundary to control the closure of the tunnel. In the third step the internal pressure is removed a support is proposed. The following three steps is performed for the analysis of underground excavation:

- a. The amount of tunnel wall deformation prior to support installation is determined. In this study, this deformation is determined by using empirical relationship proposed by Vlachopoulos and Diederichs (2009).

In this method, a model of tunnel is built to determine the deformation far from the tunnel face using a simple plane strain analysis and to determine radius of plastic zone.

- b. The internal pressure that yields the amount of tunnel wall deformation at the point of and prior to support installation is determined.

A uniform distributed load to the tunnel is added such that the magnitude and direction of the load will be equal and opposite to the in-situ stressed. There will be no deformation since the pressure is equal and opposite to the in-situ stress. Afterward, with suitable factor, the magnitude of the pressure is gradually reduced such that tunnel deformation will increase as the pressure is lowered to zero. Ten stages are considered in this analysis and the factor for each stage are diminished by 50% such that each stage has 1, 0.5, 0.25, 0.125, 0.0625, 0.0313, 0.0156, 0.0078 and 0.0039 which will decrease to 0 at the final stage.

- c. The support is assessed and it is checked whether i) the tunnel is stable, ii) tunnel wall deformation meets the specified requirements, and iii) the tunnel lining meets certain factor of safety requirements.

Care is taken that tunnel closure is not more than 4% of the tunnel span after installation of support. Support capacity diagram is generated for determining the factor of safety of the shotcrete and steel rib support. For a given factor of safety, capacity envelopes are plotted in axial force versus moment space and axial force versus shear force space. Values of axial force, moment and shear force for the liners are then compared to the capacity envelopes. The computed liners values must fall inside an envelope so that they have a factor of safety greater than envelop value. For this thesis, the factor of safety of tunnel support must be greater than two.

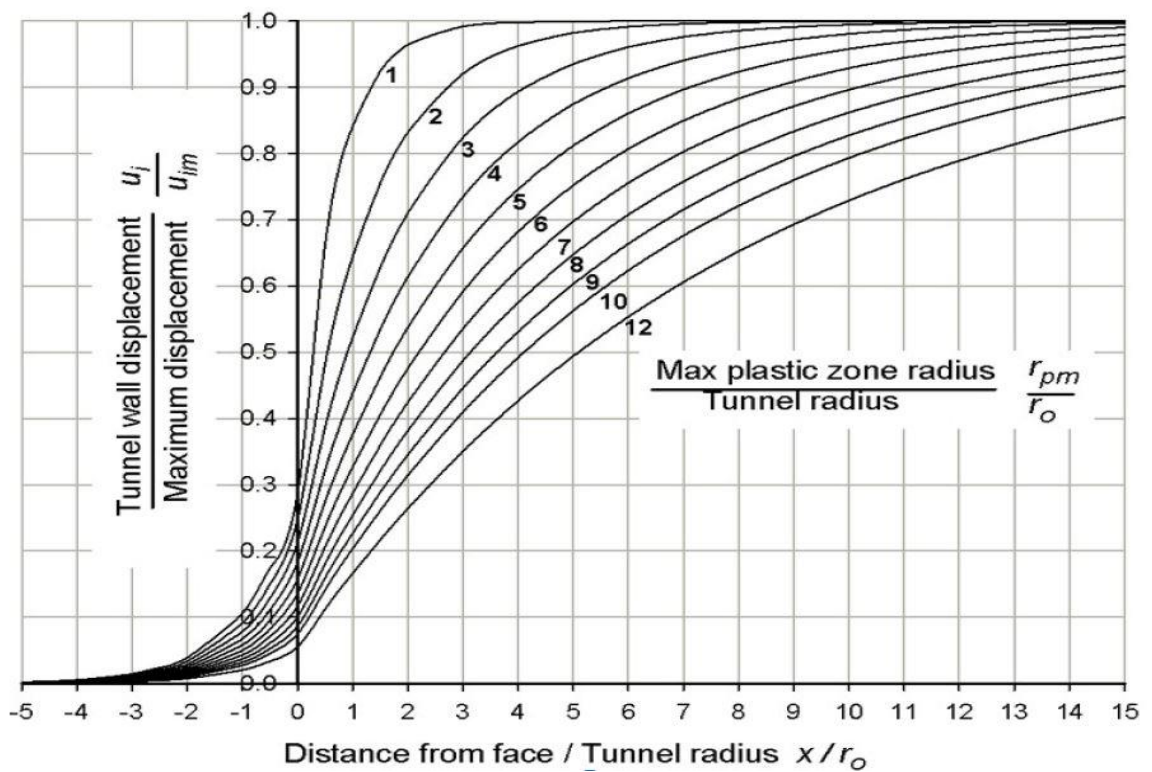


Figure 3-3: Longitudinal Displacement Profile (Vlachopoulos & Diederichs, 2009)

3.7.4 Three-Dimensional Numerical Modelling

GTS-NX has been used to carry out a three-dimensional analysis on selected zones where the longitudinal homogeneity of the tunnel breaks due to presence of additional excavations. Three of such zones are taken in this research for 3D modeling which are:

- Adit connection
- Underground Surge Shaft
- A bend in the tunnel

Analysis is carried out using construction stages and are based on the Generalized Hoek-Brown non-linear analysis.

$$\sigma_1' = \sigma_3' + \sigma_c \left(m \frac{\sigma_3'}{\sigma_c'} + s \right)^a \quad 3-8$$

Where, σ_1' and σ_3' are the axial (major) and confining (minor) effective principal stresses respectively, σ_c is the uniaxial compressive strength (UCS) of the intact rock material, m_b is a reduced value (for the rock mass) of the material constant m_i (for the intact rock) and s and a are constants which depend upon the characteristics of the rock mass. Other constants are determined as shown in table below. (Hoek & Brown, Underground Excavation in rock, 1980)

$$m_b = m_i \exp \left(\frac{GSI-100}{28-14D} \right) \quad 3-9$$

$$s = \exp \left(\frac{GSI-100}{9-3D} \right) \quad 3-10$$

$$a = \frac{1}{2} + \frac{1}{6} (e^{-GSI/15} - e^{-20/3}) \quad 3-11$$

$$GSI = RMR - 5 \quad 3-12$$

3.8 Recommendation of the support system

All of the methods mentioned above independently suggest design support depending on the scientific principles they are based on. In this thesis, empirical and analytical methods are compared and the one that gives the more demanding support is used as input for numerical modeling. If the factor of safety obtained from the numerical modeling is satisfactory, then the support system is recommended.

4 RESULTS AND DISCUSSIONS

4.1 Determination of Overburden

The overburden for each of the selected chainages were determined from the longitudinal profile of the project. The UCS is obtained from the report of the project. They are tabulated below:

Table 4-1 Overburden and uniaxial compressive strength of rock mass at selected sections

Chainages	UCS (MPa)	Overburden (m)
0+600	50	155
0+1400	50	205
0+2000	40	590
0+2500	40	345
0+3200	30	145

4.2 Calculation of Rock Mass Parameters

The rock mass deformation modulus is determined based on the section 3.4 of the literature review. Poisson ratio and Unit weight of particular rock is defined studying various literatures.

Estimation of rock mass deformation modulus

After knowing the values of Q and RMR system the value of modulus of elasticity can be estimated by averaging several empirical methods as stated in Section 3.4. All the necessary data for calculation was used studying various literatures. The estimation of rock mass deformation modulus is shown in Table 4-2.

Table 4-2: Estimation of rock mass deformation modulus

Chainage	Overburden (m)	RMR	Q	Estimated Em			
				Sarafim and Perera (1983)	Hoek et al (2002)	Barton (2002)	Average (GPa)
0+600	155	70	10	4.985	12.576	17.100	11.899
1+400	205	55	4	3.746	5.303	11.447	4.959
2+000	590	40	1	1.300	2.000	6.840	1.485
2+500	345	30	0.4	4.157	1.125	2.978	0.920
3+200	145	25	0.1	0.562	0.731	0.965	0.637

4.3 Assessment of Potential Squeezing

4.3.1 Empirical approach to squeezing

For the assessment of squeezing using empirical approach, Singh approach (1992) and Goel et al. approach (1984) were used as discussed in section 2.5.

Table 4-3: Calculation for empirical method of estimation of squeezing

Starting Chainage (m)	Overburden	RMR	Q Value	N value SRF=1	Singh 1992 $350Q^{1/3}$	Goel 1994 $275N^{0.33} \times B^{-0.1}$	Check	
							Singh	Goel
0+600	155	70	10	700	754.05	511.83	Non Squeezing	Non Squeezing
0+1400	205	55	4	165	504.78	344.01	Non Squeezing	Non Squeezing
0+2000	590	40	1	32	324.91	222.40	Squeezing	Squeezing
0+2500	345	30	0.4	1.98	141.44	97.62	Squeezing	Squeezing
0+3200	145	25	0.1	0.075	50.47	35.20	Squeezing	Squeezing

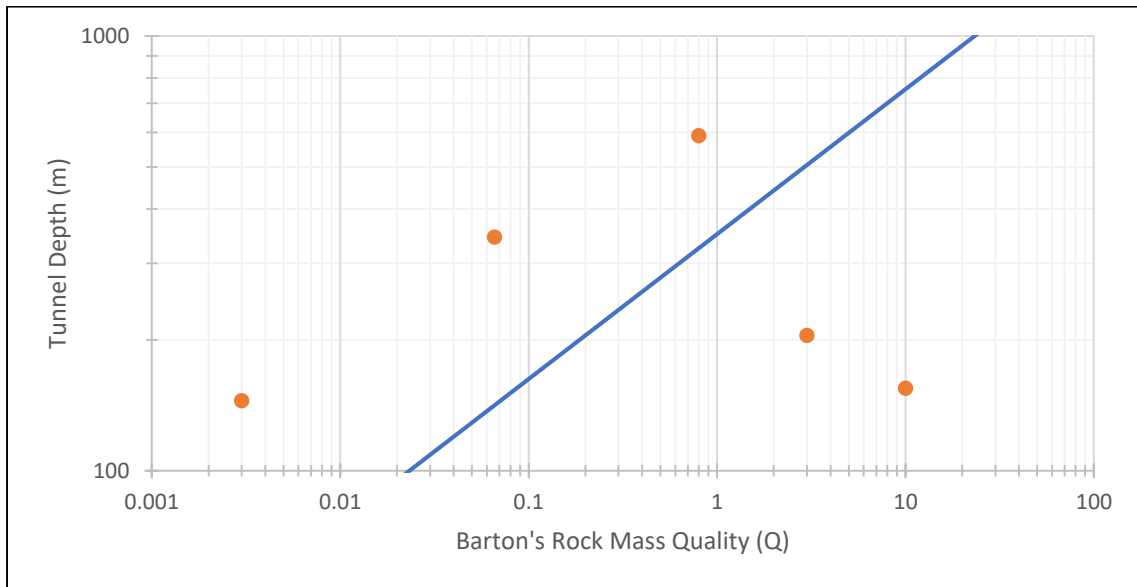


Figure 4-1: Plot showing Singh's approach to assessment of squeezing

4.3.2 Semi Empirical Approach for Squeezing

For the assessment of squeezing potential of the ground using semi-empirical approach, Jethwa et al. approach (1984) and Hoek and Marinos (2000) were used. The results of the assessments are shown in tables below:

Table 4-4: Calculations for semi-empirical method of assessment of squeezing using Jethwa et al. approach (1984) approach.

Chainage	Overburden	RMR	Q value	UCS	Unit Wt.	In-Situ Stress P_0	$N_c = UCS/P_0$	Check	FOS
0+600	155	70	10	50	26.92	4.17	11.98	Non-Squeezing	5.99
0+1400	205	55	4	50	27.05	5.54	9.01	Non-Squeezing	4.50
0+2000	590	40	1	40	26.93	15.89	2.51	Non-Squeezing	1.25
0+2500	345	30	0.4	40	27.01	9.31	4.29	Non-Squeezing	2.14
0+3200	145	25	0.1	30	26.61	3.85	7.77	Non-Squeezing	3.88

Table 4-5: Calculations for semi-empirical method of assessment of squeezing using Hoek and Marinos (2000) approach.

Chainage	Overburden	RMR	Q value	UCS	Tunnel Dia (m)	Tunnel Closure (m)	Strain without support, ϵ	Squeezing condition
0+600	155	70	10	50	4	0.0008	0.02%	Few Support Problems
0+1400	205	55	4	50	4	0.004	0.1%	Few Support Problems
0+2000	590	40	1	40	4	0.25	6.25%	Very severe squeezing problems
0+2500	345	30	0.4	40	4	0.23	5.75%	Very severe squeezing problems
0+3200	145	25	0.1	30	4	0.14	3.5%	Severe squeezing problems

From the above Table 4-3, Table 4-4 and Table 4-5, we can see that there is probability of squeezing in three chainages i.e. 0+2000, 2+500 and 3+200m. The squeezing is likely to occur due to high overburden and weak rocks. So, in order to be in safe side while designing, this must be considered because the area of squeezing requires heavy support and special considerations. More discussions about squeezing for each section are in the conclusion section of this report.

4.4 Assessment of Rock Burst

For checking rock burst, Hoek and Brown approach and Grimstad and Barton's approach has been used as mentioned in section 2.6. The detail results of rock bursting assessment by these methods are given in the table below:

Table 4-6: Calculations for prediction of rock burst

Chainage	Maximum rock cover (H)	Poisson Ratio	Tectonic stress, MPa	Unit Weight, MN/m ³	Vertical Stress, MPa	Horizontal Stress, MPa	K	σ_c	$\sigma_{\theta r}$	$\sigma_{\theta w}$
0+600	155.00	0.10	3.50	0.027	4.19	3.97	0.70	50	5.19	6.70
1+400	205.00	0.10	3.50	0.027	5.54	4.12	0.60	50	5.09	9.41
2+000	590.00	0.10	3.50	0.027	15.93	5.27	0.40	40	4.46	30.27
2+500	345.00	0.10	3.50	0.026	8.97	4.50	0.40	40	2.51	17.04
3+200	145.00	0.10	3.50	0.026	3.77	3.92	0.70	30	4.67	6.03

Table 4-7: Results of Rock Burst assessment using Hoek and Brown's approach

Chainage	For Roof		For Wall	
	$\sigma_c/\sigma_{\theta r}$	Description	$\sigma_c/\sigma_{\theta w}$	Description
0+600	9.64	Stable	7.47	Stable
1+400	9.82	Stable	5.31	Minor Sidewall Spalling
2+000	8.97	Stable	1.32	Heavy support required
2+500	15.93	Stable	2.35	Minor Sidewall Spalling
3+200	6.42	Minor sidewall spalling	4.97	Minor Sidewall Spalling

Table 4-8: Results of Rock Burst assessment using Grimstad and Barton's approach

Chainage	For Roof		For Wall	
	$\sigma_c/\sigma_{\theta r}$	Description	$\sigma_c/\sigma_{\theta w}$	Description
0+600	9.64	Medium Stress, favorable stress condition	7.47	Medium Stress, favorable stress condition

1+400	9.82	Medium Stress, favorable stress condition	5.31	Medium Stress, favorable stress condition
2+000	8.97	Medium Stress, favorable stress condition	1.32	Slabbing and rock burst after minutes in massive rocks
2+500	15.93	Medium Stress, favorable stress condition	2.35	High stress, usually favorable to stability, maybe unfavorable to wall stability
3+200	6.42	Medium Stress, favorable stress condition	4.97	Medium Stress, favorable stress condition

From the above tables we can see that the sections at chainage 2+000 and 2+500 are most susceptible for rock bursting. The Hoek and Brown approach suggest requirement of heavy support at the wall in section 2+000 while minor wall spalling in section 1+400, 2+500 and 3+200. This is mostly due to the D-shape of the tunnel as there will be high stress induced at the corners in the invert level. The Grimstad and Barton method suggest that at section 2+500, the stress is very high which is usually favorable for overall stability but it can be unfavorable for wall stability. Again, this is due to the high stress induced at the corners of the invert. It also suggests that the in the wall of the section 2+000, slabbing and rock burst will occur after minutes in case of massive rocks. This recommendation is made irrespective of the presence of discontinuities around the section, which is out of scope of this research. But major precaution should be made in this region while designing support system as the rock cover in this section is significantly high at 590m. Further discussions for each section are given in conclusion and recommendation section.

4.5 Empirical Method

Table 4-9: Support system design on the basis of RMR rock mass classification

Chainage	RMR	Rock Mass Class	Description	Support System		
				Rock Bolts 20mm End Anchored	Shotcrete	Steel Sets
0+600	70	II	Good Rock	Locally, bolts in crown 3m long, spaced 2.5m with occasional wire mesh.	50 in crown where required.	None.
1+400	55	III	Fair Rock	Systematic bolts 4 m long, spaced 1.5 - 2 m in crown and walls with wire mesh in crown.	50-100 mm in crown and 30 mm in sides.	None
2+000	40	IV	Poor Rock	Systematic bolts 4- 5 m long, spaced 1-1.5 m in crown and walls with wire mesh.	100-150 mm in crown and 100 mm in sides.	Light to medium ribs spaced 1.5 m where required.
2+500	30					
3+200	25					

Table 4-10: Support system design on the basis of Q-system (Annex C, Figure 9-1)

					<i>ESR=1.6, Bolt length=2.25m</i>
Chainage (m)	Overburden (m)	Q Value	Rock Class	Rock mass description	Support System
0+600	155	10	C	Fair Rock	5 cm thick steel fiber reinforced shotcrete and Spot bolting.
1+400	205	4	D	Poor Rock	7.5 cm thick steel fiber reinforced shotcrete and 25 mm diameter 2.5 m long grouted rock bolts @ 1.5 x 1.5 m spacing.
2+000	590	1	E	Very Poor Rock	10 cm thick steel fiber reinforced shotcrete and 25 mm diameter 2.5 m long grouted rock bolts @ 1.3 x 1.5 m spacing.
2+500	345	0.4	F	Very Poor Rock	10 cm thick steel fiber reinforced shotcrete and 25 mm diameter 2.5 m long grouted rock bolts @ 1.3 x 1.5 m spacing.
3+200	145	0.1	G	Extremely Poor	15 cm thick steel fiber reinforced shotcrete and 25 mm diameter 2.5 m long grouted rock bolts @ 1.1 x 1.3 m spacing.

4.6 Analytical Method

The support systems in five sections were designed using convergence confinement method as described in the literature review section.

Chainage 0+600

Table 4-11: Calculation of GRC of section 0+600

Radius of tunnel	R	2 m	Geological strength index	GSI	50
Overburden	H	155m	Intact rock parameter	m_b	1.889
Rock mass rating	RMR	70		s	0.0094
Unit weight	γ	27KN/m ³		a	0.5019
Poisson ratio	ν	0.1	Far Field Stress	S_o	0.0468 Mpa
Strength of intact rock	σ_{ci}	10 MPa	Scaled critical internal pressure	P_i^{cr}	0.0065 Mpa
Vertical stress	σ_v	4.17 MPa	Actual critical internal pressure	p_i^{cr}	0.3652 Mpa
Rock mass modulus	E_{rm}	11899 MPa	Rock mass shear modulus	G_{rm}	5408.63 Mpa

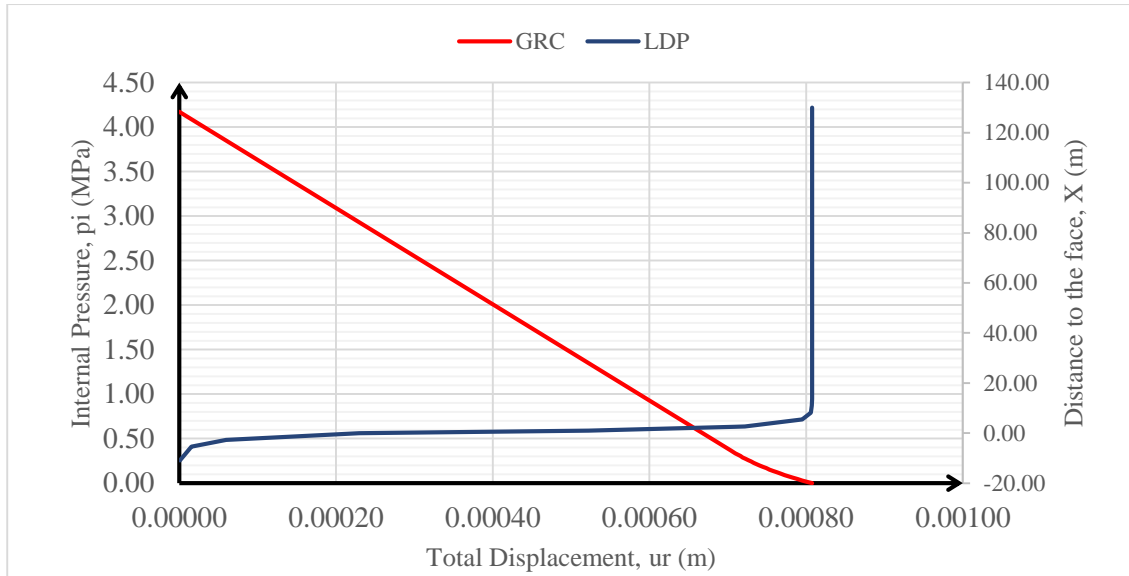


Figure 4-2: GRC and LDP of section 0+600

From this Ground reaction curve, it can be seen that the displacement without support is merely 0.001, which is 0.025% of the Tunnel diameter. Hence, an empirical support system can be provided.

Chainage 1+400

Table 4-12: Calculation of GRC of section 1+400

Radius of tunnel	R	2 m	Geological strength index	GSI	50
Overburden	H	205m	Intact rock parameter	m_b	0.925
Rock mass rating	RMR	55		s	0.00127
Unit weight	γ	27KN/m ³		a	0.5057
Poisson ratio	ν	0.1	Far Field Stress	S_o	0.1214 Mpa
Strength of intact rock	σ_{ci}	10 Mpa	Scaled critical internal pressure	P_i^{cr}	0.032 Mpa

Vertical stress	σ_v	5.54 Mpa	Actual critical internal pressure	p_i^{cr}	1.41 Mpa
Rock mass modulus	E_{rm}	4959 Mpa	Rock mass shear modulus	G_{rm}	2254 Mpa

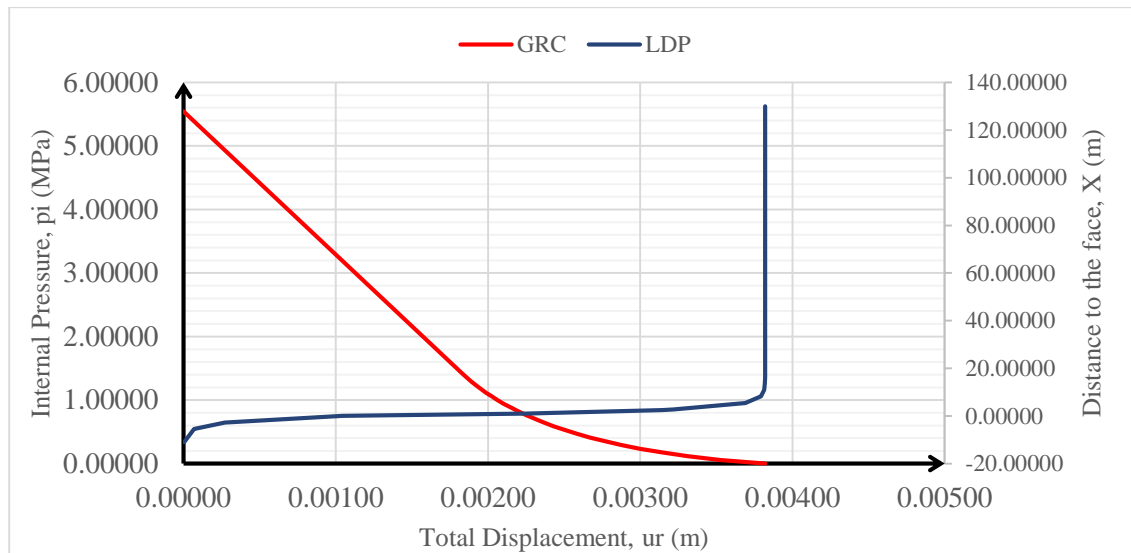


Figure 4-3: GRC and LDP of section 1+400

A: Shotcrete

Table 4-13: Calculation of SCC for section 1+400

Unconfined Compressive Strength	σ_{cc}	25	Mpa	Displacement (m)	Support Pressure (Mpa)
Young's Modulus	E_c	25000	Mpa	0.00250	0
Radius of Tunnel	R	2	Mpa	0.00372	0.920
Thickness of Shotcrete	t_c	75	mm	0.00382	0.920
Poisson's Ratio	ν	0.2		FOS	2.95
Maximum Support Pressure	P_{sma} x	0.920	Mpa		

Elastic Stiffness	K_s	753.34	Mpa/ m
Maximum Displacement	u_r	1.22×10^{-3}	m

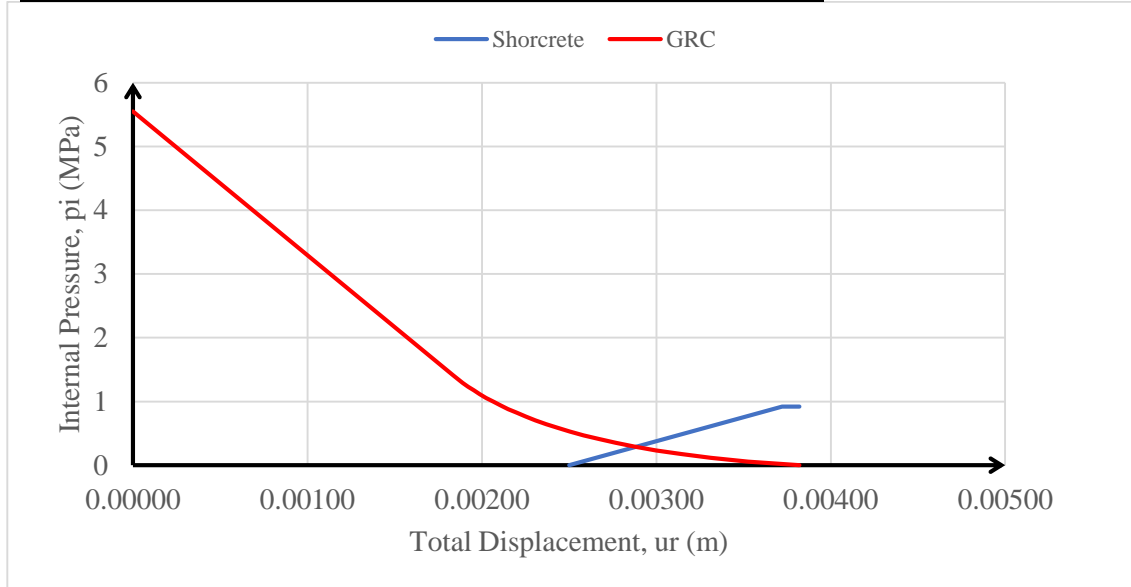


Figure 4-4: GRC and SCC for section 1+400

Chainage 2+000

Table 4-14: Calculation of GRC for section 2+000

Radius of tunnel	R	2 m	Geological strength index	GSI	35
Overburden	H	590m	Intact rock parameter	m_b	0.452
Rock mass rating	RMR	40		s	0.00017
Unit weight	γ	27KN/m ³		a	0.5159
Poisson ratio	ν	0.1	Far Field Stress	S_o	0.8785 Mpa
Strength of intact rock	σ_{ci}	10 Mpa	Scaled critical internal pressure	P_i^{cr}	0.518 Mpa

Vertical stress	σ_v	5.54 Mpa	Actual critical internal pressure	p_i^{cr}	9.37 Mpa
Rock mass modulus	E_{rm}	1485 Mpa	Rock mass shear modulus	G_{rm}	675 Mpa

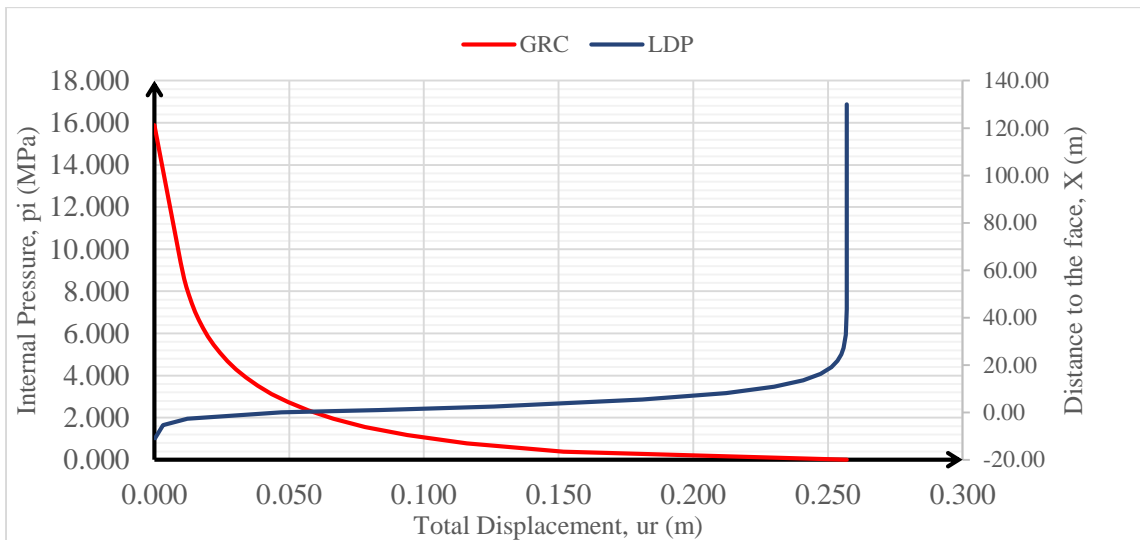


Figure 4-5: GRC and LDP of section 2+000

Table 4-15: Calculation of SCC for section 2+000

A: Shotcrete

Unconfined Compressive Strength	σ_{cc}	25	Mpa	Displacement (m)	Support Pressure (Mpa)
Young's Modulus	E_c	25000	Mpa	0.100	0
Radius of Tunnel	R	2	Mpa	0.1012	1.805
Thickness of Shotcrete	t_c	150	mm	0.257	1.805
Poisson's Ratio	ν	0.2			
Maximum Support Pressure	P_{sm} ax	1.805	Mpa		
Elastic Stiffness	K_s	1549.7 5	Mpa/ m		

Maximum Displacement	u_r	1.16×10^{-3}	m
----------------------	-------	-----------------------	---

Bolt Type		End Anchored		Displacement (m)	Support Pressure (Mpa)
Bolt Diameter	d_b	0.025	m	0.100	0.0000
Free Length of Bolt	l	2.5	m	0.1426	0.5060
Ultimate Load Pullout Test	T_{bf}	0.253	MN	0.2570	0.5060
Deformation Constant	Q	0.143	m/M N		
Youngs Modulus for Bolt	E_s	200000	Mpa		
Circumferential Bolt Spacing	S_c	0.5	m		
Longitudinal Bolt Spacing	S_l	1	m		
Maximum Support Pressure	P_{sm} ax	0.506	Mpa		
Elastic Stiffness	K_s	11.87	Mpa/ m		
Maximum Displacement	u_r	0.043	m		

C. Combined System

				Displacement(m)	Support Pressure (Mpa)
Elastic Stiffness	K_{sb}	1561.63	Mpa/m		
Max Displacement	u_r	0.0015	m	0.100	0
Maximum Support Pressure	P_{sbmx}	2.311	Mpa	0.101	2.311
Factor of Safety	FoS	2.33		0.257	2.311

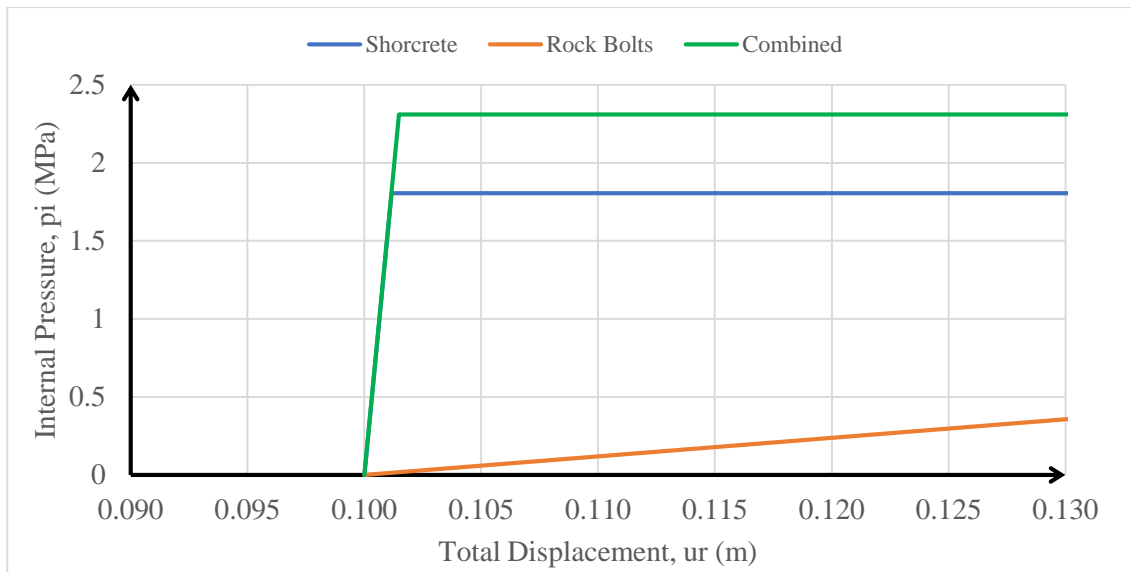


Figure 4-6: SCC for section 2+000

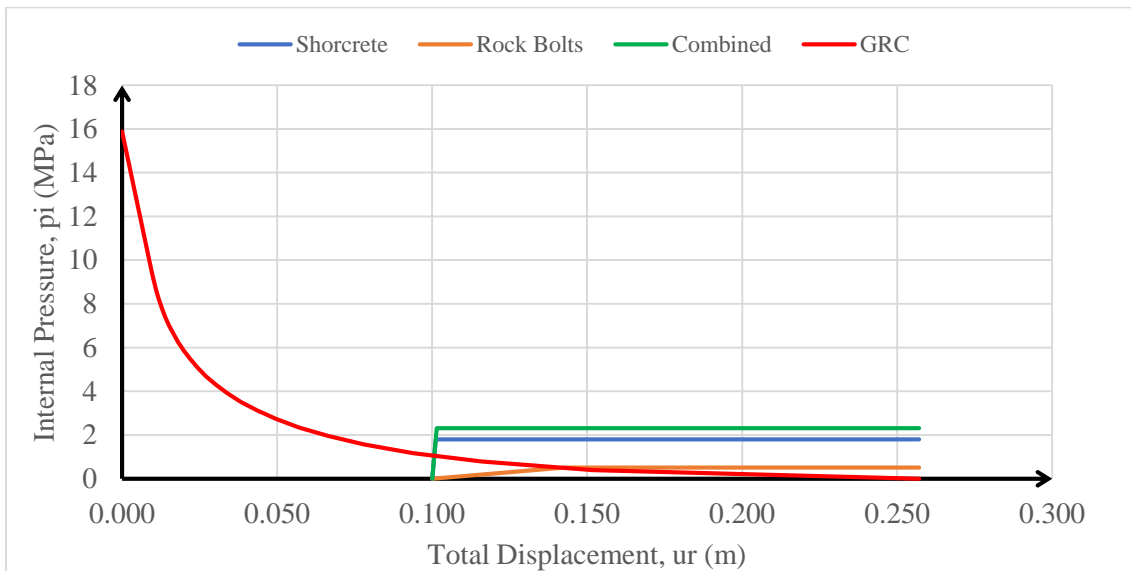


Figure 4-7: GRC and SCC of section 2+000

Chainage 2+500

Table 4-16: Calculation of GRC of section 2+500

Radius of tunnel	R	2 m	Geological strength index	GSI	25
Overburden	H	345m	Intact rock parameter	m_b	0.2811

Rock mass rating	RMR	30		s	0.0000454
Unit weight	γ	27KN/m ³		a	0.5312
Poisson ratio	ν	0.1	Far Field Stress	S_o	0.8292 Mpa
Strength of intact rock	σ_{ci}	10 Mpa	Scaled critical internal pressure	P_i^{cr}	0.482 Mpa
Vertical stress	σ_v	9.319 Mpa	Actual critical internal pressure	p_i^{cr}	5.415 Mpa
Rock mass modulus	E_{rm}	920 Mpa	Rock mass shear modulus	G_{rm}	418 Mpa

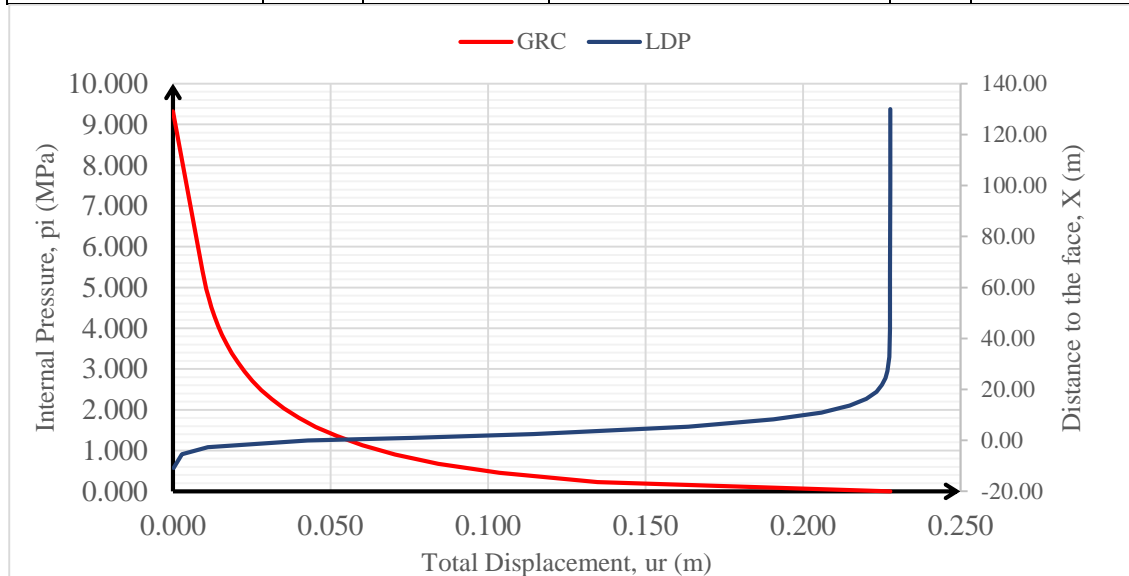


Figure 4-8: GRC and LDP of section 2+500

Table 4-17: Calculation of SCC for section 2+500

A: Shotcrete

Unconfined Compressive Strength	σ_{cc}	25	Mpa	Displacement (m)	Support Pressure (Mpa)
Young's Modulus	E_c	25000	Mpa	0.075	0

Radius of Tunnel	R	2	Mpa	0.0762	1.805
Thickness of Shotcrete	t _c	150	mm	0.228	1.805
Poisson's Ratio	v	0.2			
Maximum Support Pressure	P _{sma} x	1.805	Mpa		
Elastic Stiffness	K _s	1549.75	Mpa/ m		
Maximum Displacement	u _r	1.16×10 ⁻³	m		

B. Rock Bolts

Bolt Type		End Anchored		Displacement (m)	Support Pressure (Mpa)
Bolt Diameter	d _b	0.025	m	0.0750	0.0000
Free Length of Bolt	l	2.5	m	0.1171	0.5000
Ultimate Load Pullout Test	T _{bf}	0.253	MN	0.2277	0.5000
Deformation Constant	Q	0.143	m/M N		
Youngs Modulus for Bolt	E _s	200000	Mpa		
Circumferential Bolt Spacing	S _c	0.5	m		
Longitudinal Bolt Spacing	S _l	1	m		
Maximum Support Pressure	P _{sm} ax	0.500	Mpa		
Elastic Stiffness	K _s	11.87	Mpa/ m		
Maximum Displacement	u _r	0.042	m		

C. Combined System

Elastic Stiffness	K_{sb}	1561.6 3	Mpa/ m	Displacement(m)	Support Pressur e (Mpa)
Max Displacement	u_r	0.0015	m	0.075	0
Maximum Support Pressure	P_{sbmax}	2.305	Mpa	0.076	2.305
Factor of Safety	FoS	2.38		0.228	2.305

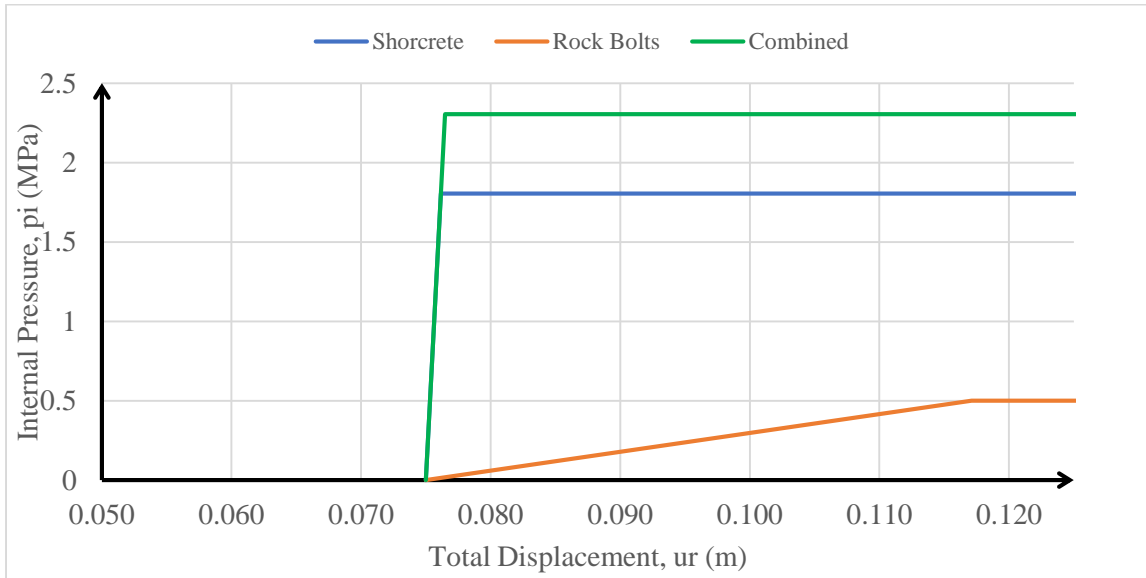


Figure 4-9: SCC for section 2+500

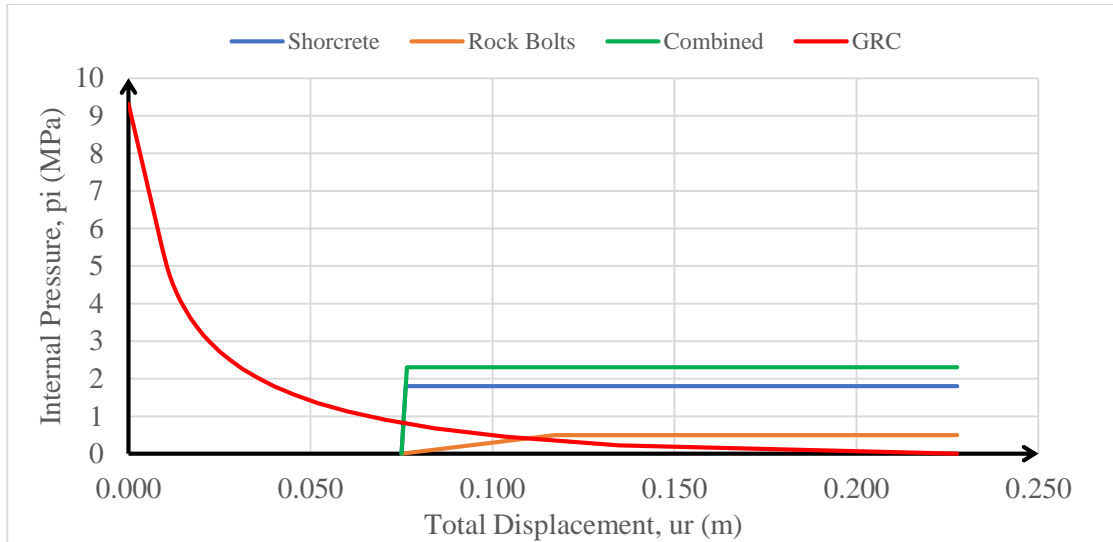


Figure 4-10: GRC and SCC of section 2+500

Chainage 3+200

Table 4-18: Calculation of GRC for section 3+200

Radius of tunnel	R	2 m	Geological strength index	GSI	20
Overburden	H	145m	Intact rock parameter	m_b	0.155
Rock mass rating	RMR	25		s	0.0000233
Unit weight	γ	27KN/m ³		a	0.5437
Poisson ratio	ν	0.1	Far Field Stress	S_o	0.8302 Mpa
Strength of intact rock	σ_{ci}	7 Mpa	Scaled critical internal pressure	P_i^{cr}	0.482 Mpa
Vertical stress	σ_v	9.319 Mpa	Actual critical internal pressure	p_i^{cr}	2.2422 Mpa
Rock mass modulus	E_{rm}	637 Mpa	Rock mass shear modulus	G_{rm}	289 Mpa

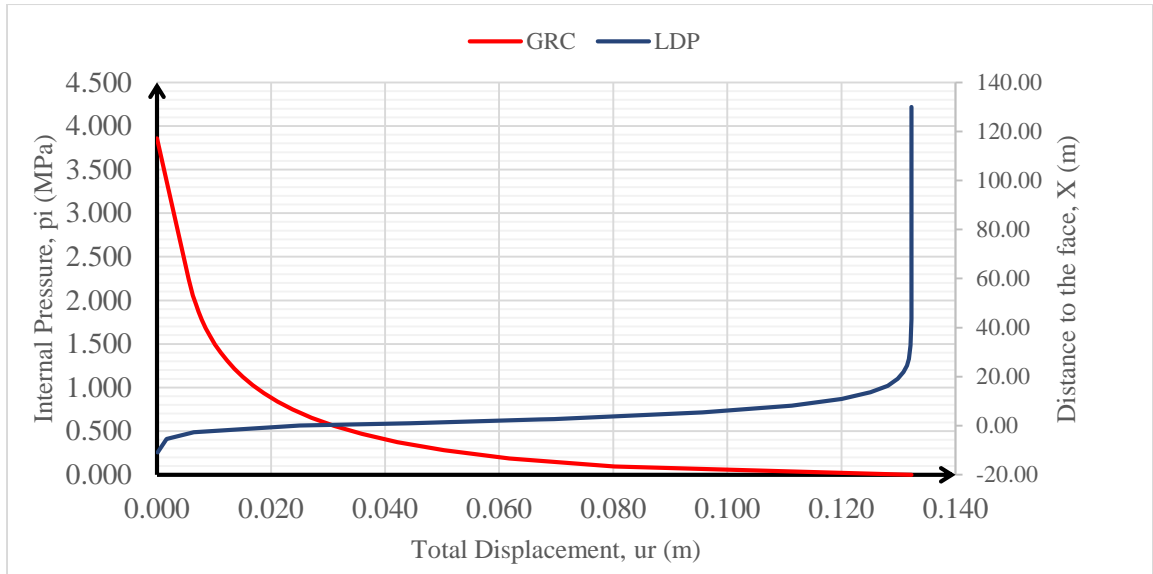


Figure 4-11: GRC and LDP of section 3+200

Table 4-19: Calculation of SCC for section 3+200

A: Shotcrete

Unconfined Compressive Strength	σ_{cc}	25	Mpa	Displacement (m)	Support Pressure (Mpa)
Young's Modulus	E_c	25000	Mpa	0.030	0
Radius of Tunnel	R	2	Mpa	0.0312	0.617
Thickness of Shotcrete	t_c	50	mm	0.132	0.617
Poisson's Ratio	ν	0.2			
Maximum Support Pressure	P_{sma}	0.617	Mpa		
Elastic Stiffness	K_s	497.53	Mpa/m		
Maximum Displacement	u_r	1.24×10^{-3}	m		

B. Rock Bolts

Bolt Type		End Anchored		Displacement (m)	Support Pressure (Mpa)
Bolt Diameter	d_b	0.025	m	0.0300	0.0000
Free Length of Bolt	l	2.5	m	0.0468	0.4000
Ultimate Load Pullout Test	T_{bf}	0.1	MN	0.1323	0.4000
Deformation Constant	Q	0.143	m/M N		
Youngs Modulus for Bolt	E_s	200000	Mpa		
Circumferential Bolt Spacing	S_c	0.5	m		
Longitudinal Bolt Spacing	S_l	0.5	m		
Maximum Support Pressure	P_{sm} ax	0.400	Mpa		
Elastic Stiffness	K_s	23.74	Mpa/ m		
Maximum Displacement	u_r	0.017	m		

C. Steel Sets

Steel Sets	ISMB 150			Displacement(m)	Support Pressure (Mpa)
Radius of Tunnel	m	2		0.030	0.000
Set Spacing	S_l	0.5	m	0.034	0.831
Cross Sectional Area	A_s	0.0019	m^2	0.132	0.831
Youngs Modulus of Steel	E_s	200000	Mpa		

Yield Strength of Steel	σ_{ys}	435	Mpa
Maximum Support Pressure	P_{smax}	0.831	Mpa
Elastic Stiffness	K_s	191	Mpa/m
Max Displacement	u_r	0.0044	m

C. Combined System

				Displacement(m)	Support Pressure (Mpa)
Elastic Stiffness	K_{sb}	712.28	Mpa/m		
Max Displacement	u_r	0.0026	m	0.030	0
Maximum Support Pressure	P_{sbmax}	1.848	Mpa	0.033	1.848
Factor of Safety	FoS	3		0.132	1.848

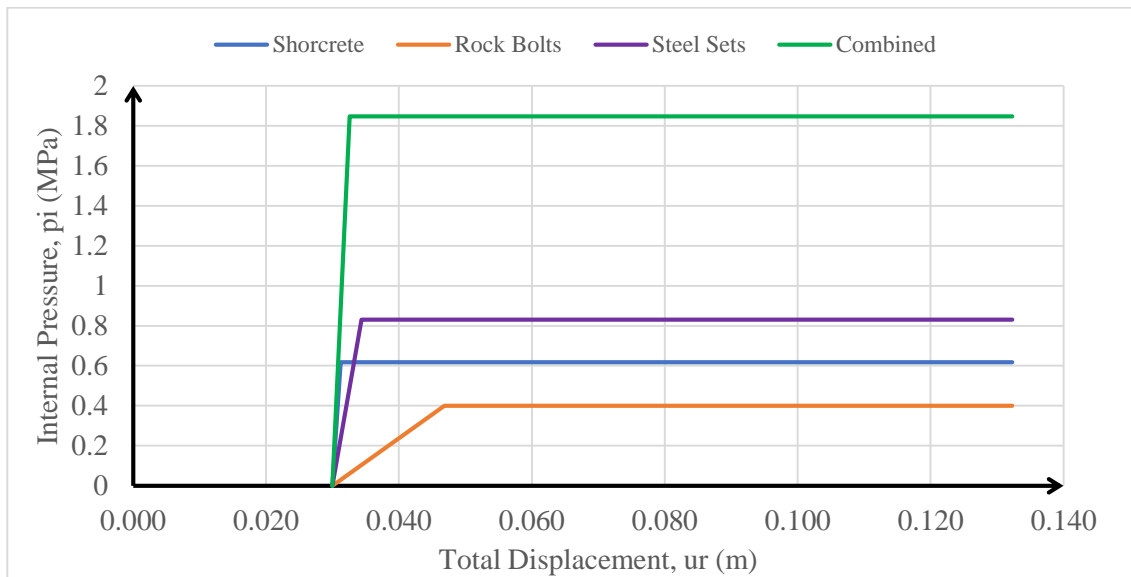


Figure 4-12: SCC of section 3+200

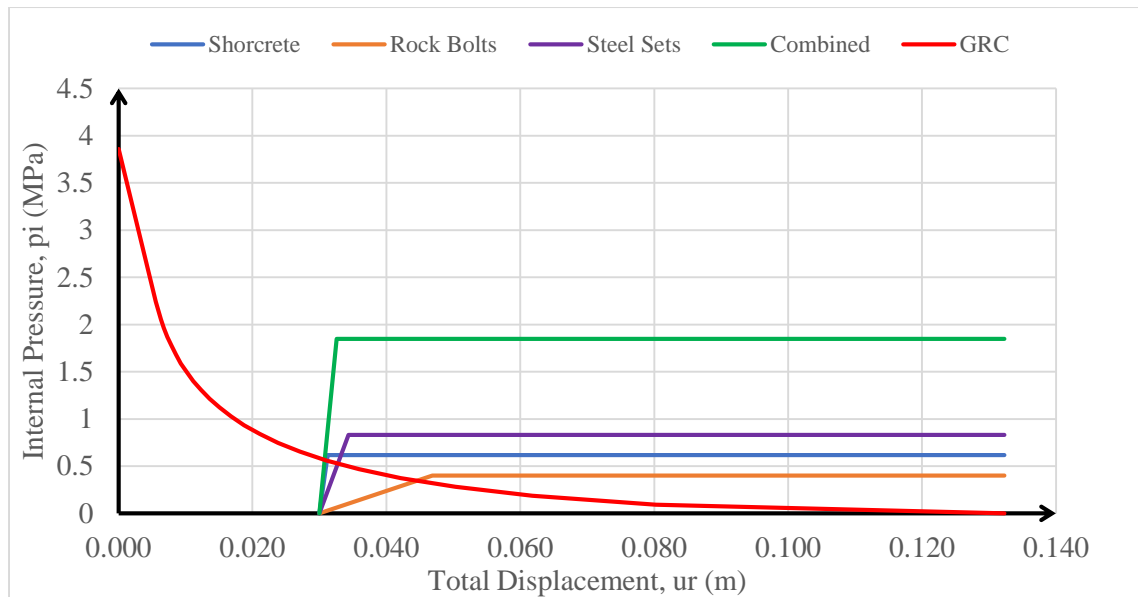


Figure 4-13: GRC and SCC of section 3+200

4.7 Numerical Modeling

Phase² was used for modeling of 5 sections keeping in mind they cover all kinds of rock types in the tunnel alignment as explained in Introduction section in 1.6.3. The support system suggested is given below. The detailed figures on the periphery of tunnel before and after support installment is given in Annex B.

Chainage 0+600

The rock mass is a monotonous sequence of garnet schist with occasional intercalation of banded gneiss with a uniaxial compressive strength of 50 MPa, Geological Strength Index of 65, Hoek-Brown constant m_i is 10, modulus ratio is 675 and rock mass deformation modulus is 11899 MPa. This corresponds to the rock mass having the Q value more than 4 which is better than Fair Rock according to that classification.

The support suggested by Q system is 50 mm of steel fiber reinforced shotcrete and some spot bolting of 2.5 m long, 25 mm diameter, fully bonded rock-bolts.

A uniform distributed load to the tunnel is in the initial stage. The factor is taken such that it will gradually reduce the magnitude of the pressure. As a result, tunnel deformation will increase as the pressure is lowered to zero. At this stage the internal pressure is removed, simulating the reduction of support due to the advance of the tunnel face.

The maximum displacement of the tunnel is calculated as (u_{max}) 0.0014 m. This is only 0.035% of the tunnel span. The location of this displacement is at the floor of the excavation. The extent of the plastic zone (R_p) is about 2.8 m as shown in Figure 8. The unsupported section (X) will be at maximum of 4 m distance from the tunnel face. The ratio of distance from tunnel face to tunnel radius (X/R_t) is 2 and plastic zone to tunnel radius (R_t/R_p) is 1.4.

By using Vlachopoulos and Diederichs method, the above values are plotted which gives ratio of closure to maximum closure equal to 0.92. Therefore, the closure equals 0.00132 m. This is about 91.67% of the total closure of 0.00144 m. This means that 91.67% of deformation will already have taken place before the support can be installed. Internal pressure factor of 0.005 yields the tunnel wall displacement computed above for the point of support installation.

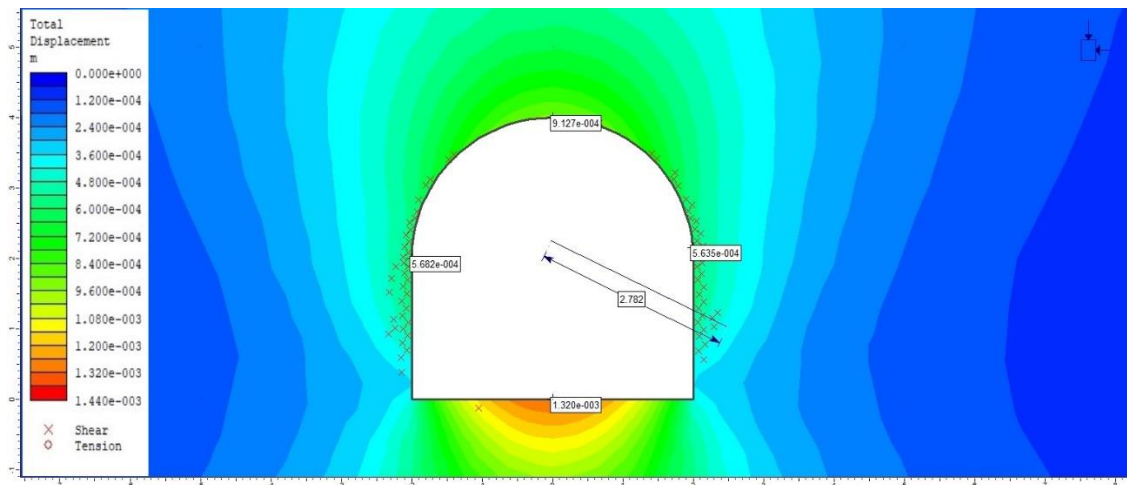


Figure 4-14: Plastic zone and tunnel closure for section 0+600

The support system suggested by empirical methods is installed and analysis is given below:

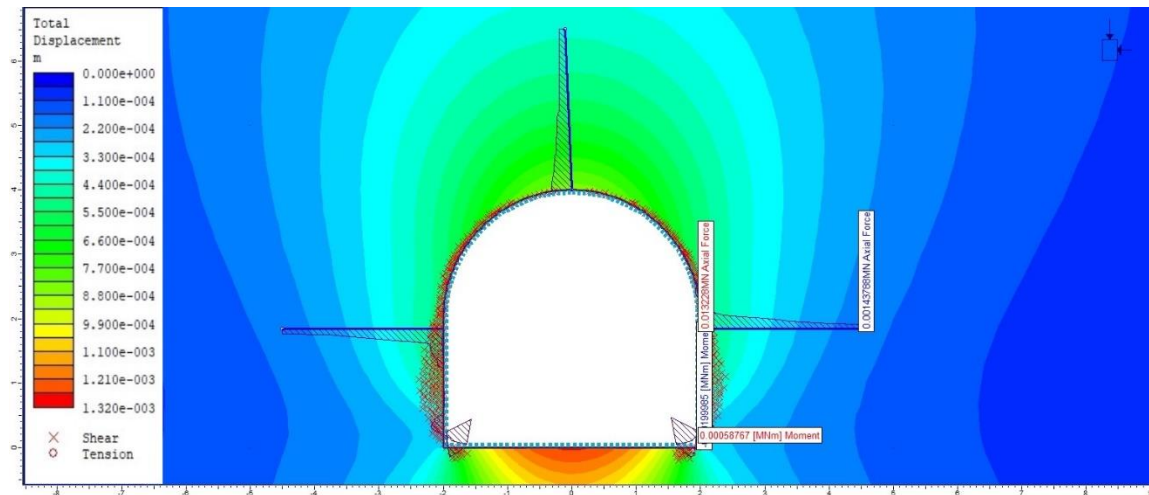


Figure 4-15: Axial force on bolts and BM in liners for section 0+600

The support capacity diagrams, which are presented as Thrust Vs Shear Force and Thrust Vs Moment, for fiber reinforced shotcrete of 50 mm is generated and presented in the Figure

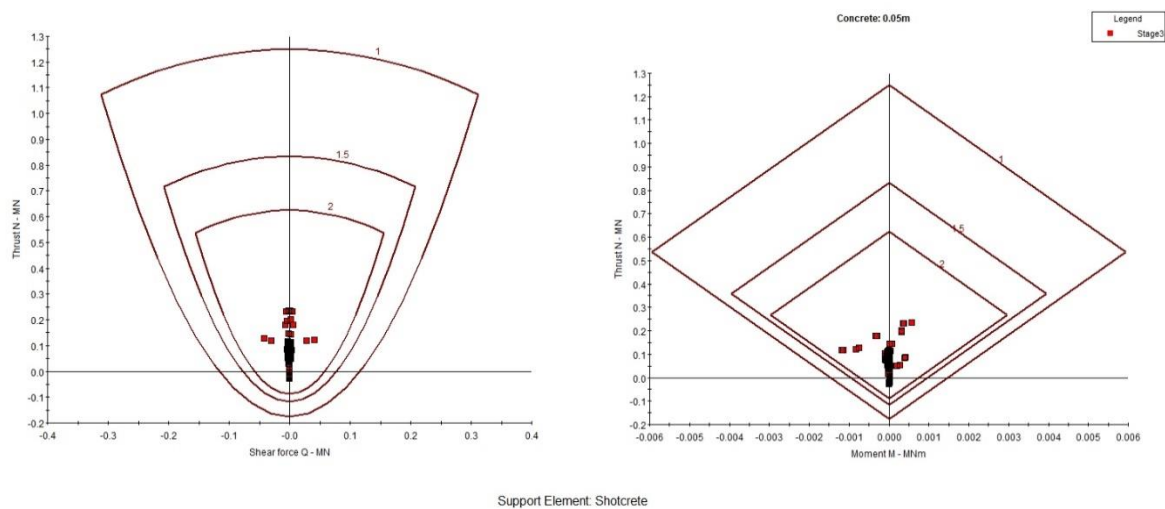


Figure 4-16: Safety envelope for section 0+600

From the above plot, all the points fall within the factor of safety of '2' envelope on both plots. Also, no yielding is observed in any of the rock-bolts. This means that the support system has a factor of safety greater than 2 thus achieving the design factor of safety.

Table 4-20: Support system suggested by Numerical Modeling for section 0+600

Rock Bolts		Shotcrete	
Type	End Anchored	UCS	25Mpa
Length	2.5m	Youngs Modulus	25000 MPa
Diameter	25 mm	Thickness of shotcrete	50mm
Bolt Modulus	2×10^5 MPa	Poisson's Ratio	0.2
Out of Plane Spacing	3 m	Tensile Strength	3.5 MPa

Chainage 1+400

The rock mass is a monotonous sequence of garnet schist with occasional intercalation of banded gneiss with a uniaxial compressive strength of 50 MPa, Geological Strength Index of 50, Hoek-Brown constant m_i is 10, modulus ratio is 675 and rock mass deformation modulus is 4959 MPa. This corresponds to the rock mass having the Q value ranging between 1 to 4 which is Poor Rock according to that classification.

The support suggested by Q system is 75 mm of steel fibre reinforced shotcrete and systematic bolting spaced at 1.5 m x 1.5 m, 2.5 m long, 25 mm diameter, fully bonded rockbolts.

A uniform distributed load to the tunnel is in the initial stage. The factor is taken such that it will gradually reduce the magnitude of the pressure. As a result, tunnel deformation will increase as the pressure is lowered to zero. At this stage the internal pressure is removed, simulating the reduction of support due to the advance of the tunnel face.

The maximum displacement of the tunnel is calculated as (u_{max}) 0.006 m. This is only 0.15% of the tunnel span. The location of this displacement is at the bottom of the excavation. The extent of the plastic zone (R_p) is about 3.276 m as shown in Figure below. The unsupported section (X) will be at maximum of 2 m distance from the tunnel face.

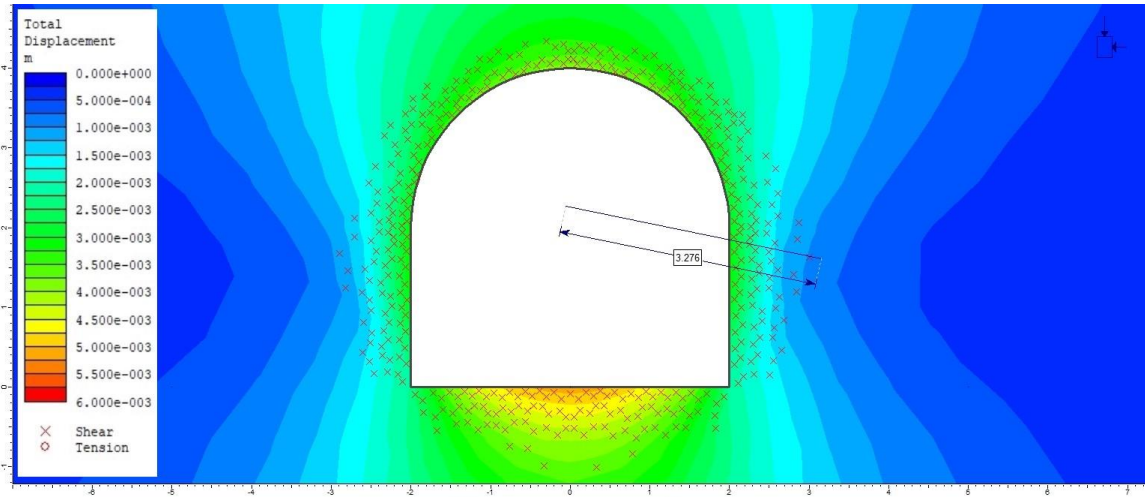


Figure 4-17: Plastic zone and tunnel closure for section 1+400

The ratio of distance from tunnel face to tunnel radius (X/R_t) is 1 and plastic zone to tunnel radius (R_t/R_p) is 1.63

By using Vlachopoulos and Diederichs method, the above values are plotted which gives ratio of closure to maximum closure equal to 0.8. Therefore, the closure equals 0.0048 m. This is about 80% of the total closure of 0.006 m. This means that 80% of deformation will already have taken place before the support can be installed. Ipressure factor of 0.02 yields the tunnel wall displacement computed above for the point of support installation.

The support system suggested by empirical methods is installed and analysis is given below:

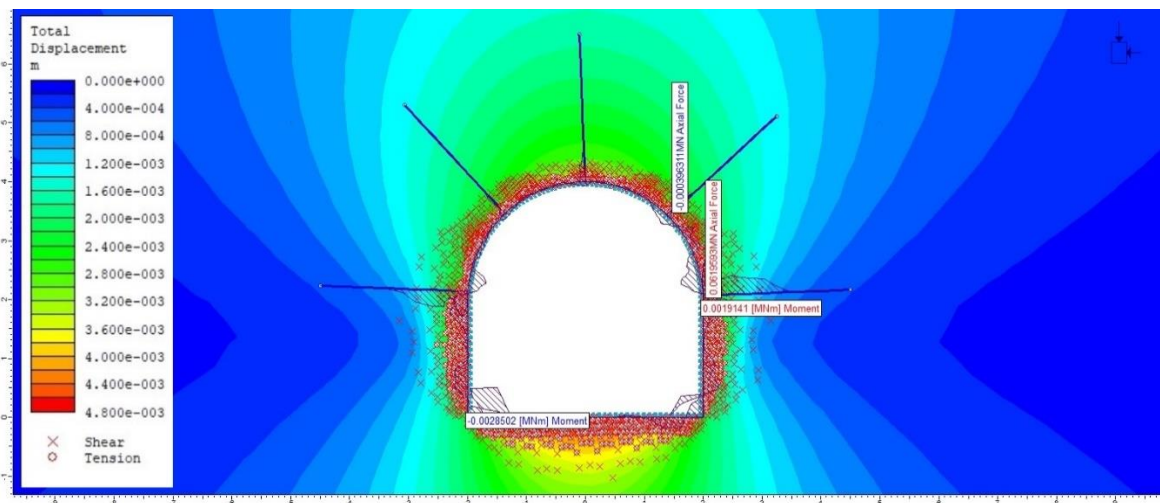


Figure 4-18: Axial force and BM in supports for section 1+400

The support capacity diagrams, which are presented as Thrust Vs Shear Force and Thrust Vs Moment, for fiber reinforced shotcrete of 50 mm is generated and presented in the Figure

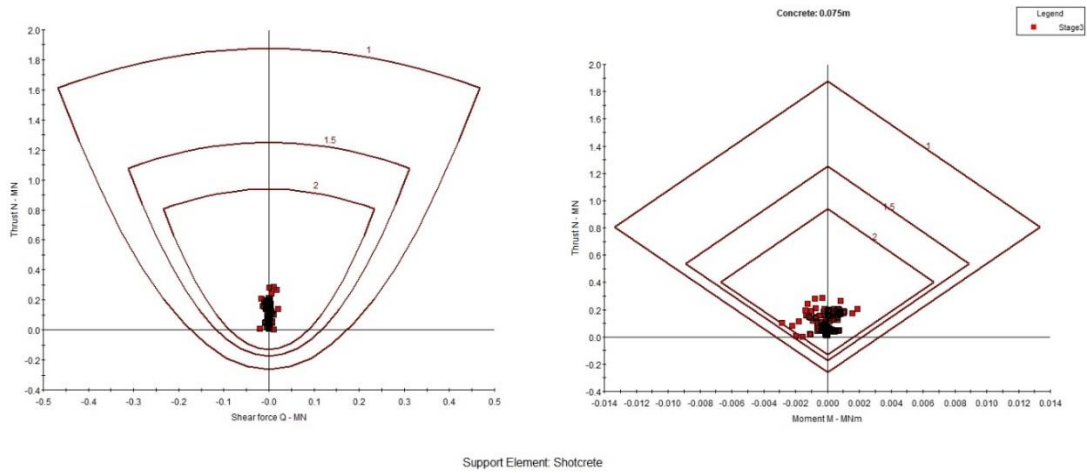


Figure 4-19: Safety envelope for section 1+400

From the above plot, all the points fall within the factor of safety of ‘2’ envelope on both plots. Also, no yielding is observed in any of the rock-bolts. This means that the support system has a factor of safety greater than 2 thus achieving the design factor of safety.

Table 4-21: Supports suggested by numerical modeling for section 1+400

Rock Bolts		Shotcrete	
Type	End Anchored	UCS	25Mpa
Length	2.5m	Youngs Modulus	25000 MPa
Diameter	25 mm	Thickness of shotcrete	75mm
Bolt Modulus	2×10^5 MPa	Poisson's Ratio	0.2
Out of Plane Spacing	1.5 m	Tensile Strength	3.5 MPa

Chainage 2+000

The rock mass is a monotonous sequence of garnet schist with occasional intercalation of banded gneiss with a uniaxial compressive strength of 40 MPa, Geological Strength Index of 35, Hoek-Brown constant m_i is 10, modulus ratio is 650 and rock mass deformation modulus is 1485 MPa. This corresponds to the rock mass having the Q value ranging between 0.1 to 1 which is Very Poor Rock according to that classification.

The support suggested by Q system is 100 mm of steel fiber reinforced shotcrete and systematic bolting spaced at 1.3 m x 1.5 m, 2.5 m long, 25 mm diameter, fully bonded rock bolts.

A uniform distributed load to the tunnel is in the initial stage. The factor is taken such that it will gradually reduce the magnitude of the pressure. As a result, tunnel deformation will increase as the pressure is lowered to zero. At this stage the internal pressure is removed, simulating the reduction of support due to the advance of the tunnel face.

The maximum displacement of the tunnel is calculated as (u_{max}) 0.216 m. This is only 5.4% of the tunnel span. The location of this displacement is at both the walls of the excavation. The extent of the plastic zone (R_p) is about 9.027 m as shown in Figure below. The unsupported section (X) will be at maximum of 4 m distance from the tunnel face.

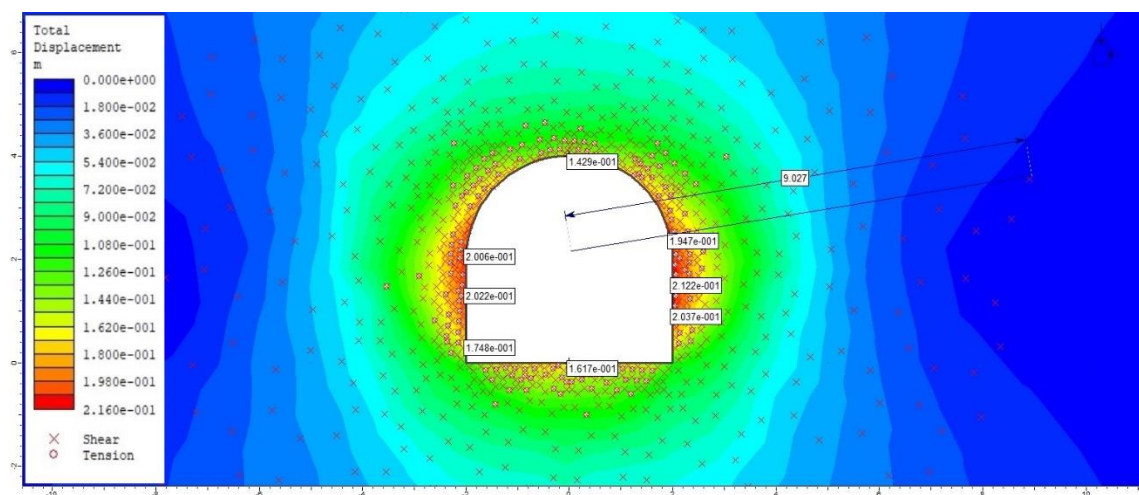


Figure 4-20: Plastic displacement and tunnel closure for section 2+000

The ratio of distance from tunnel face to tunnel radius (X/R_t) is 2 and plastic zone to tunnel radius (R_t/R_p) is 4.51

By using Vlachopoulos and Diederichs method, the above values are plotted which gives ratio of closure to maximum closure equal to 0.44. Therefore, the closure equals 0.096 m. This is about 44% of the total closure of 0.216 m. This means that 44% of deformation will already have taken place before the support can be installed. An Internal pressure factor of 0.02 yields the tunnel wall displacement computed above for the point of support installation.

The support system suggested by empirical methods is installed and analysis is given below:

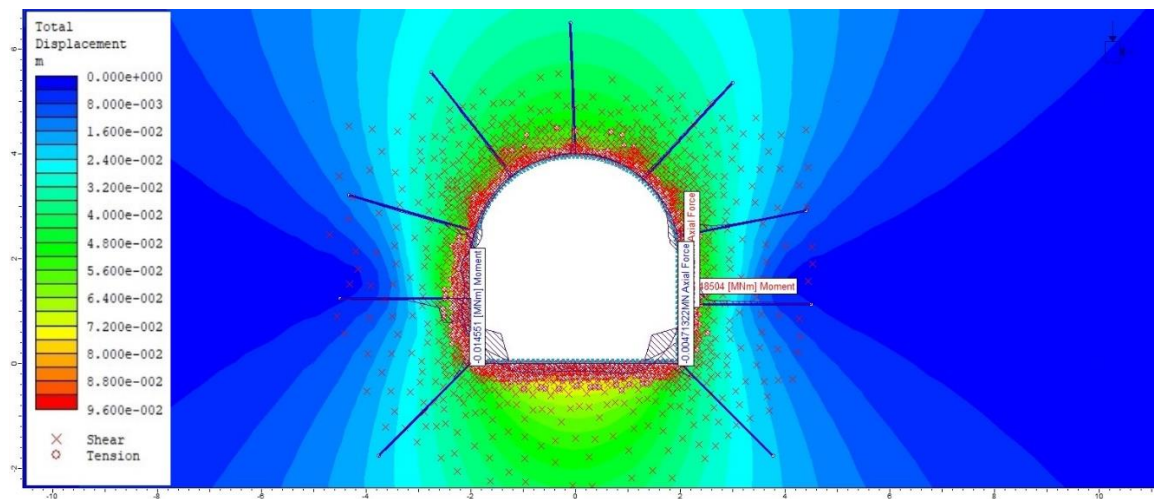


Figure 4-21: Axial force and BM on supports in section 2+000

The support capacity diagrams, which are presented as Thrust Vs Shear Force and Thrust Vs Moment, for fiber reinforced shotcrete of 100 mm is generated and presented in the Figure below

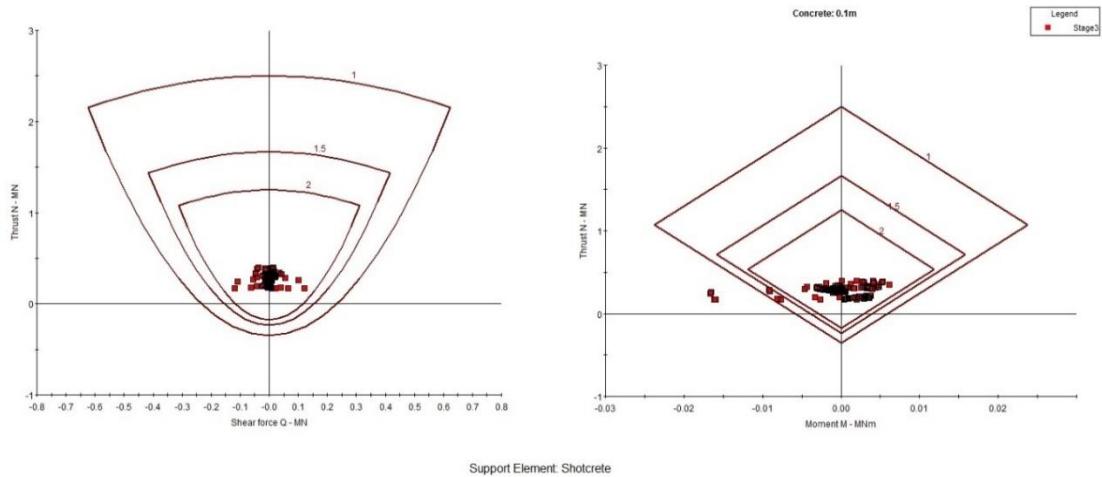


Figure 4-22: Safety envelope for section 2+000 with 100mm shotcrete

From the above plot, some of the elements are out of the envelope of factor of safety of 1 which does not satisfy our design. This asks for the support to be modified for this tunnel stretch which has a very high overburden of 590m. The excavation is remodeled with 120 mm thickness and similar rock bolt pattern and the result is shown below:

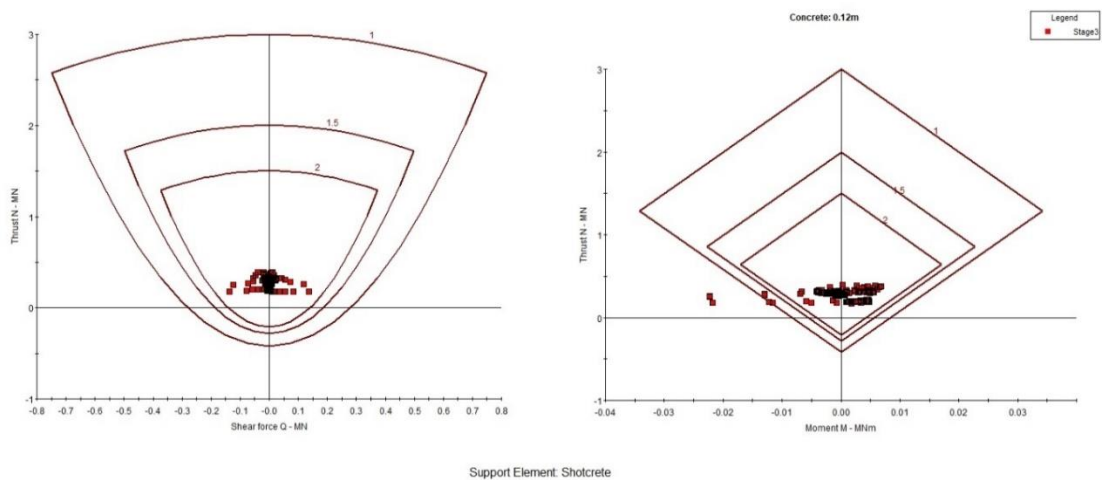


Figure 4-23: Safety envelope for section 2+000 with 120mm shotcrete

Applying 120 mm of shotcrete is not enough to withstand the stress generated by the very high overburden of 590 meters. Again, using 200mm of shotcrete with similar rock bolt patterns, results are shown below:

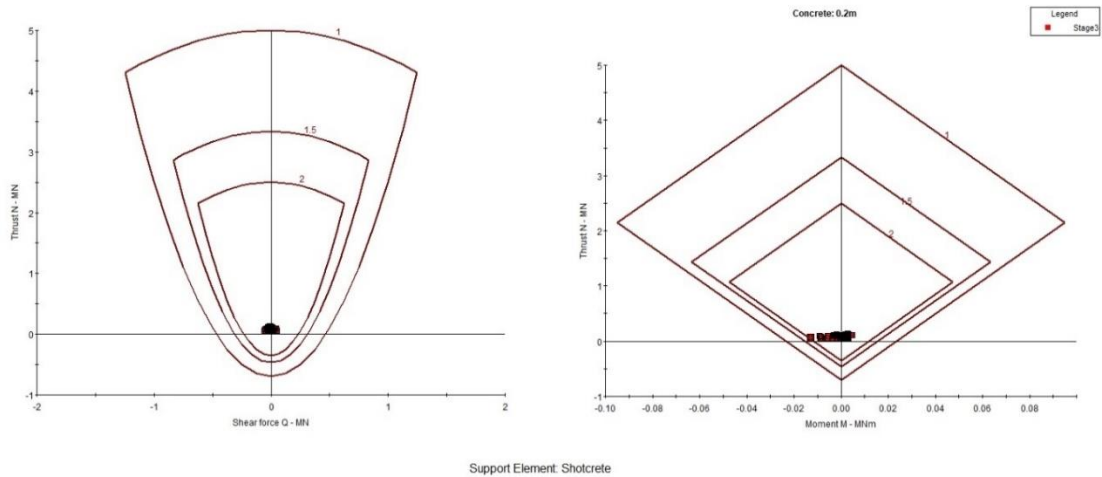


Figure 4-24: Safety envelope for section 2+000 with 200mm shotcrete

Applying 200 mm shotcrete brings all the liner elements within the factor of safety envelop of 1.5 to 2. However, there are still couple of elements which lie just at or outside of that envelop which are mainly from the flat invert which can be treated by invert concrete layer. Also, no yielding is observed in any of the rock-bolts. This means that the support system has a factor of safety between 1.5 to 2 thus achieving the design factor of safety.

Table 4-22: Supports suggested by Numerical Modeling for section 2+000

Rock Bolts		Shotcrete	
Type	End Anchored	UCS	25Mpa
Length	2.5m	Youngs Modulus	25000 MPa
Diameter	25 mm	Thickness of shotcrete	200mm
Bolt Modulus	2×10^5 MPa	Poisson's Ratio	0.2
Out of Plane Spacing	1.5 m	Tensile Strength	3.5 MPa

Chainage 2+500

The rock mass is a monotonous sequence of garnet schist with occasional intercalation of banded gneiss with a uniaxial compressive strength of 40 MPa, Geological Strength

Index of 25, Hoek-Brown constant m_i is 10, modulus ratio is 650 and rock mass deformation modulus is 920 MPa. This corresponds to the rock mass having the Q value ranging between 0.01 to 0.1 which is Extremely Poor Rock according to that classification.

The support suggested by Q system is 150 mm of steel fiber reinforced shotcrete and systematic bolting spaced at 1.1 m x 1.3 m, 2.5 m long, 25 mm diameter, fully bonded rock bolts.

A uniform distributed load to the tunnel is in the initial stage. The factor is taken such that it will gradually reduce the magnitude of the pressure. As a result, tunnel deformation will increase as the pressure is lowered to zero. At this stage the internal pressure is removed, simulating the reduction of support due to the advance of the tunnel face.

The maximum displacement of the tunnel is calculated as (u_{max}) 0.036 m. This is only 0.9% of the tunnel span. The location of this displacement is at both the walls of the excavation. The extent of the plastic zone (R_p) is about 4.53 m as shown in Figure below. The unsupported section (X) will be at maximum of 2 m distance from the tunnel face.

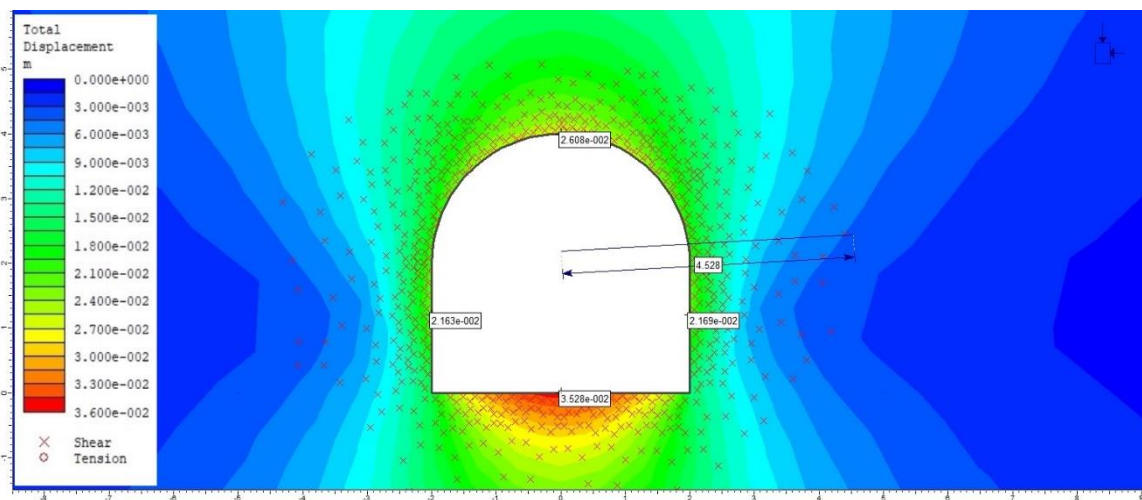


Figure 4-25: Plastic zone and Tunnel Closure for section 2+500

The ratio of distance from tunnel face to tunnel radius (X/R_t) is 1 and plastic zone to tunnel radius (R_t/R_p) is 2.265.

By using Vlachopoulos and Diederichs method, the above values are plotted which gives ratio of closure to maximum closure equal to 0.5. Therefore, the closure equals 0.018 m.

This is about 50% of the total closure of 0.036 m. This means that 50% of deformation will already have taken place before the support can be installed. An internal pressure factor of 0.05 yields the tunnel wall displacement computed above for the point of support installation. Support system suggested by the empirical method is installed to the excavation with the parameters stated above and analysed as shown in Figure below.

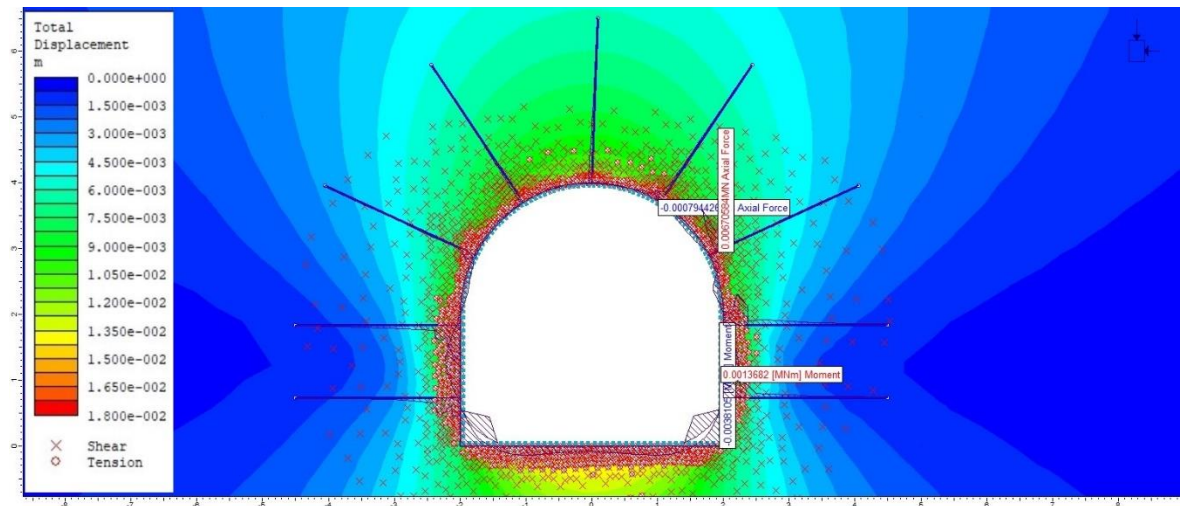


Figure 4-26: Axial force and BM on supports in section 2+500

The support capacity diagrams, which are presented as Thrust Vs Shear Force and Thrust Vs Moment, for fiber reinforced shotcrete of 150 mm is generated and presented in the Figure 25.

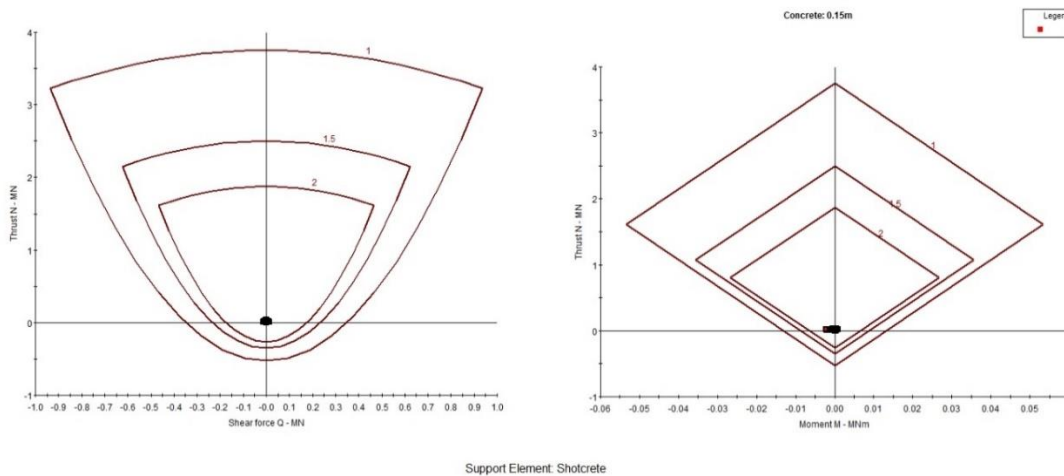


Figure 4-27: Safety envelope for section 2+500

From the above plot, most of the elements are within the envelope of the factor of safety of 2 on both plots. Also, no yielding is observed in any of the rock-bolts. This means that the support system has a factor of safety between 1.5 to 2 thus achieving the design factor of safety.

Table 4-23: Supports suggested by numerical modeling for section 2+500

Rock Bolts		Shotcrete	
Type	End Anchored	UCS	25Mpa
Length	2.5m	Youngs Modulus	25000 MPa
Diameter	25 mm	Thickness of shotcrete	150mm
Bolt Modulus	2×10^5 MPa	Poisson's Ratio	0.2
Out of Plane Spacing	1.3 m	Tensile Strength	3.5 MPa

Chainage 3+200

The rock mass is a monotonous sequence of garnet schist with occasional intercalation of banded gneiss with a uniaxial compressive strength of 30 MPa, Geological Strength Index of 20, Hoek-Brown constant m_i is 7, modulus ratio is 600 and rock mass deformation modulus is 637 MPa. This corresponds to the rock mass having the Q value 0.1 which is Extremely Poor Rock according to that classification.

The support suggested by Q system is 200 mm of steel fiber reinforced shotcrete supported by steel rib ISMB 150 spaced at 1.0 m and systematic bolting at 1.1 m x 1.3 m spacing of 2.5 m long, 25 mm diameter, fully bonded rock-bolts.

A uniform distributed load to the tunnel is in the initial stage. The factor is taken such that it will gradually reduce the magnitude of the pressure. As a result, tunnel deformation will increase as the pressure is lowered to zero. At this stage the internal pressure is removed, simulating the reduction of support due to the advance of the tunnel face.

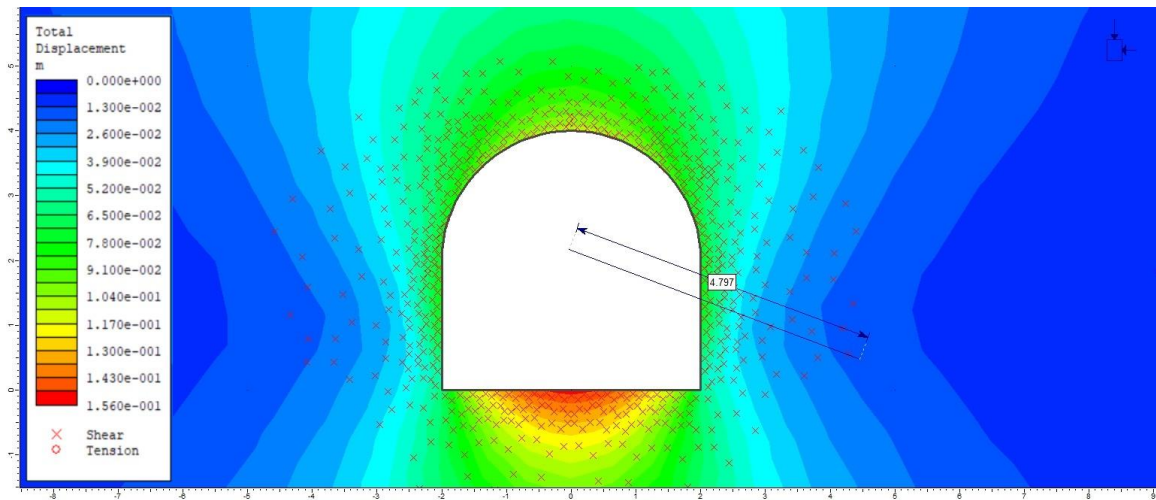


Figure 4-28: Plastic zone and Tunnel Closure in section 3+200

The maximum displacement of the tunnel is calculated as (u_{\max}) 0.156 m. This is only 3.9% of the tunnel span. The location of this displacement is at the floor of the excavation. The extent of the plastic zone (R_p) is about 4.797 m as shown in Figure. The unsupported section (X) will be at maximum of 2 m distance from the tunnel face.

The ratio of distance from tunnel face to tunnel radius (X/R_t) is 1 and plastic zone to tunnel radius (R_t/R_p) is 2.32.

By using Vlachopoulos and Diederichs method, the above values are plotted which gives ratio of closure to maximum closure equal to 0.86. Therefore, the closure equals 0.0156 m. This is about 84% of the total closure of 0.0168 m. This means that 84% of deformation will already have taken place before the support can be installed. An internal pressure factor of 0.01 yields the tunnel wall displacement computed above for the point of support installation.

Support system suggested by the empirical method is installed to the excavation with the parameters stated above and analysed as shown in Figure below.

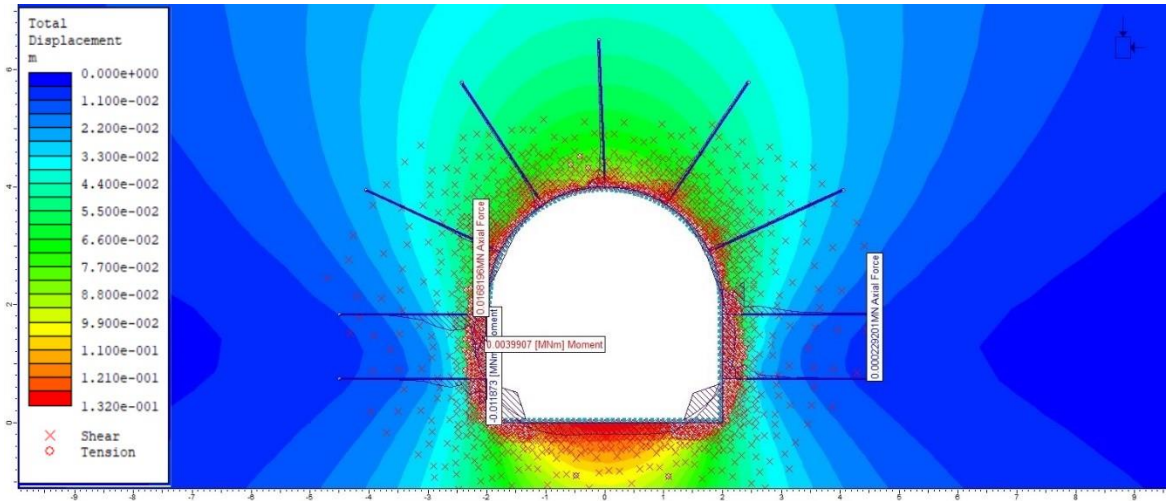


Figure 4-29: Axial force and BM at section 3+200

The support capacity diagrams, which are presented as Thrust Vs Shear Force and Thrust Vs Moment, for steel fiber reinforced shotcrete of 200 mm as well as steel rib ISMB 150 is generated and presented in the Figure below.

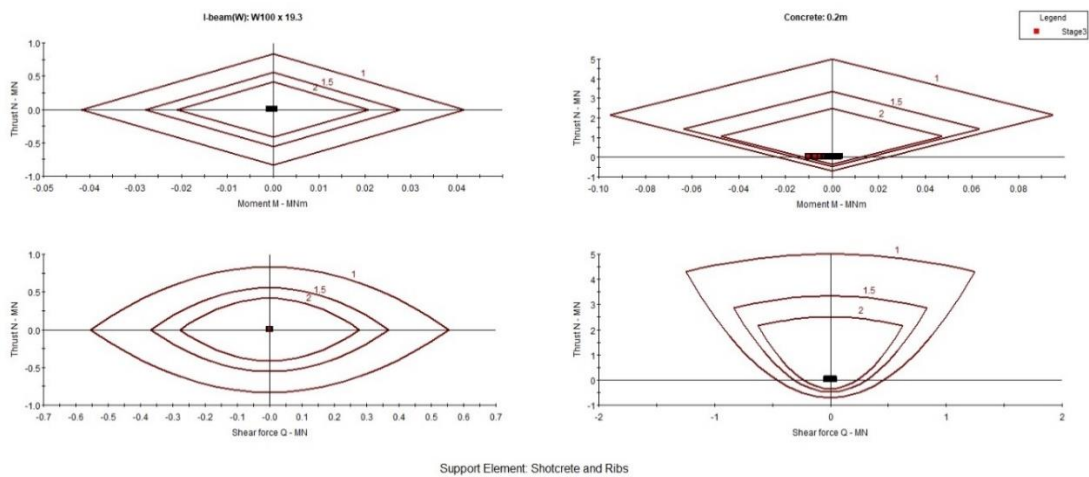


Figure 4-30: Safety envelope for section 3+200

From the above plot, all the elements fall within the factor of safety of '2' envelope on both plots for ISMB 150 and reinforced concrete. Also, no yielding is observed in any of the rock bolts. This means that the support system has a factor of safety greater than 2 thus achieving the design factor of safety.

Table 4-24: Supports suggested by Numerical Modeling for section 3+200

Steel Sets		Rock Bolts	
Type	ISMB 150	Type	End Anchored
Sectional depth	0.15 m	Length	2.5m
Area	0.00191 m ²	Diameter	25 mm
Youngs Modulus	2 × 10 ⁵ MPa	Bolt Modulus	2 × 10 ⁵ Mpa
Poisson Ratio	0.25	Out of plane Spacing	1.3 m
Spacing	1 m	Shotcrete	
Compressive Strength	435 MPa	Unconfined Compressive Strength	40Mpa
Tensile Strength	435 MPa	Youngs Modulus	30000 Mpa
Weight	15 Kg/m	Thickness of shotcrete	200mm
Moment of Inertia	7.18e-06m ⁴	Poisson's Ratio	0.15

The mean stress around the tunnel at different sections in supported and unsupported condition is given in Annex B.

4.8 Three-Dimensional Numerical Modelling

GTS-NX has been used to carry out 3D-Modelling in selected region of the tunnel alignment, where stress distribution changes along the alignment of the tunnel. Three such zones are selected:

- Adit Connection: The region where the adit meets the tunnel
- Underground Surge Shaft
- A bend in the tunnel

4.8.1 3D Adit Connection

In the Headrace Tunnel of the Upper Balephi 'A' Hydropower, an Adit of similar shape and size to the main tunnel is connected to the main tunnel at chainage 3+185 as shown in the figure below the overburden at the Adit connection is 170m.

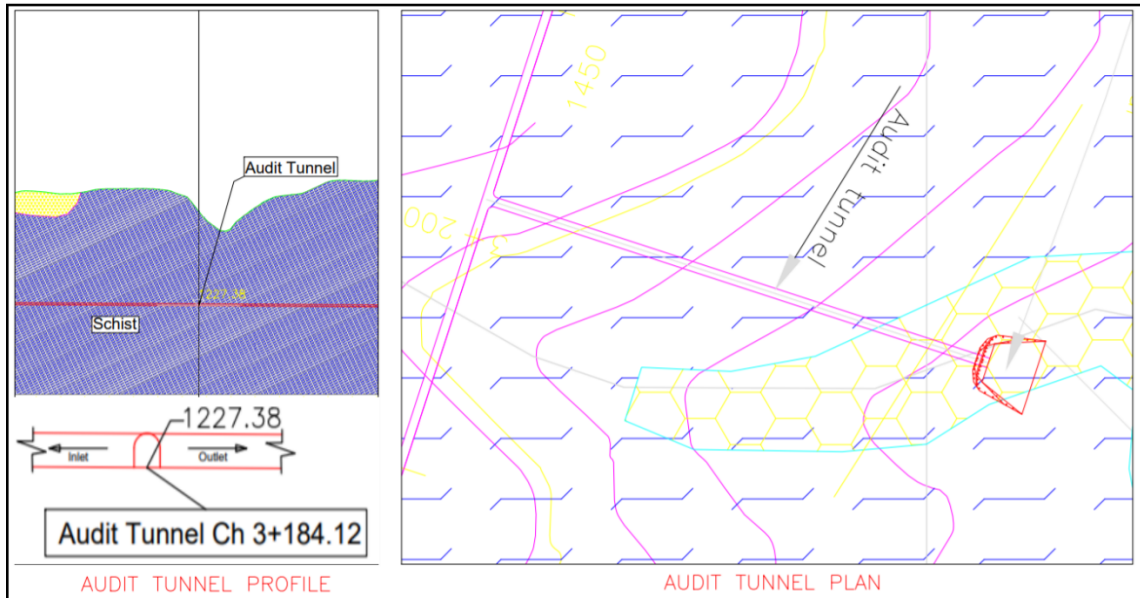


Figure 4-31: Location of Adit

Geometric Modelling

The symmetry of the connection is considered and the modelling is done for half of the adit section and the downstream face of the Main Tunnel. A control volume of 20m*40m*40m is modeled and YZ-plane is taken as symmetric plane which bisects the adit tunnel as shown in figure below.

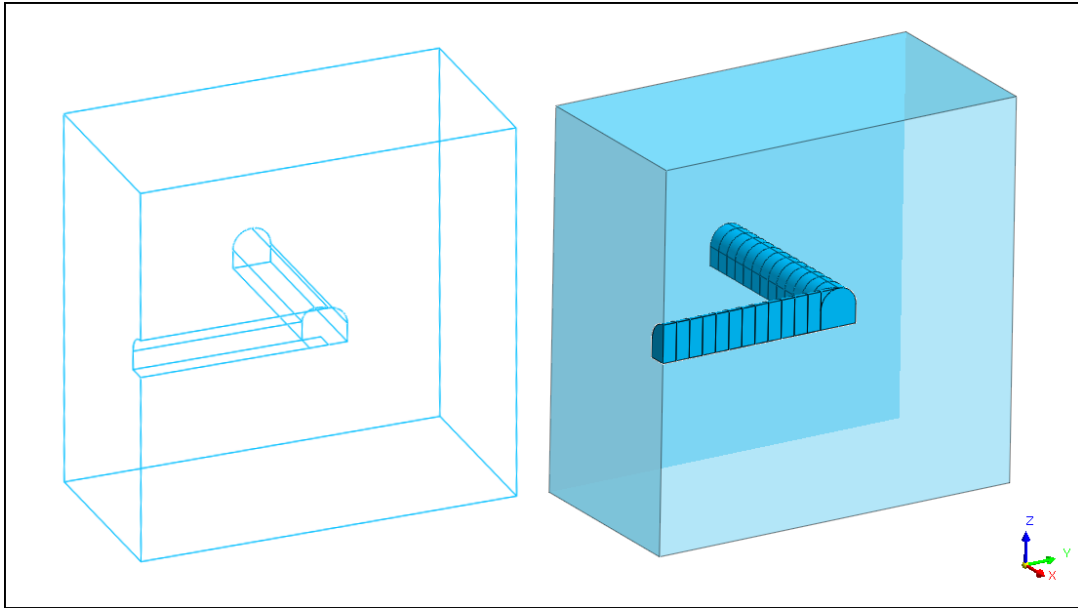


Figure 4-32: 3D Geometric modeling of Adit connection

Material Modeling, Loading and Boundary condition

The meshing, loading and boundary condition can be shown in the figure below.

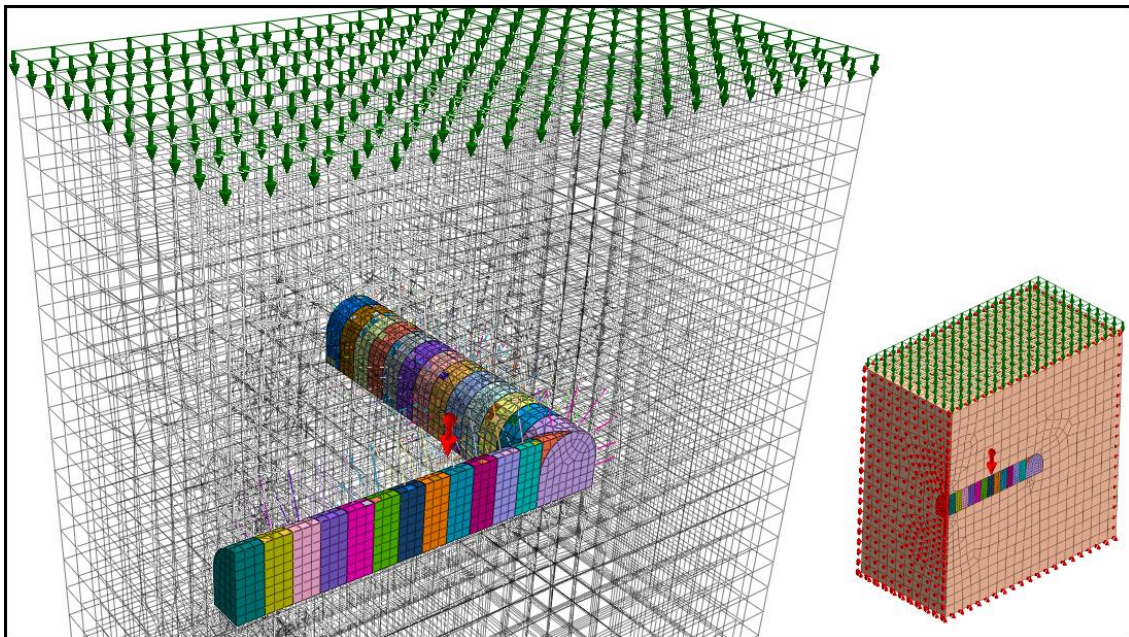


Figure 4-33: 3D Material modeling of Adit connection

Hybrid meshing is done throughout the model and mesh refinement is fine around the tunnel and gradually increasing in size as the distance from the excavation increases.

Self-weight of the model is assigned and the remaining overburden is provided as vertical load from the top face of the material model.

The model is restricted in translation at the four faces in the sides along the direction perpendicular to those faces and is restricted for translation along all three axes at the bottom face.

Material Properties

The tunnel, adit and the periphery around the excavation is assigned with rock properties obtained from the geological report of the project which is shown in section 1.6 above.

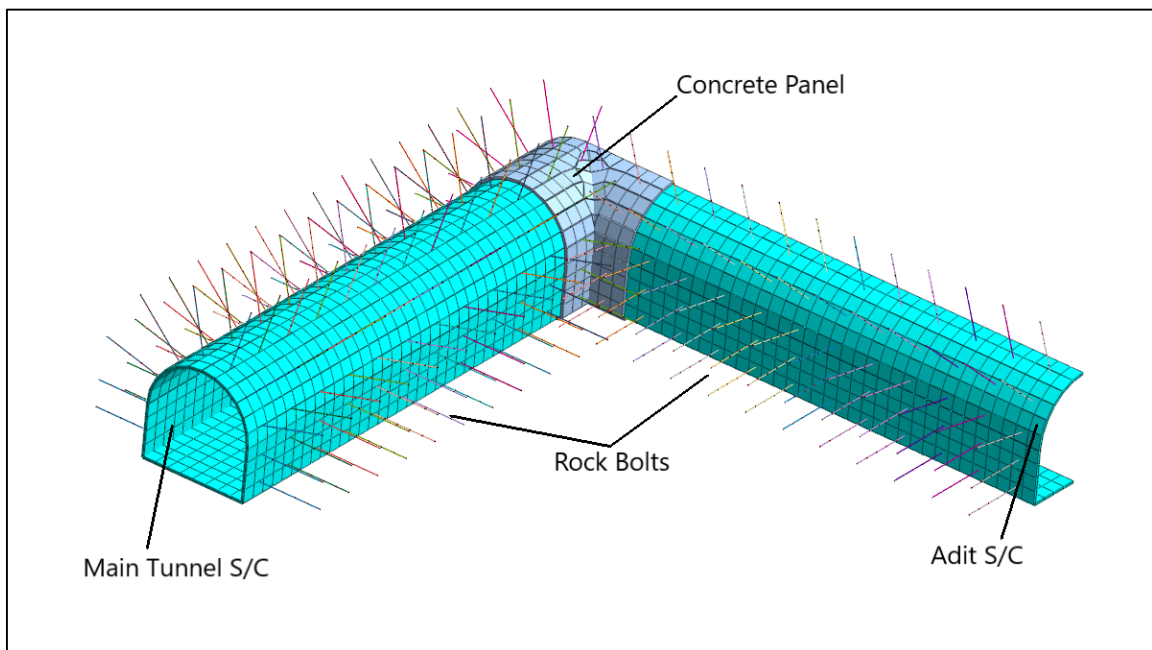


Figure 4-34: 3D presence of Concrete panel, Shotcrete and Rock Bolt in adit connection

The shotcrete lining and the rock bolts are assigned random properties and the property that gives the required factor of safety is selected as the support system. The shotcrete lining is assumed to possess 2D elastic shell property and the Rock Bolts are assumed to possess 1D elastic properties. The figure below shows the 3D appearance of the shotcrete lining with rock bolts in Main Tunnel and the Adit.

Construction stages and Analysis

The analysis is carried out in 28 stages. The Main Tunnel and Adit are so divided that an excavation of 1.5m is carried out in each step. In the first stage, the first 1.5 meters of the

adit is excavated and in the second stage the next 1.5 meters, along with installing support in the portion that was excavated in the previous stage. This can be illustrated from the figure below:

Set Type	Set Name Prefix	I.S.	S1	S2	S3	S4	S5	S6	S7	S8	S9	S10	S11	S12	S13	
Mesh set	Adit #-	A: 1to13	R: 1	R: 2	R: 3	R: 4	R: 5	R: 6	R: 7	R: 8	R: 9	R: 10	R: 11	R: 12	R: 13	
Mesh set	Adit R/B #-			A: 1	A: 2	A: 3	A: 4	A: 5	A: 6	A: 7	A: 8	A: 9	A: 10	A: 11	A: 12	
Mesh set	Adit S/C #-			A: 1	A: 2	A: 3	A: 4	A: 5	A: 6	A: 7	A: 8	A: 9	A: 10	A: 11	A: 12	
Boundary Set	Constraint	A: -														
Mesh set	Default Mesh Set															
Mesh set	Ground	A: -														
Mesh set	Main Tunnel #-	A: 1to13														
Mesh set	Main Tunnel R/B #-															
Mesh set	Main Tunnel S/C #-															
Load Set	Overburden	A: -														
Load Set	Self Weight	A: -														
Set Type	Set Name Prefix	S14	S15	S16	S17	S18	S19	S20	S21	S22	S23	S24	S25	S26	S27	S28
Mesh set	Adit #-															
Mesh set	Adit R/B #-	A: 13														
Mesh set	Adit S/C #-	A: 13														
Boundary Set	Constraint															
Mesh set	Default Mesh Set															
Mesh set	Ground															
Mesh set	Main Tunnel #-		R: 1	R: 2	R: 3	R: 4	R: 5	R: 6	R: 7	R: 8	R: 9	R: 10	R: 11	R: 12	R: 13	
Mesh set	Main Tunnel R/B #-			A: 1	A: 2	A: 3	A: 4	A: 5	A: 6	A: 7	A: 8	A: 9	A: 10	A: 11	A: 12	A: 13
Mesh set	Main Tunnel S/C #-			A: 1	A: 2	A: 3	A: 4	A: 5	A: 6	A: 7	A: 8	A: 9	A: 10	A: 11	A: 12	A: 13
Load Set	Overburden															
Load Set	Self Weight															

Figure 4-35: Construction stages in analysis of Adit connection

This construction stage analysis is carried out using a non-linear analysis based on Generalized Hoek-Brown criterion. The tolerance is kept at 0.001 for load and 1e-06 for work done. Newton-Raphson method was used to solve the non-linear equations at created nodes.

Results from Analysis

A construction stage analysis is carried out in GTS-NX using following support systems with following properties:

Table 4-25: Supports suggested by 3D numerical analysis of adit connection

Rock Bolts		Shotcrete		Concrete Panel	
Type	1D	Type	2D	Type	2D
Model	Embedded Truss	Model	Shell	Model	Shell

Poisson's Ratio	0.25	Poisson's Ratio	0.2	Poisson's Ratio	0.2
In plane Spacing	1m	Compressive Strength	25MPa	Compressive Strength	40MPa
Out of plane spacing	1.5m	Tensile Strength	3.5MPa	Tensile Strength	4MPa
Section Shape	Solid Round	Thickness	0.1m	Thickness	0.3m
Diameter	0.025m	Young's Modulus	25000MPa	Young's Modulus	25000MPa
Tensile capacity	0.1MN	Unit Weight	24 KN/m ³	Unit Weight	25 KN/m ³
Bolt Modulus	200000 MPa				

The displacement in and around the junction, shear force in shotcrete and concrete panel, and the axial force on Rock Bolts are discussed below

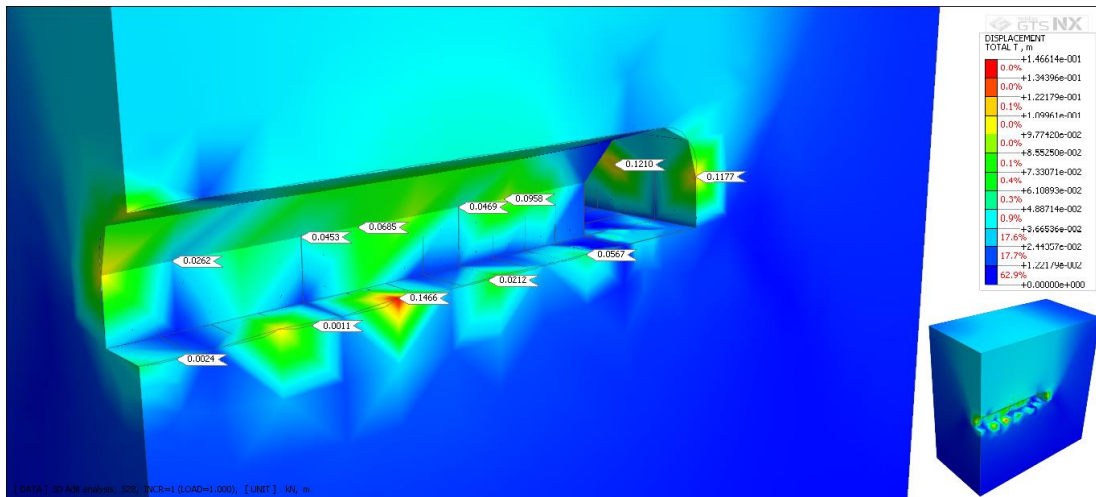


Figure 4-36: Displacement around adit connection

The above figure shows the displacement in and around the adit connection. Considering the symmetry of the geometric model, only half of the adit section is shown here, connected to the main tunnel. Probes has been used to query the displacement at few random nodes in the model which show the value of displacement at that point. We can see how the displacement has increased as we approach the junction of the adit with the Main Tunnel. There are a couple of nodes where the displacement is uncharacteristically high and this is because of the limitations of the control volume we can make to simulate the real field condition. The displacement is maximum at the spring line at the junction of the Adit and Main Tunnel.

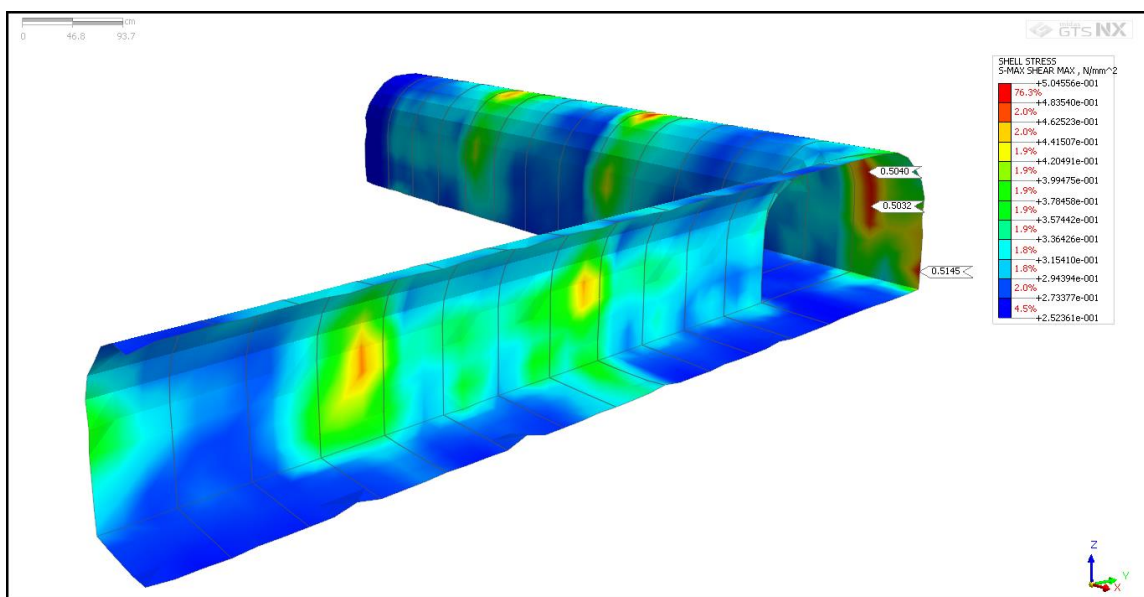


Figure 4-37: Maximum shear stress in shotcrete lining and concrete panel

The figure above shows the maximum shear stress imposed on the shotcrete and concrete lining. We can see here that as we approach the junction, the shear stress goes on increasing and is the highest at the junction. This is because at the junction, the unsupported span of the excavation increases and the stress distribution varies in all three dimensions.

The maximum shear strength of shotcrete of 100mm thickness for a tunnel radius diameter of 4m is 1.219 MPa, obtained by using the property of hollow cylinder as explained in section ... above. Here, the maximum shear stress induced is 0.504 MPa.

This gives a minimum factor of safety of 2.42 at the junction. Besides, the excavation at the junction is lined using concrete panel which is even stronger than shotcrete.

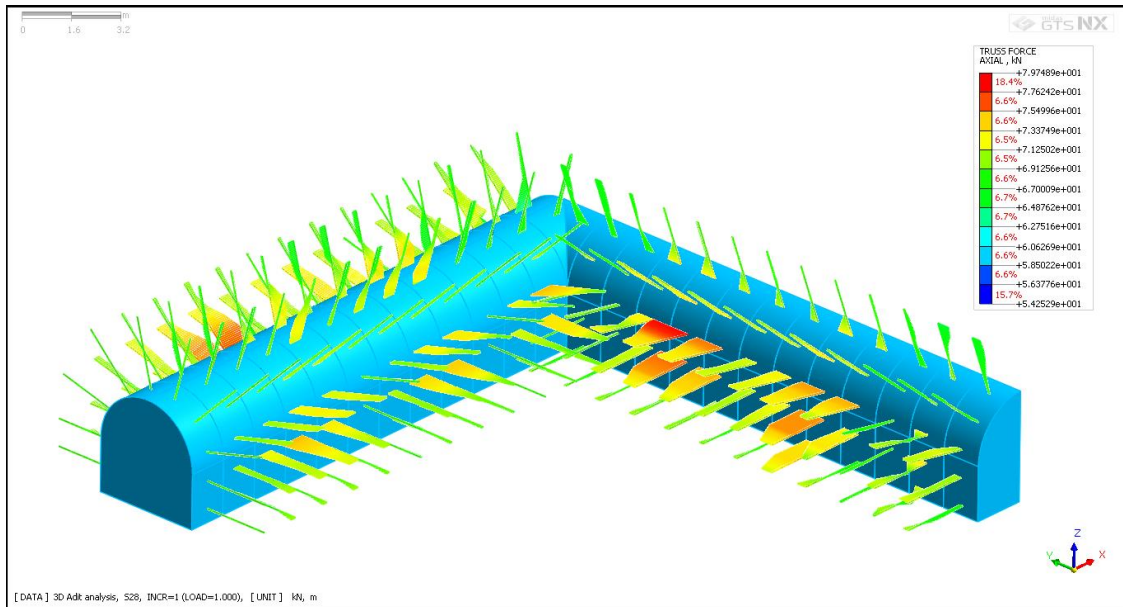


Figure 4-38: Axial force in rock bolts around adit

The figure above shows the axial force imposed on the rock bolts in the Main Tunnel and Adit. The axial force on the model is somewhat homogeneous. This is because the additional force that is supposed to be imposed on the rock bolts at the junction is attenuated by the concrete panel casted at the junction.

The maximum tensile capacity of the bolt used is 0.1MN, i.e. 100 KN. The maximum axial force induced in the Rock Bolt here is 79 KN. This gives factor of safety of 1.27 at the junction. Considering the junction is lined using concrete panel, this value of safety factor is safe.

The mean stresses around the adit connection and excavation construction stages are shown on Annex C.

4.8.2 3D Surge Shaft and Ventilation Tunnel

At a chainage of 4+520, there's an underground vertical surge shaft of 8m diameter and 48m height. A ventilation tunnel is attached to the top of the surge shaft that protrudes into the ground surface as shown in the figure below.

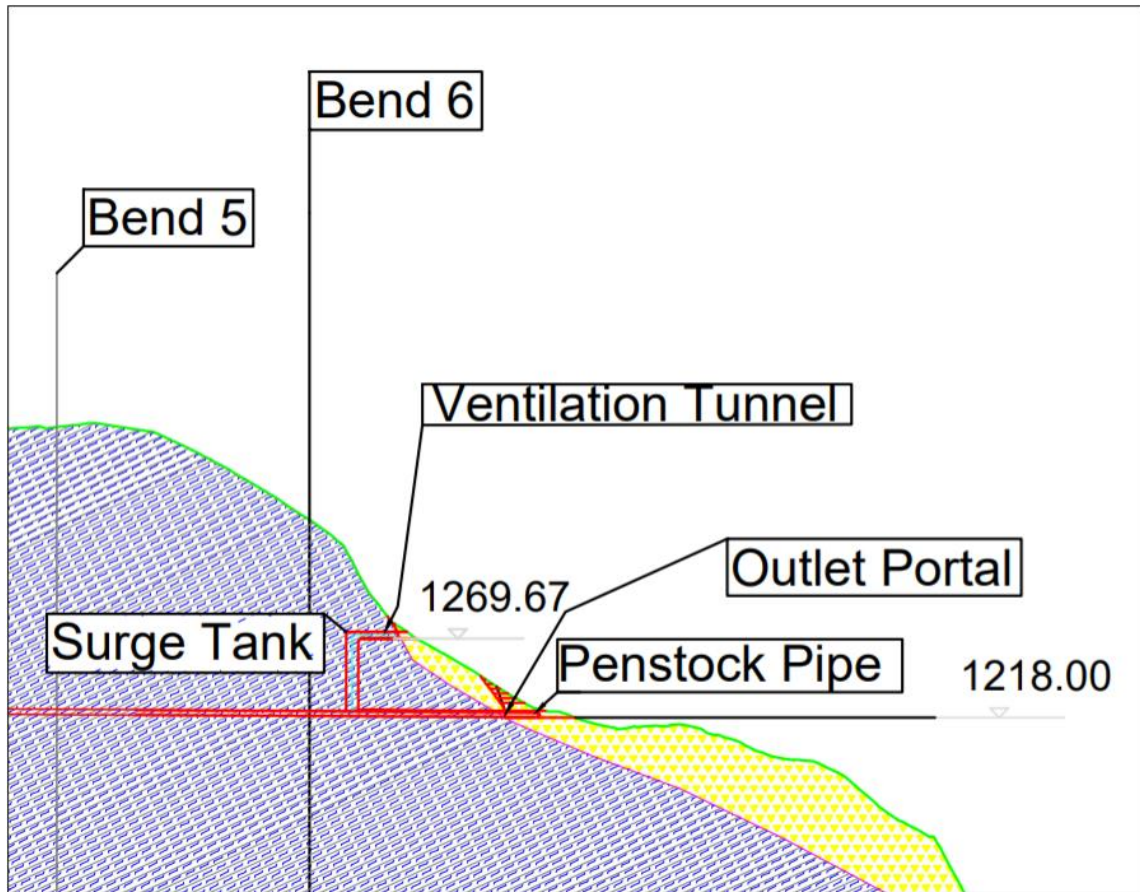


Figure 4-39: Location of Surge Shaft in HRT

Geometric Modelling

Considering the symmetry plane passing vertically through the axis of the main tunnel, the geometric model is prepared as shown in the figure below. The plane of symmetry is XZ-plane and a control volume of width 20m and of length 20m upstream from the surge shaft and the length of the ventilation tunnel i.e. 33.425m downstream of the shaft is considered for modelling. The topmost face of the model is made by extruding a spline in order to represent the real ground surface above the surge shaft.

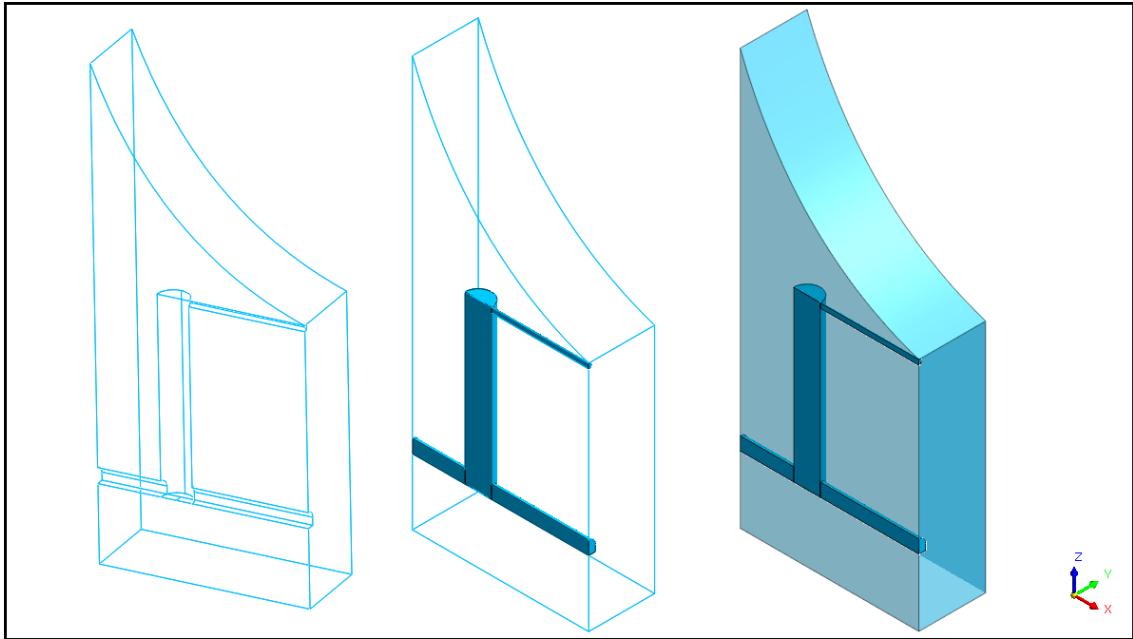


Figure 4-40: 3D geometric model of surge shaft

Material Modeling, Loading and Boundary Condition

The meshing, loading and boundary conditions are shown in the figure below.

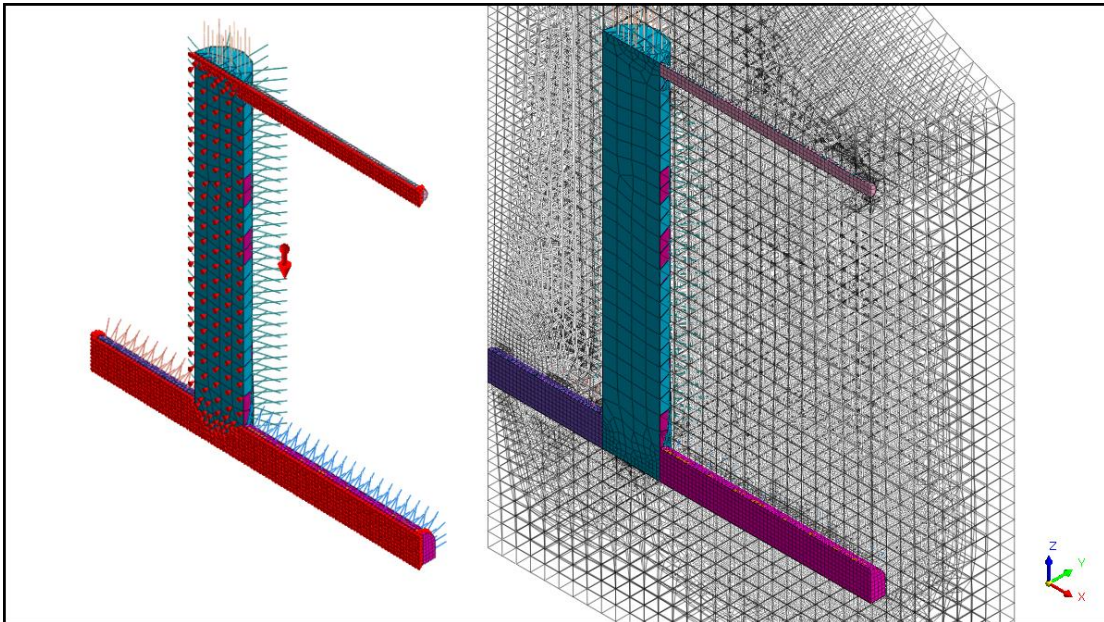


Figure 4-41: 3D meshing, loading and boundary conditions of Surge Shaft

Hybrid meshing is done throughout the model and mesh refinement is fine around the tunnel and gradually increasing in size as the distance from the excavation increases.

The upper face of the model represents the real ground surface so only self-weight of the model is applied and no extra overburden in the form of pressure from the top has to be applied.

The material model is restricted in translation at the four faces in the sides along the direction perpendicular to those faces and is restricted for translation along all three axes at the bottom face. The upper face of the model is free to move in all three direction.

Material Properties

The main tunnel, surge shaft, the ventilation tunnel and the periphery around the excavation is assigned with rock properties obtained form the geological report of the project which is shown in section above.

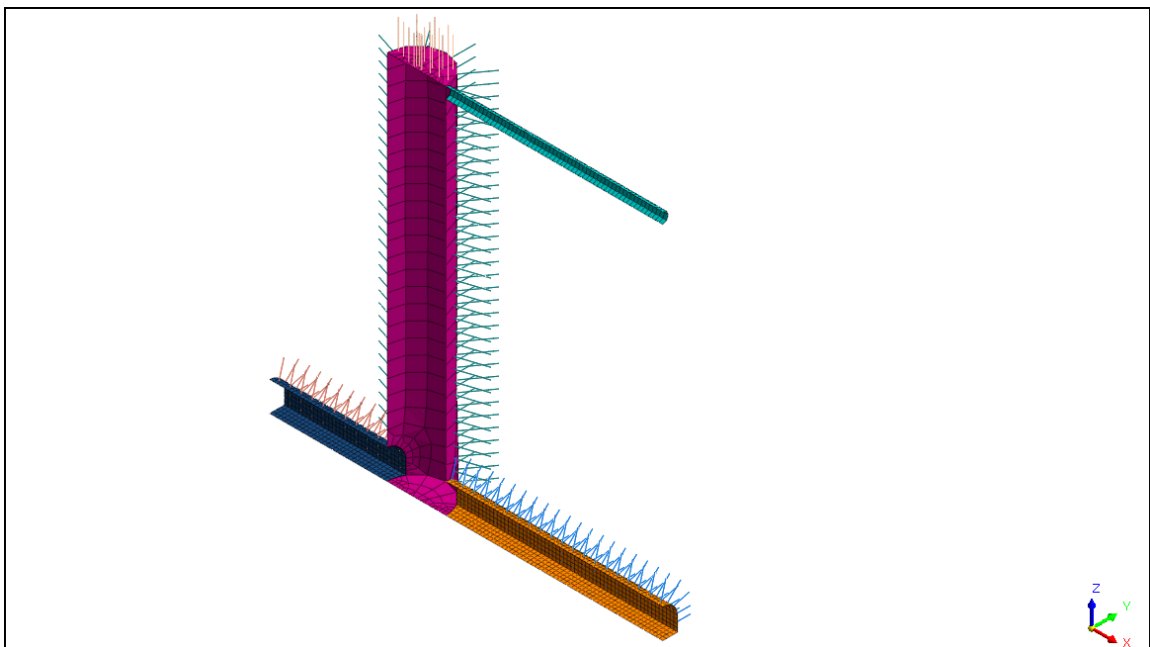


Figure 4-42: 3D presence of shotcrete lining and rock bolts in Surge Shaft, main tunnel and ventilation tunnel.

The shotcrete lining and the rock bolts are assigned random properties and the property that gives the required factor of safety is selected as the support system. The shotcrete lining is assumed to possess 2D elastic shell property and the Rock Bolts are assumed to possess 1D elastic properties. The figure above shows the 3D appearance of the shotcrete lining with rock bolts in the region of vertical surge shaft.

Results from Analysis

This analysis is carried out using a non-linear analysis based on Generalized Hoek-Brown criterion. The tolerance is kept at 0.001 for load and 1e-06 for work done. Newton-Raphson method was used to solve the non-linear equations at created nodes. This three-dimensional analysis is carried out in GTS-NX using following support systems with following properties:

Table 4-26: Supports suggested by 3D numerical analysis of Surge Shaft

Rock Bolts		Shotcrete	
Type	1D	Type	2D
Model	Embedded Truss	Model	Shell
Poisson's Ratio	0.25	Poisson's Ratio	0.2
In plane Spacing	1m	Compressive	25MPa
Out of plane	1.5m	Tensile Strength	3.5MPa
Section Shape	Solid Round	Thickness	0.1m
Diameter	0.025m	Young's Modulus	25000MPa
Tensile capacity	0.1MN	Unit Weight	24 KN/m ³
Bolt Modulus	200000 MPa		

The displacement in and around the junction, shear force in shotcrete, and the axial force on rock bolts are discussed below.

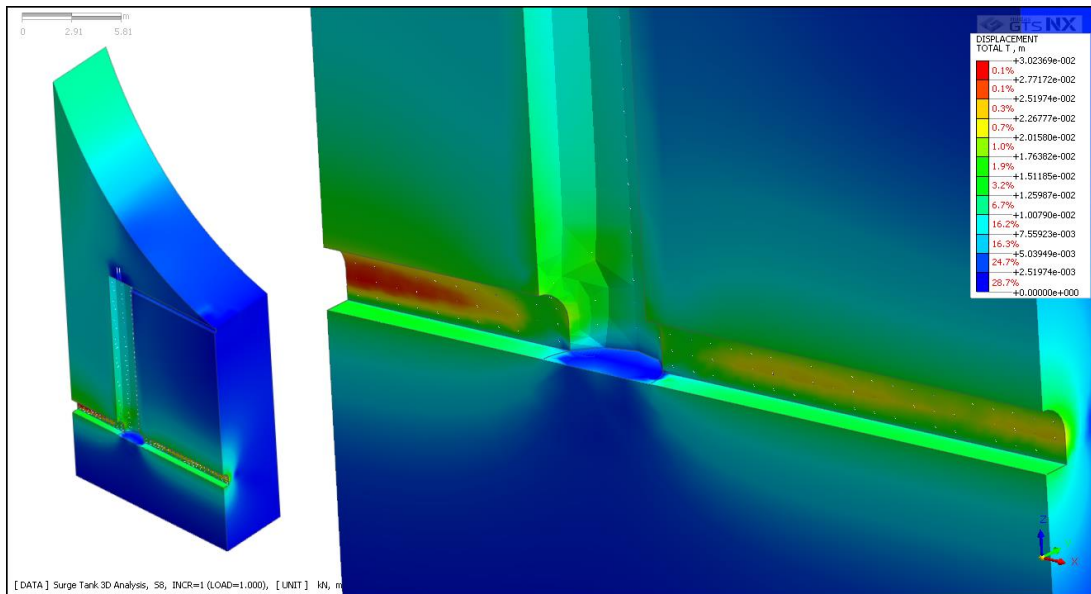


Figure 4-43: Displacement around the Surge Shaft

In the figure above, we can see the displacement in the periphery of the surge shaft. The displacement in the upstream of the surge shaft is high and this is due to the changing level of ground surface and hence the overburden as we move upstream from the surge shaft.

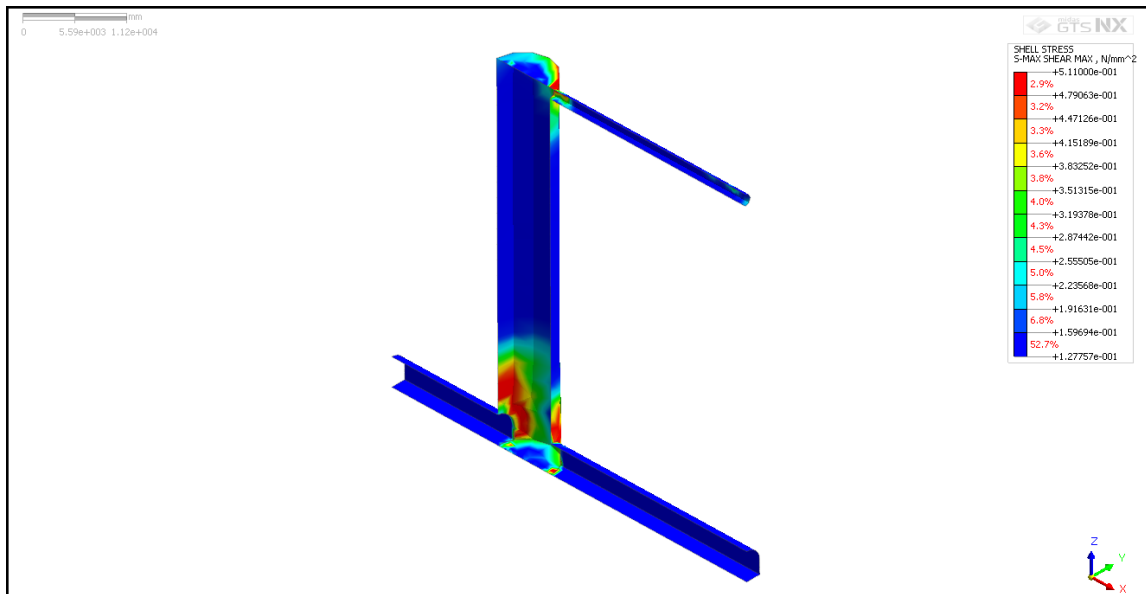


Figure 4-44: Maximum shear stress around the Surge Shaft

The figure above shows the maximum shear stress imposed on the shotcrete lining. The stress is maximum at the junction of the surge shaft with the main tunnel. This stress has increased from top to bottom of the surge shaft as the vertical in-situ stress goes on increasing.

The maximum shear strength of shotcrete of 100mm thickness for a tunnel radius diameter of 4m is 1.219 MPa, obtained by using the property of hollow cylinder as explained in section ... above. Here, the maximum shear stress induced is 0.511 MPa. This gives a minimum factor of safety of 2.38 at the junction. Since, the factor of safety is above two, this can be considered safe.

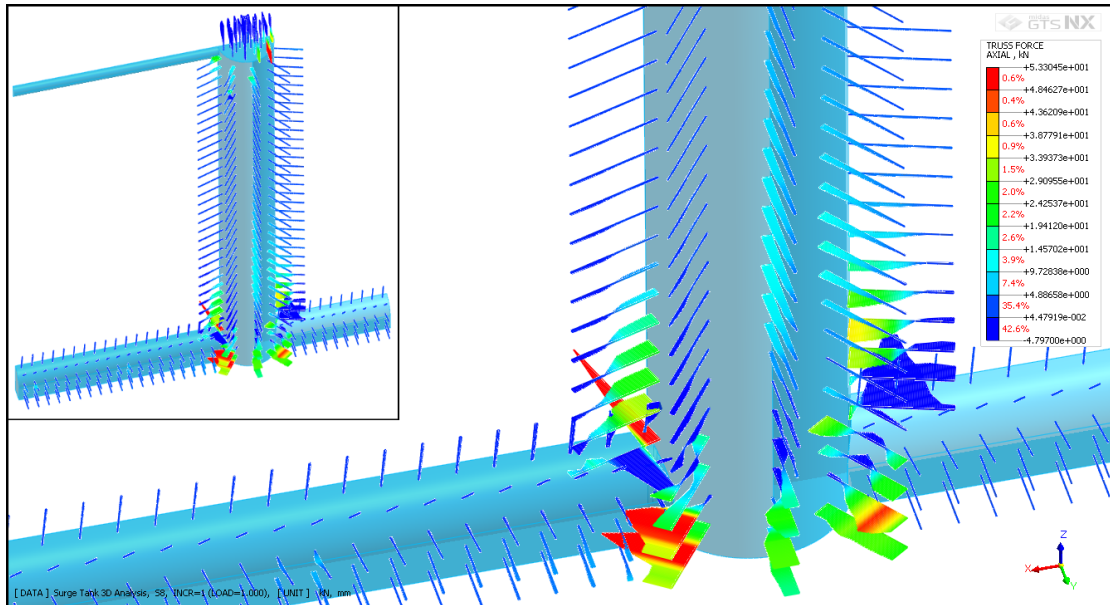


Figure 4-45: Axial force imposed on rock bolts around the Surge Shaft

The figure above shows the axial force in the rock bolts in the periphery of the surge shaft. Here, it can be seen that the axial force is maximum at the main tunnel-surge shaft junction, near the flat invert of the tunnel.

The maximum tensile capacity of the bolt used is 0.1MN, i.e. 100 KN. The maximum axial force induced in the Rock Bolt here is 53.3 KN. This gives factor of safety of 1.87 at the junction. Considering the junction is lined using concrete panel, this value of safety factor is safe.

The mean stresses around the junction are shown on the Annex C.

4.8.3 3D bend in the tunnel

As far as possible, it is desirable to construction a straight tunnel as it would keep the instability problems to the minimum. But geological conditions don't always permit this and sometimes bends are unavoidable. In bends, the influence of the two members that connect at the bend overlaps and the stress distribution becomes three dimensional.

In the plan of the headrace tunnel of the project, there are several bends at different chainage. One of such bends at a chainage of 1+460 as shown in the figure below is taken for three-dimensional modeling.

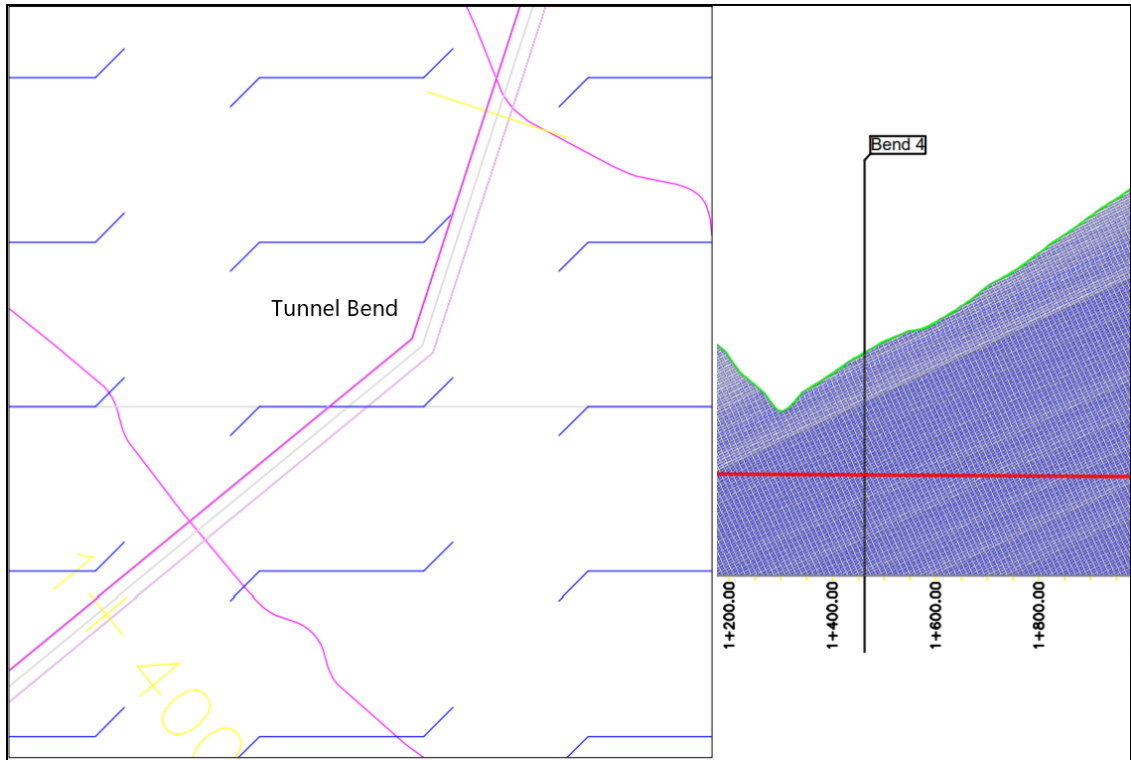


Figure 4-46: Location of a bend in the tunnel

The bend shown above has an overburden of 239m. The properties of the rock around the bend are explained in geological summary of the project in section 1.6.3 above.

Geometric Modeling

Since, this model represents a bend, the symmetry cannot be considered and a control volume of 40m*40m*40m is considered for numerical modeling.

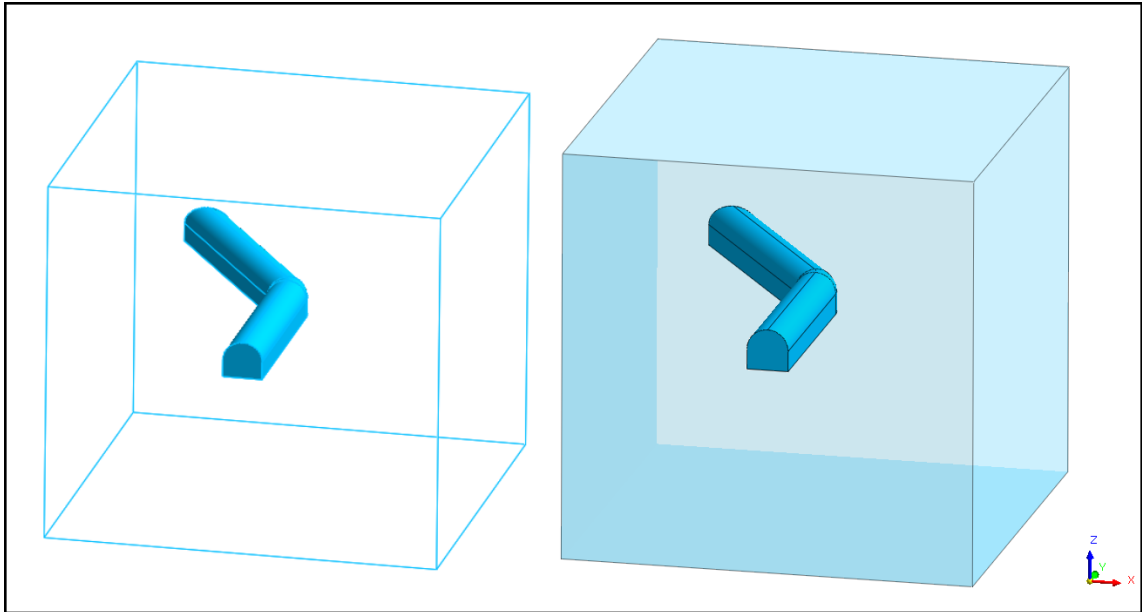


Figure 4-47: 3D geometric model of a tunnel bend

Material Modeling, Loading and Boundary condition:

The meshing, loading and boundary condition can be shown in the figure below:

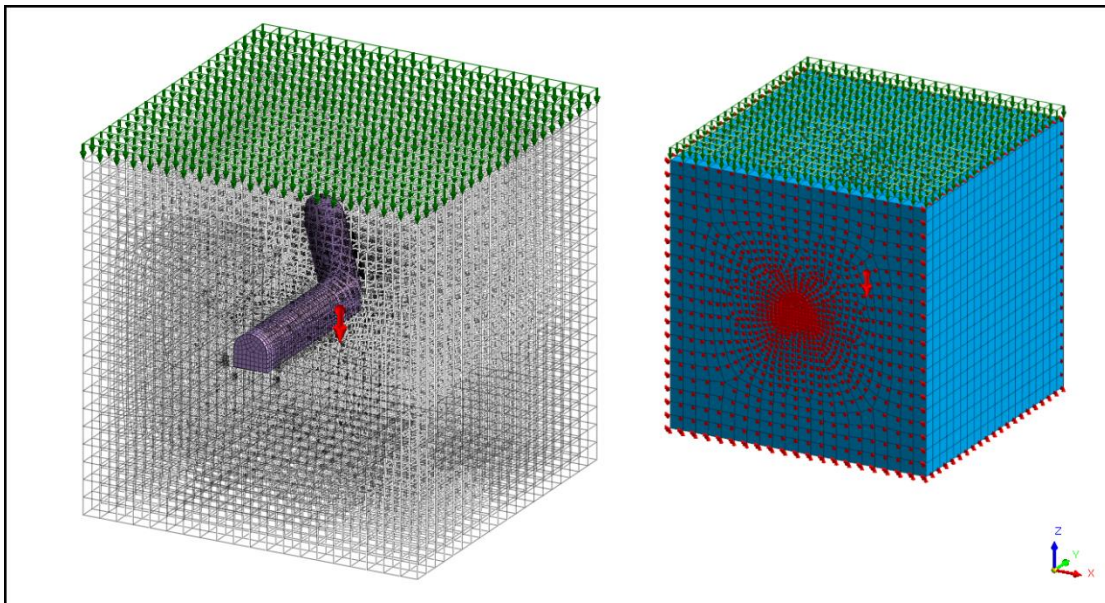


Figure 4-48: Meshing, Loading and boundary conditions around the tunnel bend

Hybrid meshing is done throughout the model and mesh refinement is fine around the tunnel and gradually increasing in size as the distance from the excavation increases.

Self-weight of the model is assigned and the remaining overburden is provided as vertical load from the top face of the material model.

The material model is restricted in translation at the four faces in the sides along the direction perpendicular to those faces and is restricted for translation along all three axes at the bottom face. The upper face of the model is free to move in all three direction.

Materials Properties

The main tunnel around the bend and the periphery around the excavation is assigned with rock properties obtained from the geological report of the project which is shown in section 1.6.3 above.

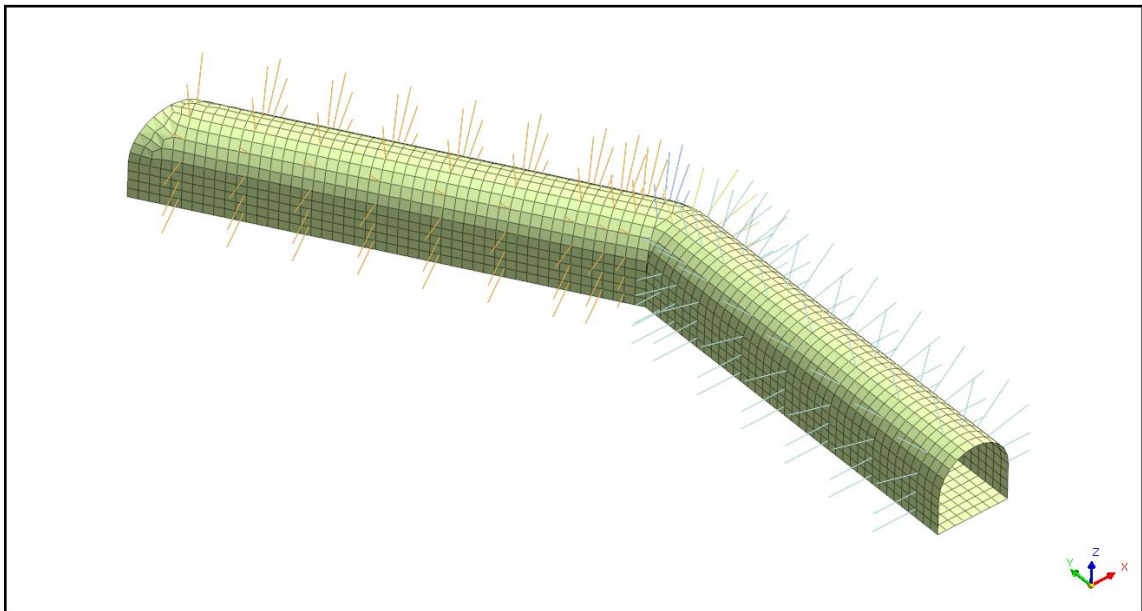


Figure 4-49: 3D presence of shotcrete and rock bolts around the bend

The shotcrete lining and the rock bolts are assigned random properties and the property that gives the required factor of safety is selected as the support system. The shotcrete lining is assumed to possess 2D elastic shell property and the Rock Bolts are assumed to possess 1D elastic properties. The figure above shows the 3D appearance of the shotcrete lining with rock bolts in the region of vertical surge shaft.

Results from Analysis

This analysis is carried out using a non-linear analysis based on Generalized Hoek-Brown criterion. The tolerance is kept at 0.001 for load and 1e-06 for work done. Newton-Raphson method was used to solve the non-linear equations at created nodes. This three-dimensional analysis is carried out in GTS-NX using following support systems with following properties:

Table 4-27: Supports suggested on the tunnel bend by 3D numerical modeling

Rock Bolts		Shotcrete	
Type	1D	Type	2D
Model	Embedded Truss	Model	Shell
Poisson's Ratio	0.25	Poisson's Ratio	0.2
In plane Spacing	1m	Compressive Strength	25MPa
Out of plane spacing	3m (1m at bend)	Tensile Strength	3.5MPa
Section Shape	Solid Round	Thickness	0.5m
Diameter	0.025m	Young's Modulus	25000MPa
Tensile capacity	0.1MN	Unit Weight	24 KN/m ³
Bolt Modulus	200000 MPa		

The displacement in and around the junction, shear force in shotcrete, and the axial force on rock bolts are discussed below:

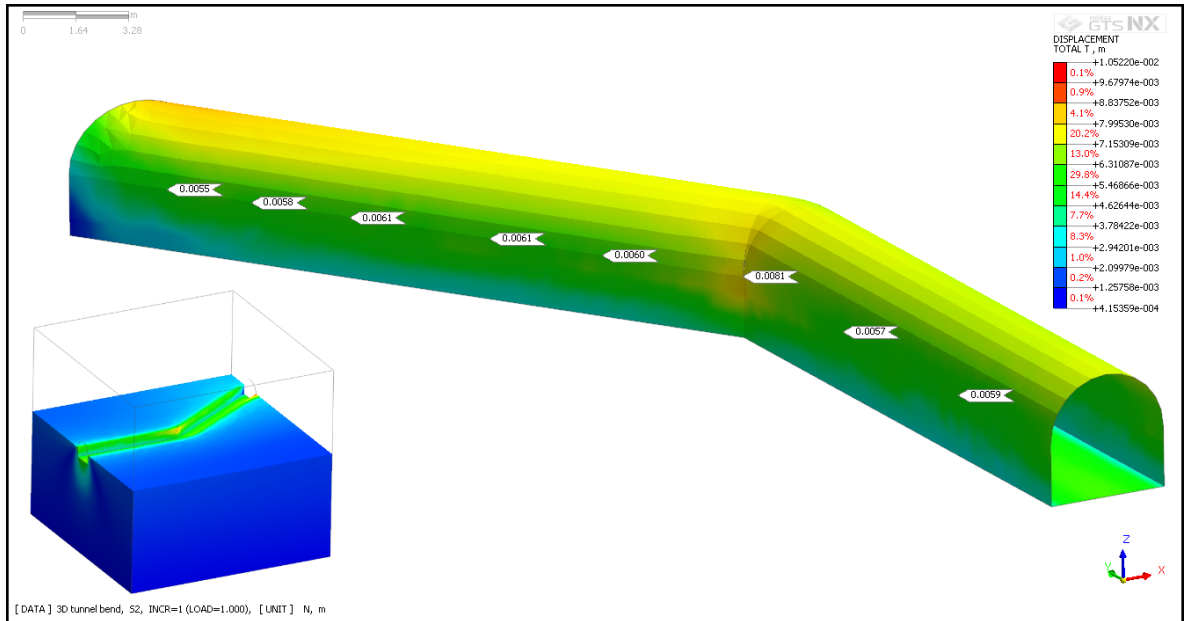


Figure 4-50: Displacement around the tunnel bend

In the figure above we can see that the displacement is largest at the bend which is caused due to the influence zone of two excavations overlapping. Probes are used to query displacement at discrete points along the spring line of the tunnel.

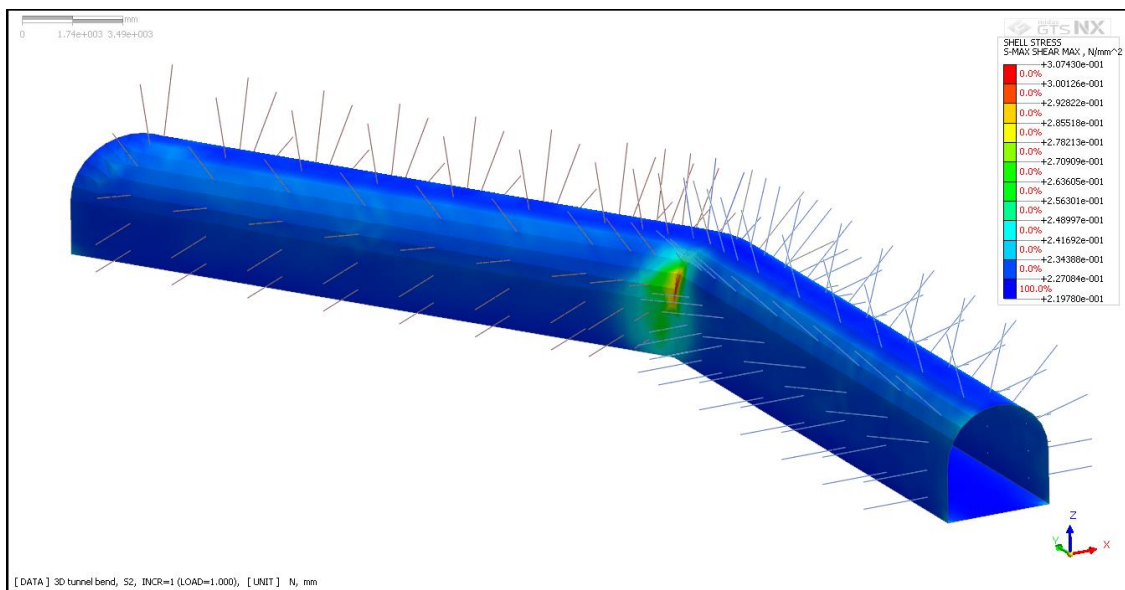


Figure 4-51: Maximum shear stress around the tunnel bend

The figure above shows the maximum shear stress imposed on the shotcrete lining. The stress is maximum at the bend as can be seen from the color contour. This stress has

increased from top to bottom of the surge shaft as the vertical in-situ stress goes on increasing.

The maximum shear strength of shotcrete of 50mm thickness for a tunnel radius diameter of 4m is 0.617 MPa, obtained by using the property of hollow cylinder as explained in section ... above. Here, the maximum shear stress induced is 0.307 MPa. This gives a minimum factor of safety of 2.09 at the junction. Since, the factor of safety is above two, this can be considered safe.

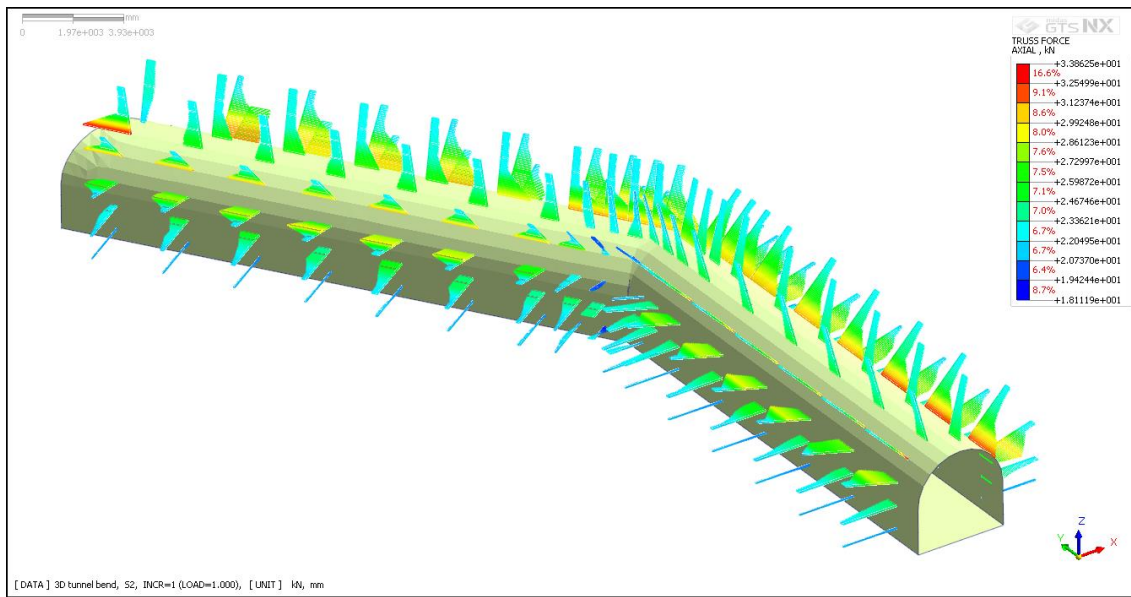


Figure 4-52: Axial force in the rock bolts around the tunnel bend

The figure above shows the axial force imposed on the bolts in the periphery of the tunnel. Here, the axial force on the bolt near the bend is not significantly higher than that imposed on rock bolts away from the bend. This is because the support system is designed in such a way that the out of plane spacing of the rock bolts goes on decreasing as we approach the bend.

The maximum tensile capacity of the bolt used is 0.1MN, i.e. 100KN. The maximum axial force imposed in the rock bolt here is 33.86KN. This gives a minimum factor of safety of 2.95, which can be considered significantly desirable.

The mean stresses around the tunnel bend are presented on the Annex.

4.9 Discussions

The study explored the design of a support system for a 4 m diameter underground D-shaped tunnel. Overall, this study found that a comprehensive design of an adequate tunnel support system cannot be accomplished using only one approach. Moreover, it is wise to conduct a three-dimensional analysis and design of support systems in case of certain features that break the longitudinal homogeneity of the tunnel. The required support selected should be the most accurate result of the different solutions. The highest capacity of the support represents the highest factor of safety, a universal engineering design concept. Through rigorous designs, underground geotechnical engineering instability problems causing tunnel failure can be minimized. The conclusion drawn can be summarized as:

General observations and discussion:

- Soft rocks are more prone to squeezing problems whereas hard, intact rock masses succumb to bursting phenomenon.
- The solution of an instability problem varies depending on the method used to analyze it.
- The analytical, FEM and empirical methods are independent with no correlations. They provide certain suggestions based on the principles or assumptions they are built upon.
- The empirical method gives very first estimate for the support analysis. The Q and RMR method also help in rock mass classification which is helpful in further design. The empirical method suggests same type of support if they fulfil a certain criterion but geological condition has to be verified.
- The analytical method provides better result considering the individual section. Factor of Safety more than one is considered safe. In this thesis the supports are designed so that factor of safety is greater than or equal to 2.
- The analytical method provides the information about when the support should be installed and the deformation that can be allowed before the installation of support through the GRC and SCC. It also gives information on how far away from the face the support should be installed through LDP.

- The numerical modeling is the most accurate method for support system design as it gives detail information in the form of readily available axial force and moment diagrams, and safety envelopes.
- The results obtained from the three-dimensional methods has the highest efficacy and is easy and less tedious to understand as it provides results in form of contour maps in three dimensional spaces.

Case specific observations and discussion:

- At section 0+600, the ground reaction curve plot using convergence confinement method showed the maximum tunnel closure of 0.0008m. This is almost negligible amount of displacement and the tunnel is unlikely to fail due to deformation. Hence, support suggested by empirical methods are sufficient. The numerical modeling was done using the support system suggested by Q-value method and the factor of safety obtained was more than 2, which is satisfactory. Since, the RMR value of the rock mass is 70, this section was checked for possibility of rock burst but it was found to be stable. Also, the empirical and semi-empirical methods of prediction of squeezing suggested no squeezing in this section.
- At section 1+400, FOS of 2.95 was obtained by using 75mm thick shotcrete only. So, the support system suggested by the empirical method was input in the Numerical Model and the result was well within the envelope of safety factor 2. No squeezing condition was found in this section and while Hoek and Brown method of assessing rock burst suggested minor spalling on wall, Grimstad and Barton's method suggested that the stress condition was favorable.
- At section 2+000, the overburden is drastically high (590m). The support suggested by empirical method did not yield a satisfactory safety factor when put against the analytical method. The RMR of this section was 40 but it was checked against both squeezing and rock burst, especially due to such a high amount of rock cover. The empirical method of assessment of squeezing by Singh and Goel both suggested squeezing to occur while the semi-empirical method by Jethwa et al suggested no squeezing. However, due to significantly high overburden, the

Grimstad and Barton method suggests that slabbing and bursting will occur in minutes in the wall of this section.

- At section 2+500, the support suggested by empirical method was tested against CCM and Numerical modeling and both gave satisfactory factor of safety, more than 2. Upon analyzing for rock burst, it was found to be stable. As the rock cover is high (345m), Grimstad and Barton's method of assessment of rock burst suggested that there is very high stress around the tunnel which is usually favorable to overall stability but maybe unfavorable to stability of the wall. Thus, special care should be done while providing the support system. While, semi-empirical method suggested by Jethwa et al suggested no squeezing but the empirical method of squeezing analysis suggested squeezing to occur. This might be because the SRF of the rock is assumed as 1 in semi-empirical approach but that might not be the real case.
- At section 3+200, the rock has RMR value of 25. The support system suggested by empirical method did not give a satisfactory FOS when checked against the analytical method. Rather, the analytical method demanded rock bolt with spacing 0.5×0.5 and an ISMB steel rib with spacing 0.5m. But when the support system suggested by empirical method was input in Numerical modelling, the safety factor was found to be above two. This might put a light on the limitations of convergence confinement method as it considers a hydrostatic condition and assumes the tunnel shape to be circular, whereas in reality this isn't the case. Upon assessment of rock bursting, this section was found to show minor spalling on the sidewall whereas, in analysis of squeezing, the method suggested by Jethwa et al suggested no squeezing to occur.
- The three-dimensional analysis of the adit connection suggested that by providing a concrete panel at the junction of the main tunnel and adit, desired factor of safety can be attained. The actual FOS attained was 2.42 in case of shotcrete lining and 1.27 for bolt around the junction, which can be considered safe considering that concrete panel is provided in the junction where the axial force on the rock bolts is the highest. Similar FOS were obtained in case of surge shaft and tunnel bend.

5 CONCLUSIONS AND RECOMMENDATIONS

5.1 Conclusions

The following are the conclusions made by this research.

1. The deformation at section 0+600 is 0.0008 mm which is significantly low. This section is rather prone to failure by rock burst. But upon prediction of rock burst using the approaches suggested by various researchers, the section was found stable against rock burst. A support system of 3m long rock bolt in crown spaced 2.5m with wire mesh and 50mm thick shotcrete where required is suggested for section 0+600.
2. The maximum tunnel closure at section 1+400 is 0.004 mm which is also significantly low, so rock burst is the major risk for failure. Upon assessment of potential rock burst or squeezing, it was found to be stable against both. The support suggested is 75mm thick shotcrete lining with 25mm diameter, 2.5m long grouted rock bolts at a in place spacing 1.5m and out of plane spacing of 1.5m.
3. The maximum tunnel closure at section 2+000 is 0.25m which is significantly high and squeezing was found to be the major cause of potential failure in this section. The support system suggested at section 2+000 is 200mm thick shotcrete with 2.5m long 25mm diameter rock bolts at a spacing of 1.3 circumferential and 1.5 tangential.
4. The support recommended for section 2+500 is 150mm thick shotcrete with 2.5m long 25mm rock bolts at a spacing of 1.1×1.3m. For potential rock burst the stress condition is favorable for roof but not so favorable for wall. But for this section squeezing problem was found to be the major cause of failure. Therefore, special precaution should be taken.
5. The support recommended for section 3+200 is 200 mm thick shotcrete lining with 2.5m long 25mm rock bolts with spacing of 1.1×1.3m. Steel rib ISMB 150 with spacing 1m also should be provided as the rock mass in this section is found to be very weak. Special measures should be taken against squeezing.
6. Different support systems were tried in this section like, decreasing the out of plane spacing of the rock bolts as we move towards the junction, increasing length

of rock bolts as we move towards the junction, etc. But most satisfactory results were obtained when a concrete panel was provided at the junction. Supports suggested for adit connection are rock bolts of 25mm diameter and 2.5m length with 1×1.5m spacing, 100mm thick shotcrete lining and 300mm thick concrete panel at the junction where the unsupported span is high.

7. For surge shaft, 100mm shotcrete lining around the surge shaft and 4m long 25mm rock bolts placed in pattern throughout the 48m high surge shaft is recommended. At the roof of the surge shaft, a set of rock bolts should be provided with low to high spacing from the center to the circumference.
8. The support system recommended is 50mm thick shotcrete with 2.5m long 25mm diameter rock bolts with in plane spacing of 1m and out of plane spacing of 1m at the bend increasing to 3m as we move away from the bend.

5.2 Recommendations:

The recommendations made by this research and suggestions for future works are given below:

1. While two-dimensional analysis is sufficient for analysis of stress distribution and design of support system, in places where the longitudinal symmetry breaks and stress varies along the longitudinal direction, only three-dimensional approach can give accurate results.
2. Most of the designs today involving tunnel junctions with adit, with surge shaft or in cases of bends in the tunnel are made using empirical methods assuming conservative design with high factor of safety. But this might turn out to be uneconomical and numerical modeling is necessary to properly design support system for exceptional regions as such.
3. The results obtained can be verified with stress measurements. This will help determine whether the provided support is sufficient or not.
4. For more accurate design of the support system, numerical modeling can be done considering discontinuities.

5. Study of mineralogical properties of the rock mass around the tunnel can be done which will provide the basis for detailed study on squeezing potential in the tunnel walls.

6 REFERENCES

- Abel, J., & Desai, C. (1987). *Introduction to the Finite Element Method*.
- Atkinson, K. (2007). Numerical analysis. *Scholarpedia*, 2(8).
- Balasubramanian, A. (2017). *Tunnel-types and importance*. Research gate.
- Barton, N., & Grimstad, E. (2014). Forty years with the Q-system in Norway and Abroad. *GEOTEKNIKK*.
- Brady and Brown. (2004). *Rock Mechanics for Underground Mining*. New York.
- Carranza-Torres, C., & Fairhurst, C. (1999). General formulation of the elasto-plastic response of openings in rock using the Hoek-Brown failure criterion. *Int. J. Rock Mech. Min. Sci.*
- Carranza-Torres, C., & Fairhurst, C. (2000). Application of the convergence-confinement method of tunnel design to rock masses that satisfy the Hoek-Brown failure criterion. *Tunneling and Underground Space Technology*, 187-213.
- Duncan Fama, M. (1993). Numerical modelling of yield zones in weak rocks. *Journal of Comprehensive rock engineering*.
- Duncan, M. E. (1993). In M. E. Duncan, *Numerical Modelling of yield zones in weak rocks* (pp. 49-75).
- Gercek, H. (1986). Stability Considerations for underground excavation intersections. *Elsevier Science Publishers*.
- Goel, R. (1994). *Correlation for predicting support pressures and closure in tunnel*. PhD thesis, nagpur University, India.
- Goodier, S. T. (1951). *Theory of Elasticity*. New York: McGraw-Hill Book Company.
- Grimstad, E., & Barton, N. (1993). Updating the Q-system for NMT. *Proceedings of the international symposium on sprayed concrete, Norwegian concrete association, Oslo, Norway*.
- Hoek et al. (n.d.). Hoek-Brown failure criterion-2002 edition. *H Proceedings of NARMS-TAC*.
- Hoek, & Brown. (1980). *Underground Excavation in rock*. Institution of Mining and Metallurgy.
- Hoek, & Brown. (1980). *Underground Excavation in rock*. Institution of Mining and Metallurgy.
- Hoek, E., & Marinos, P. (2000). Predicting tunnel squeezing problems in weak heterogeneous rock masses. *Tunnels and Tunnelling International*.

- Hoek, E., Kaiser, P., & Bawden, W. (1995). *Support of underground excavation in hard rock*. Balkema, Rotterdam.
- Ismail-Zadeh, A., & Tackley, P. (2010). Computational methods for geodynamics.
- Jaeger and Cook. (1976). *Fundamentals of Rock Mechanics*.
- Jethwa, L. (1984). Estimation of ultimate rock pressure for tunnel linings under squeezing rock conditions. *Brown E.T and Hudson*, 231-8.
- Kaiser, e. (1986). *Evaluation of rock classification at B.C Rail tumbler ridge tunnels*. Rock Mechanics and Rock Engineering.
- Kirsch, G. (1898). Die Theorie der Elastizität und die Bedürfnisse der Festigkeitslehre. *Springer*.
- Lance, G., Anderson, J., & Lamont, D. (2007). Third Party Safety Issues in International Urban Tunneling. *Underground Space - 4th Dimesnion of metropolies*. London: Taylor and Francis Group.
- MIDAS IT Co., L. (2020). *About GTS NX*. Retrieved from https://www.midasgeotech.com/solution/gtsnx?utm_referrer=https%3A%2F%2Fwww.midasgeotech.com%2Fmain#none
- P.R.Sheorey. (1994). A theory for In Situ stresses in isotropic and transverseley isotropic rock. *ELSEVIER*.
- Panthi, K. (2006). *Analysis of Engineering Geological Uncertainties Related to Tunnelling in Himalayan Rock Mass Conditions*. Norwegian University of Science and Technology .
- Powderham, A. (1994). An overview of the observational method: development in cut and cover and bored tunnelling projects. *Géotechnique*, 18.
- R.C.Firth, B. W. (1990). *Tunnelling- Design,Stability and Construction*.
- Ramamurthy, T. (2011). *Engineering in rocks for Slopes, Foundation and Tunnels*. New Delhi: PHI Learning Private Limited.
- Rehman et al. (2018). Review of Rock-Mass Rating and Tunneling Quality. *Multidisciplinary digital publishing institute*.
- (2017). *Report on Rock Support Analysis of Underground Excavation*. Kathmandu, Nepal.
- Sakurai, S. (1983). Displacement measurements associated with the design of underground openings. *Proc. Int. Symp. Field Measurements in Geomechanics*.
- Singh, B., & Goel, R. (2006). *Tunnelling in weak rocks*. ELSEVIER GEO-ENGINEERING BOOK SERIES VOLUME 5.

- Terzaghi and Richart. (1952). *Stresses in rock about cavities*. Cambridge : Harvard University.
- Vlachopoulos, N., & Diederichs, M. (2009). Improved Longitudnal Displacement Profiles for Convergence Confinment Analysis of Deep Tunnels. *Rock Mechanics and Rock Engineering*.

7 ANNEX A: DETAILS OF CALCULATION

Chainage 0+600

Table 7-1: Detail calculation of GRC for section 0+600

SN	Internal Pressure	Scaled Internal Pressure	Radius of Plastic Disp	Elastic Disp.	Plastic Disp.	Disp.
1	4.173	0.047	0.000	0	0.000	0.0000
2	0.365	0.007	0.000	0.001	0.000	0.0007
3	0.335	0.006	2.008	0	0.001	0.0007
4	0.320	0.006	2.012	0	0.001	0.0007
5	0.304	0.006	2.016	0	0.001	0.0007
6	0.289	0.006	2.021	0	0.001	0.0007
7	0.274	0.006	2.025	0	0.001	0.0007
8	0.259	0.005	2.030	0	0.001	0.0007
9	0.243	0.005	2.034	0	0.001	0.0007
10	0.228	0.005	2.039	0	0.001	0.0007
11	0.213	0.005	2.043	0	0.001	0.0007
12	0.198	0.005	2.048	0	0.001	0.0007
13	0.183	0.005	2.053	0	0.001	0.0007
14	0.167	0.004	2.058	0	0.001	0.0007
15	0.152	0.004	2.063	0	0.001	0.0008
16	0.137	0.004	2.068	0	0.001	0.0008

17	0.122	0.004	2.073	0	0.001	0.0008
18	0.107	0.004	2.079	0	0.001	0.0008
19	0.091	0.004	2.084	0	0.001	0.0008
20	0.076	0.003	2.090	0	0.001	0.0008
21	0.061	0.003	2.096	0	0.001	0.0008
22	0.046	0.003	2.102	0	0.001	0.0008
23	0.030	0.003	2.108	0	0.001	0.0008
24	0.015	0.003	2.114	0	0.001	0.0008
25	0.000	0.003	2.121	0	0.001	0.0008

Table 7-2: Detail calculation of LDP for section 0+600

Maximum Displacement	U_r^m	0.0008
Maximum normalized plastic zone radius	R^*	1.06
Normalized Displacement at face	u_o^*	0.284m

Point	$X^*=X/R$	Distance to the Face, X,m	U_r,m	Remarks
1	-5	-10.90	0.000001	Min
2	-3	-5.40	0.000015	
3	-1	-2.70	0.000060	
4	0	0.00	0.000230	Face
5	0.50	1.00	0.000523	

6	1.25	2.50	0.000709	
7	1.35	2.70	0.000722	
8	2.70	5.40	0.000795	
9	4.10	8.20	0.000806	
10	5.45	10.90	0.000807	
11	6.80	13.60	0.000808	
12	8.15	16.30	0.000808	
13	9.55	19.10	0.000808	
14	10.90	21.80	0.000808	
15	12.25	24.50	0.000808	
16	13.60	27.20	0.000808	
17	16.35	32.70	0.000808	
18	21.80	43.60	0.000808	
19	27.25	54.50	0.000808	
20	32.70	65.40	0.000808	
21	50.00	100.00	0.000808	
22	65.00	130.00	0.000808	Max

Chainage 1+400

Table 7-3: Detail calculation for GRC in section 1+400

SN	Internal Pressure	Scaled Internal Pressure	Radius of Plastic Disp.	Elastic Disp.	Plastic Disp.	Disp.
1	5.546	0.121	0.000	0	0.000	0.0000
2	1.411	0.032	0.000	0.002	0.000	0.0018
3	1.293	0.029	2.029	0	0.002	0.0019
4	1.234	0.028	2.044	0	0.002	0.0019
5	1.176	0.027	2.060	0	0.002	0.0020
6	1.117	0.026	2.076	0	0.002	0.0020
7	1.058	0.024	2.093	0	0.002	0.0020
8	0.999	0.023	2.111	0	0.002	0.0021
9	0.940	0.022	2.129	0	0.002	0.0021
10	0.882	0.021	2.147	0	0.002	0.0022
11	0.823	0.019	2.167	0	0.002	0.0022
12	0.764	0.018	2.187	0	0.002	0.0023
13	0.705	0.017	2.208	0	0.002	0.0023
14	0.647	0.015	2.230	0	0.002	0.0024
15	0.588	0.014	2.254	0	0.002	0.0024
16	0.529	0.013	2.278	0	0.003	0.0025
17	0.470	0.012	2.305	0	0.003	0.0026
18	0.411	0.010	2.333	0	0.003	0.0027

19	0.353	0.009	2.363	0	0.003	0.0028
20	0.294	0.008	2.396	0	0.003	0.0029
21	0.235	0.007	2.432	0	0.003	0.0030
22	0.176	0.005	2.473	0	0.003	0.0031
23	0.118	0.004	2.519	0	0.003	0.0033
24	0.059	0.003	2.575	0	0.004	0.0035
25	0.000	0.001	2.648	0	0.004	0.0038

Table 7-4: Detail Calculation for LDP pf section 1+400

Maximum Displacement			U_r^m	0.00382
Maximum normalized plastic zone radius			R^*	1.32
Normalized Displacement at face			u_o^*	0.273m
Point	$X^*=X/R$	Distance to the Face, X,m	U_r,m	Remarks
1	-5	-10.90	0.000004	Min
2	-3	-5.40	0.000070	
3	-1	-2.70	0.000271	
4	0	0.00	0.001044	Face
5	0.50	1.00	0.002244	
6	1.25	2.50	0.003146	
7	1.35	2.70	0.003218	
8	2.70	5.40	0.003690	

9	4.10	8.20	0.003793	
10	5.45	10.90	0.003814	
11	6.80	13.60	0.003819	
12	8.15	16.30	0.003820	
13	9.55	19.10	0.003820	
14	10.90	21.80	0.003820	
15	12.25	24.50	0.003820	
16	13.60	27.20	0.003820	
17	16.35	32.70	0.003820	
18	21.80	43.60	0.003820	
19	27.25	54.50	0.003820	
20	32.70	65.40	0.003820	
21	50.00	100.00	0.003820	
22	65.00	130.00	0.003820	Max

Chainage 2+000

Table 7-5: Detail calculation for GRC in section 2+000

SN	Internal Pressure	Scaled Internal Pressure	Radius of Plastic Disp.	Elastic Disp.	Plastic Disp.	Disp.
1	15.892	0.879	0.000	0	0.000	0
2	9.373	0.519	0.000	0.010	0.000	0.010
3	8.592	0.475	2.126	0	0.011	0.011

4	8.202	0.454	2.195	0	0.012	0.012
5	7.811	0.432	2.267	0	0.013	0.013
6	7.421	0.411	2.344	0	0.014	0.014
7	7.030	0.389	2.425	0	0.015	0.015
8	6.639	0.368	2.511	0	0.016	0.016
9	6.249	0.346	2.604	0	0.018	0.018
10	5.858	0.324	2.703	0	0.020	0.020
11	5.468	0.303	2.809	0	0.022	0.022
12	5.077	0.281	2.923	0	0.024	0.024
13	4.687	0.260	3.047	0	0.027	0.027
14	4.296	0.238	3.182	0	0.030	0.030
15	3.906	0.217	3.329	0	0.034	0.034
16	3.515	0.195	3.491	0	0.038	0.038
17	3.124	0.173	3.671	0	0.043	0.043
18	2.734	0.152	3.873	0	0.050	0.050
19	2.343	0.130	4.102	0	0.057	0.057
20	1.953	0.109	4.367	0	0.066	0.066
21	1.562	0.087	4.679	0	0.078	0.078
22	1.172	0.066	5.060	0	0.094	0.094
23	0.781	0.044	5.551	0	0.116	0.116
24	0.391	0.022	6.258	0	0.152	0.152
25	0.000	0.001	7.967	0	0.257	0.257

Table 7-6: Detail calculation of LDP for section 2+000

Maximum Displacement	U_F^m	0.257
Maximum normalized plastic zone radius	R^*	3.98
Normalized Displacement at face	u_o^*	0.183m

Point	$X^*=X/R$	Distance to the Face, X,m	U_r,m	Remarks
1	-5	-10.90	0.000203	Min
2	-3	-5.40	0.003168	
3	-1	-2.70	0.012220	
4	0	0.00	0.047138	Face
5	0.50	1.00	0.083159	
6	1.25	2.50	0.125939	
7	1.35	2.70	0.130784	
8	2.70	5.40	0.181097	
9	4.10	8.20	0.212213	
10	5.45	10.90	0.230077	
11	6.80	13.60	0.240822	
12	8.15	16.30	0.247286	
13	9.55	19.10	0.251283	
14	10.90	21.80	0.253578	
15	12.25	24.50	0.254958	
16	13.60	27.20	0.255788	
17	16.35	32.70	0.256597	
18	21.80	43.60	0.256984	
19	27.25	54.50	0.257034	
20	32.70	65.40	0.257041	
21	50.00	100.00	0.257042	
22	65.00	130.00	0.257042	Max

Chainage 2+500

Table 7-7: Detail calculations for GRC in section 2+500

SN	Internal Pressure	Scaled Internal Pressure	Radius of Plastic Disp.	Elastic Disp.	Plastic Disp.	Disp.
1	9.320	0.829	0.000	0	0.000	0
2	5.415	0.482	0.000	0.009	0.000	0.009
3	4.964	0.442	2.122	0	0.011	0.011
4	4.739	0.422	2.187	0	0.011	0.011
5	4.513	0.402	2.257	0	0.012	0.012
6	4.287	0.382	2.330	0	0.013	0.013
7	4.062	0.362	2.408	0	0.014	0.014
8	3.836	0.342	2.491	0	0.016	0.016
9	3.610	0.322	2.580	0	0.017	0.017
10	3.385	0.302	2.674	0	0.019	0.019
11	3.159	0.281	2.775	0	0.021	0.021
12	2.933	0.261	2.884	0	0.023	0.023
13	2.708	0.241	3.002	0	0.025	0.025
14	2.482	0.221	3.130	0	0.028	0.028
15	2.256	0.201	3.270	0	0.031	0.031
16	2.031	0.181	3.423	0	0.035	0.035
17	1.805	0.161	3.593	0	0.040	0.040
18	1.580	0.141	3.784	0	0.045	0.045

19	1.354	0.121	4.000	0	0.052	0.052
20	1.128	0.101	4.248	0	0.060	0.060
21	0.903	0.081	4.541	0	0.071	0.071
22	0.677	0.061	4.898	0	0.084	0.084
23	0.451	0.041	5.357	0	0.104	0.104
24	0.226	0.021	6.017	0	0.135	0.135
25	0.000	0.001	7.644	0	0.228	0.228

Table 7-8: Detail calculation of LDP at section 2+500

Maximum Displacement	U_R^m	0.228
Maximum normalized plastic zone radius	R^*	3.82m
Normalized Displacement at face	u_o^*	0.188m

Point	$X^*=X/R$	Distance to the Face, X,m	U_r,m	Remarks
1	-5	-10.90	0.000184	Min
2	-3	-5.40	0.002875	
3	-1	-2.70	0.011089	
4	0	0.00	0.042774	Face
5	0.50	1.00	0.075716	
6	1.25	2.50	0.114458	
7	1.35	2.70	0.118814	

8	2.70	5.40	0.163580	
9	4.10	8.20	0.190666	
10	5.45	10.90	0.205879	
11	6.80	13.60	0.214834	
12	8.15	16.30	0.220106	
13	9.55	19.10	0.223296	
14	10.90	21.80	0.225088	
15	12.25	24.50	0.226143	
16	13.60	27.20	0.226764	
17	16.35	32.70	0.227351	
18	21.80	43.60	0.227617	
19	27.25	54.50	0.227648	
20	32.70	65.40	0.227652	
21	50.00	100.00	0.227653	
22	65.00	130.00	0.227653	Max

Chainage 3+200

Table 7-9: Detail calculation for LDP in chainage 3+200

SN	Internal Pressure	Scaled Internal Pressure	Radius of Plastic Disp.	Elastic Disp.	Plastic Disp.	Disp.
1	3.859	0.830	0.000	0	0.000	0
2	2.242	0.483	0.000	0.006	0.000	0.006

3	2.055	0.443	2.122	0	0.006	0.006
4	1.962	0.423	2.187	0	0.007	0.007
5	1.869	0.403	2.257	0	0.007	0.007
6	1.775	0.382	2.330	0	0.008	0.008
7	1.682	0.362	2.408	0	0.009	0.009
8	1.588	0.342	2.491	0	0.009	0.009
9	1.495	0.322	2.579	0	0.010	0.010
10	1.401	0.302	2.674	0	0.011	0.011
11	1.308	0.282	2.775	0	0.012	0.012
12	1.215	0.262	2.884	0	0.014	0.014
13	1.121	0.242	3.002	0	0.015	0.015
14	1.028	0.222	3.130	0	0.017	0.017
15	0.934	0.202	3.269	0	0.019	0.019
16	0.841	0.182	3.423	0	0.021	0.021
17	0.747	0.162	3.593	0	0.024	0.024
18	0.654	0.142	3.783	0	0.027	0.027
19	0.561	0.121	3.998	0	0.031	0.031
20	0.467	0.101	4.247	0	0.036	0.036
21	0.374	0.081	4.539	0	0.042	0.042
22	0.280	0.061	4.894	0	0.050	0.050
23	0.187	0.041	5.351	0	0.062	0.062
24	0.093	0.021	6.006	0	0.080	0.080

25	0.000	0.001	7.543	0	0.132	0.132
----	-------	-------	-------	---	-------	-------

Table 7-10: Detail calculations for LDP in section 3+200

Maximum Displacement	U_r^m	0.132
Maximum normalized plastic zone radius	R^*	3.77m
Normalized Displacement at face	u_o^*	0.189m

Point	$X^*=X/R$	Distance to the Face, X,m	U_r ,m	Remarks
1	-5	-10.90	0.000108	Minimum
2	-3	-5.40	0.001683	
3	-1	-2.70	0.006493	
4	0	0.00	0.025045	Face
5	0.50	1.00	0.044385	
6	1.25	2.50	0.067058	
7	1.35	2.70	0.069601	
8	2.70	5.40	0.095646	
9	4.10	8.20	0.111292	
10	5.45	10.90	0.120016	
11	6.80	13.60	0.125115	
12	8.15	16.30	0.128096	
13	9.55	19.10	0.129886	

14	10.90	21.80	0.130885	
15	12.25	24.50	0.131469	
16	13.60	27.20	0.131810	
17	16.35	32.70	0.132129	
18	21.80	43.60	0.132271	
19	27.25	54.50	0.132288	
20	32.70	65.40	0.132289	
21	50.00	100.00	0.132290	
22	65.00	130.00	0.132290	Maximum

8 ANNEX B: NUMERICAL MODELLING RESULTS

Chainage 0+600

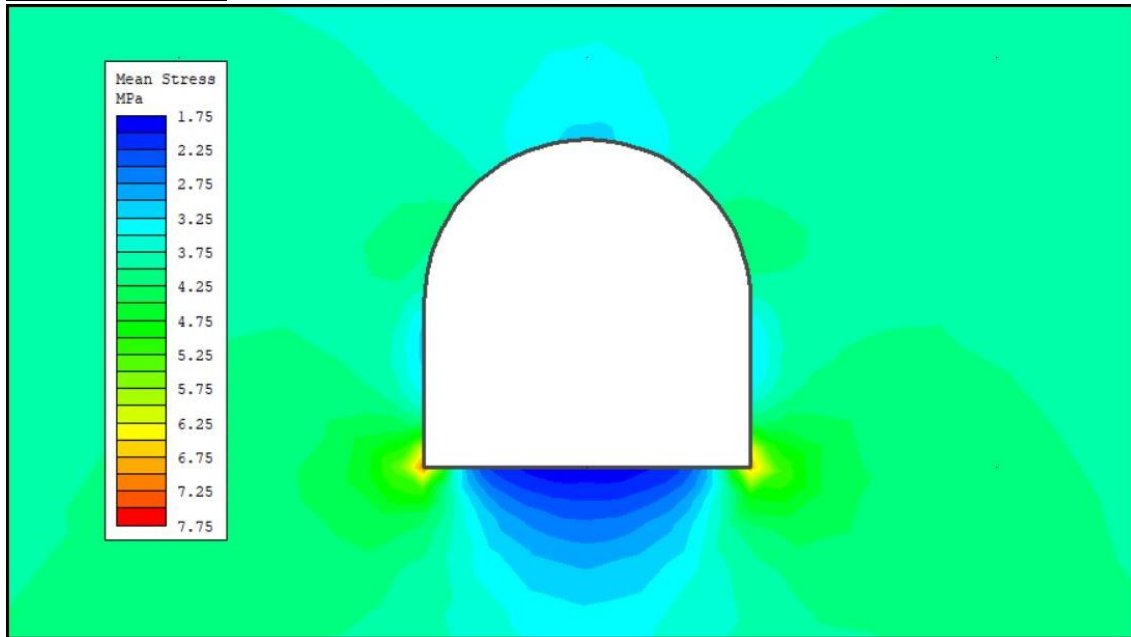


Figure 8-1: Mean stress around tunnel without support at section 0+600

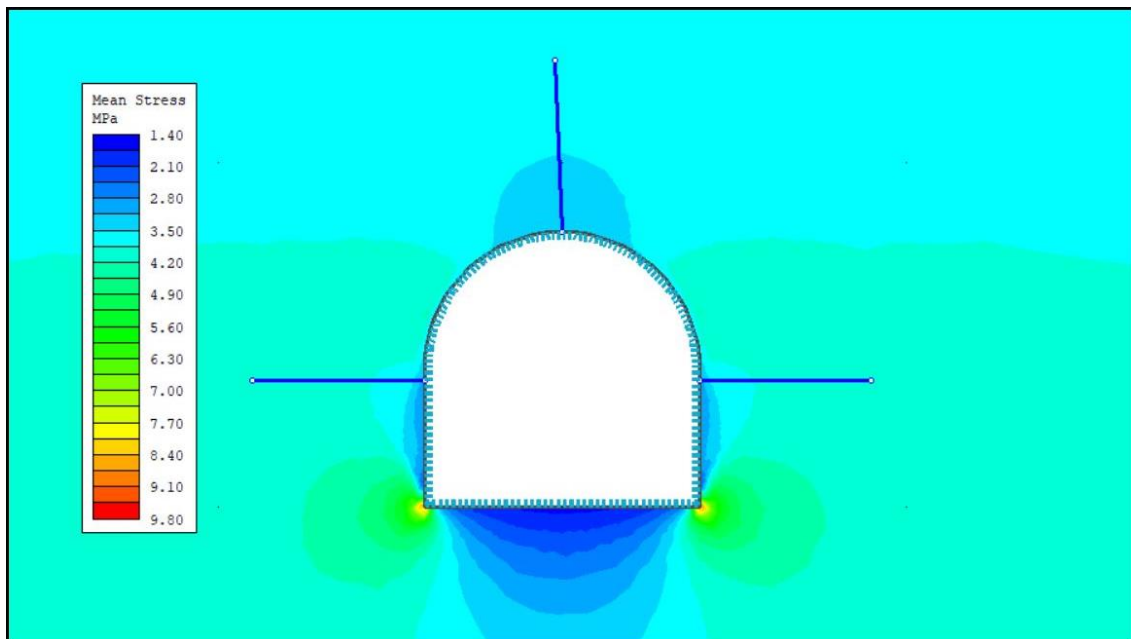


Figure 8-2: Mean stress around tunnel with support at section 0+600

Chainage 1+400

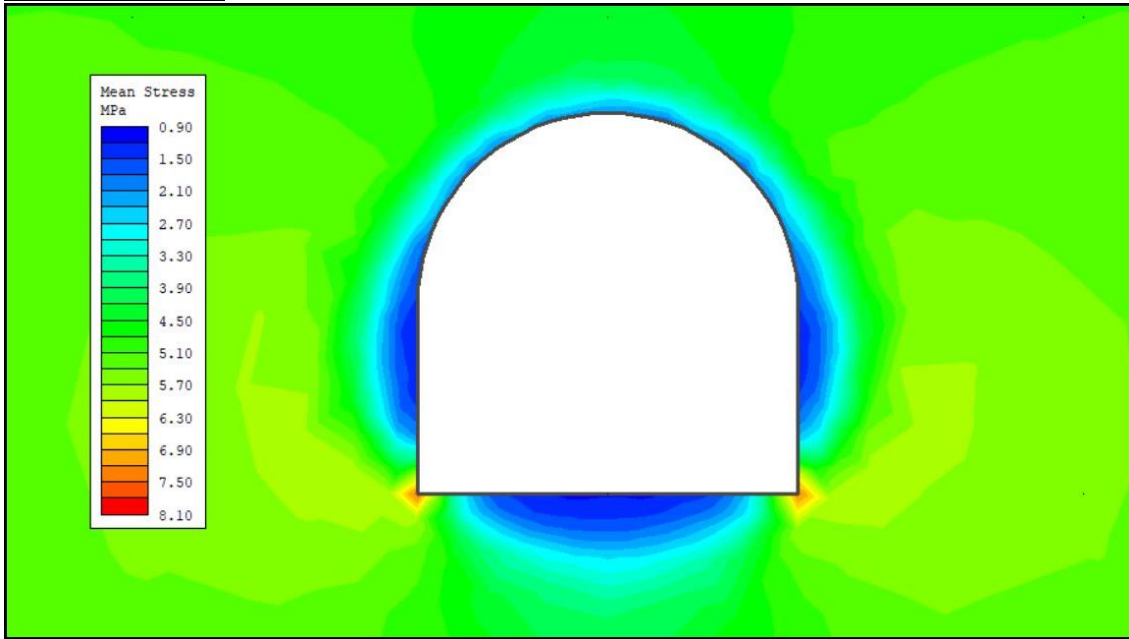


Figure 8-3: Mean stress around tunnel without support at section 1+400

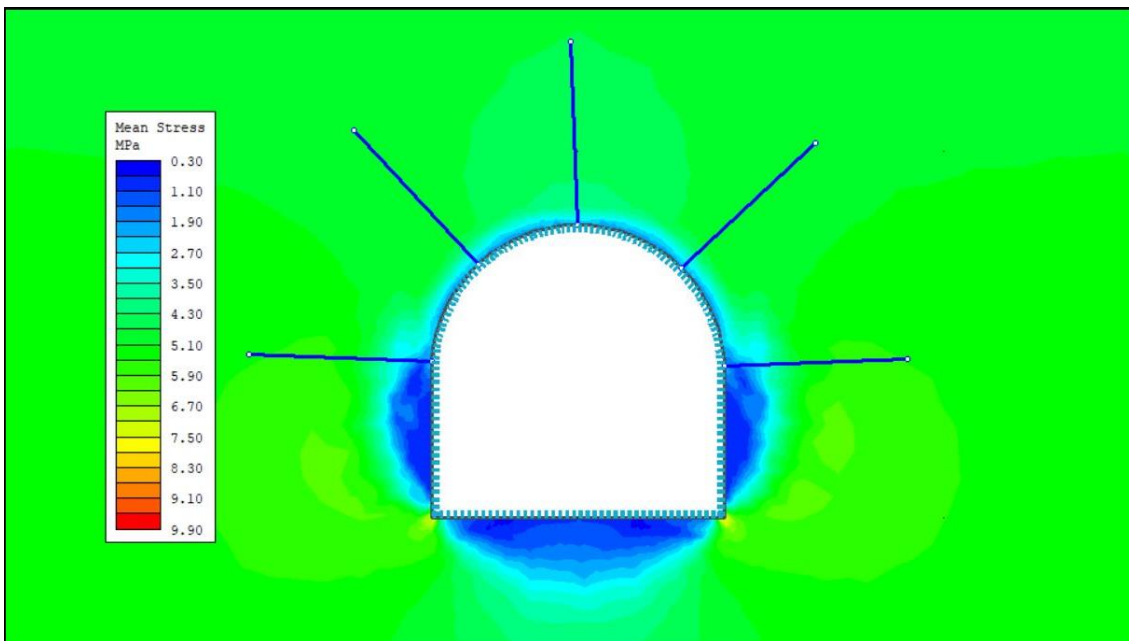


Figure 8-4: Mean stress around tunnel with support at section 1+400

Chainage 2+000

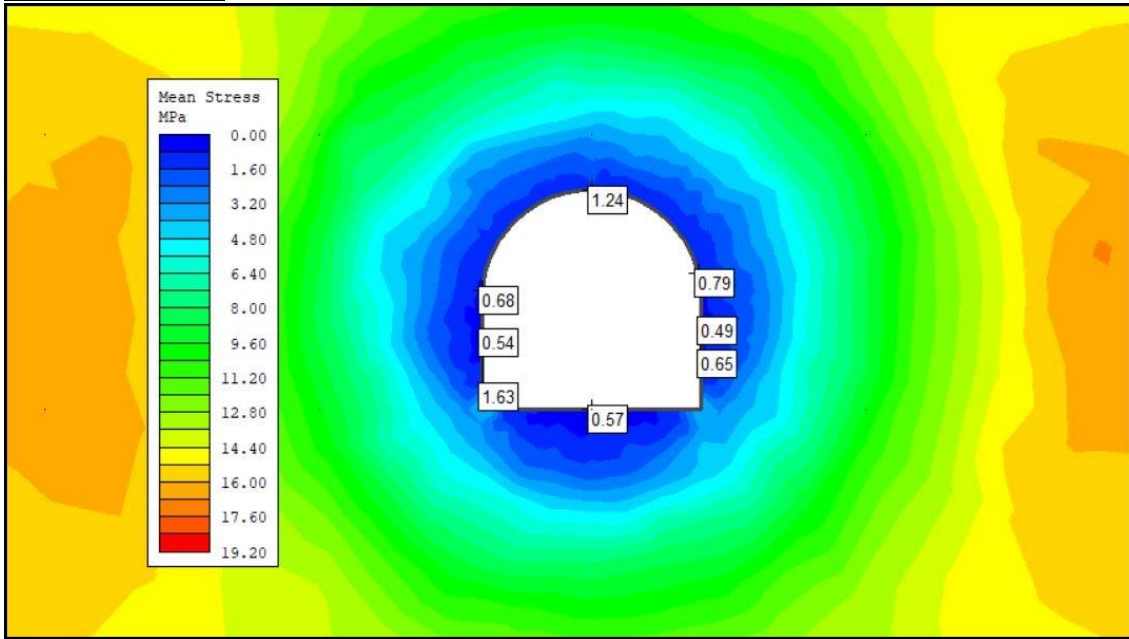


Figure 8-5: Mean stress around tunnel without support at section 2+000

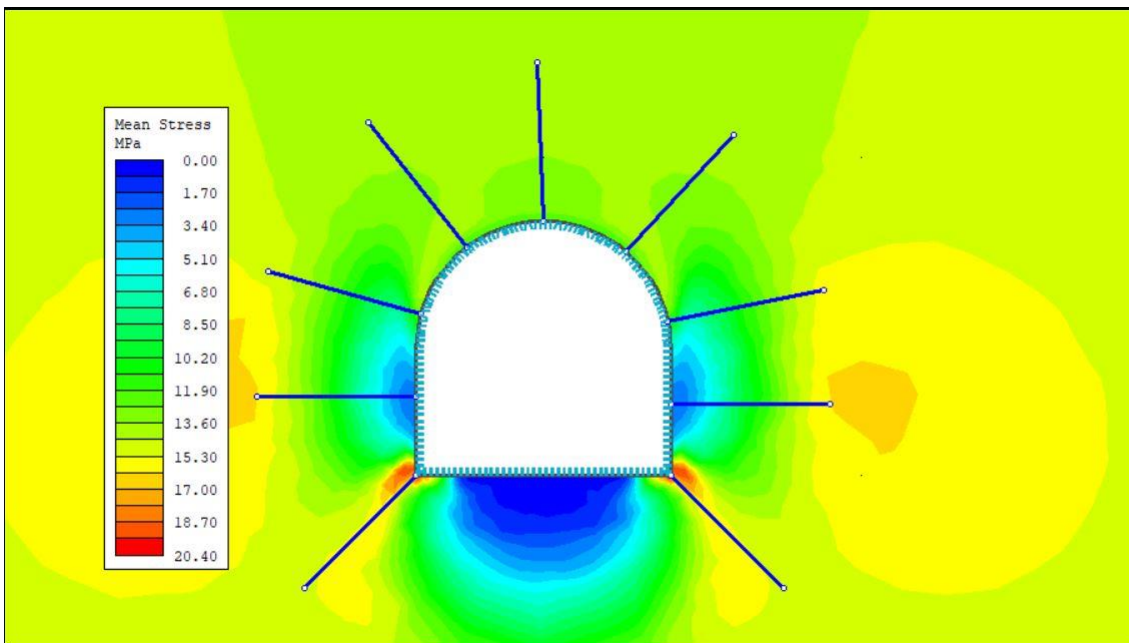


Figure 8-6: Mean stress around tunnel with support at section 2+000

Chainage 2+500

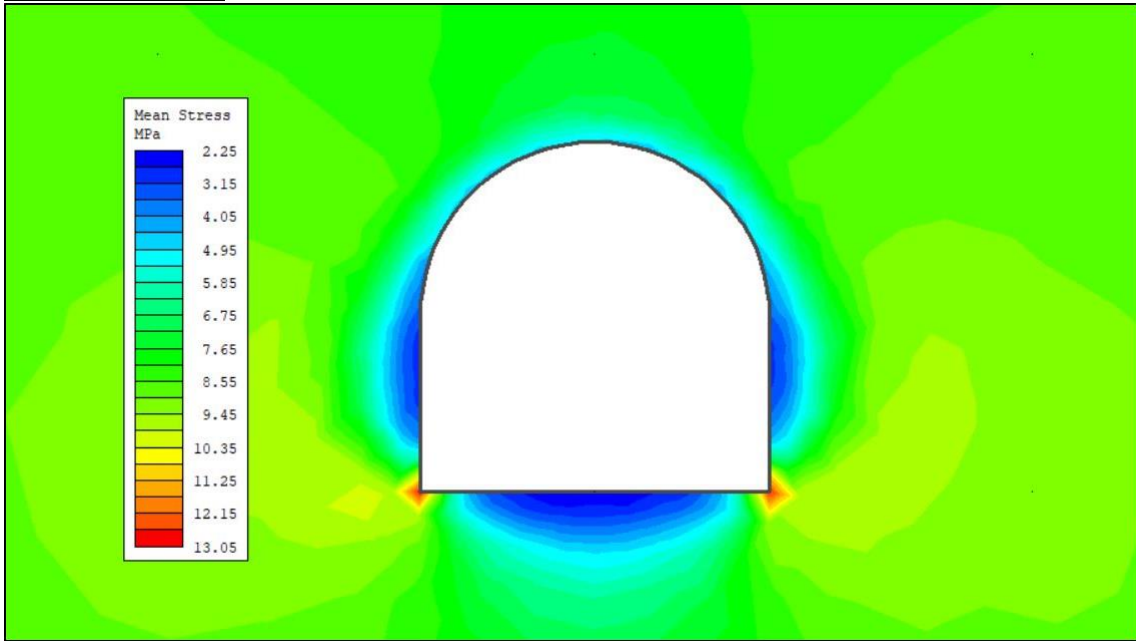


Figure 8-7: Mean stress around tunnel without support at section 2+500

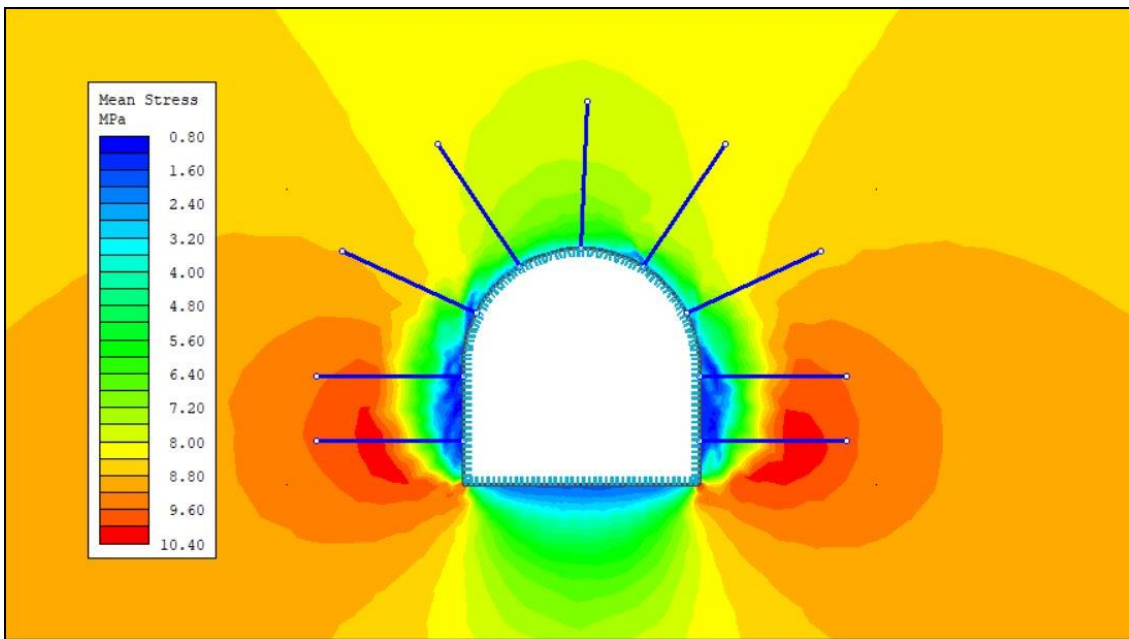


Figure 8-8: Mean stress around tunnel with support at section 2+500

Chainage 3+200

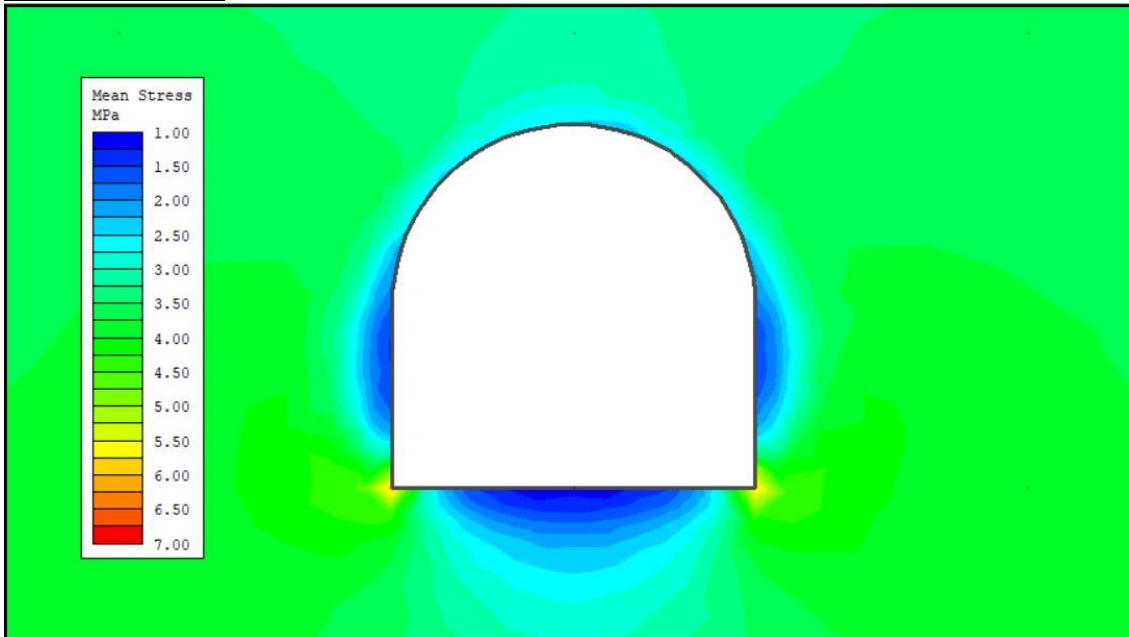


Figure 8-9: Mean stress around tunnel without support at section 3+200

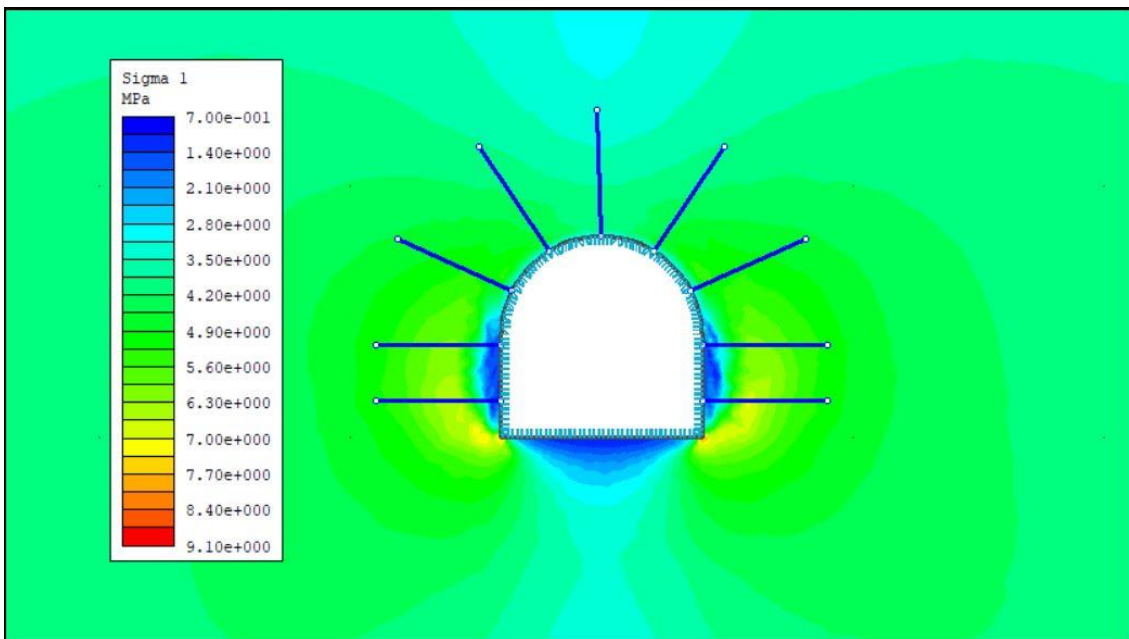


Figure 8-10: Mean stress around tunnel with support at section 3+200

3D Adit Connection

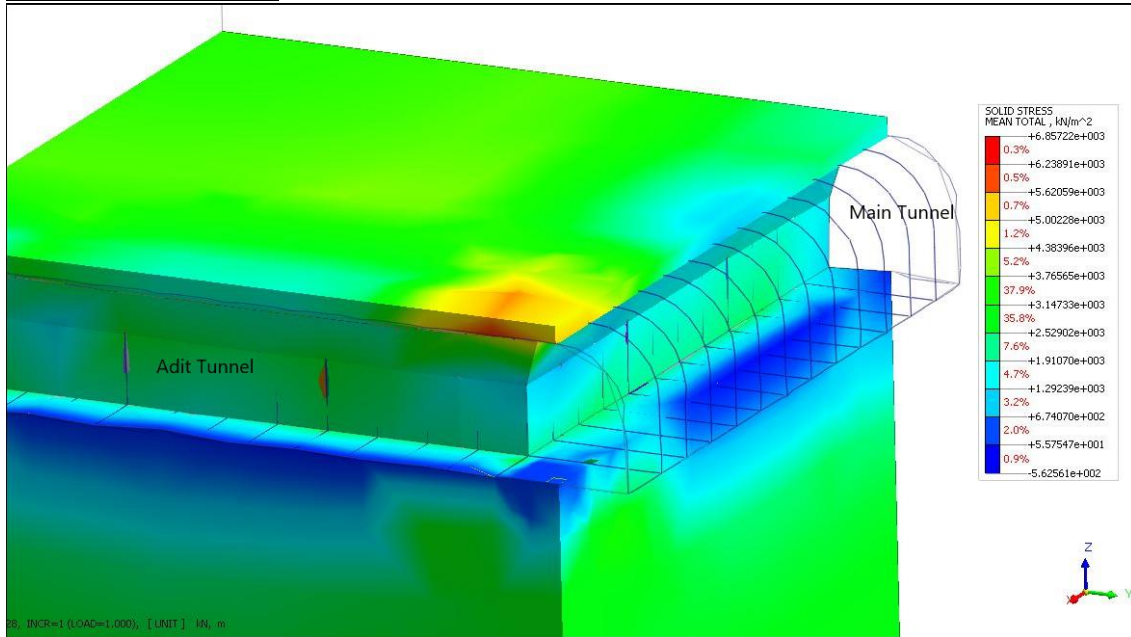


Figure 8-11: Mean stress around 3D Adit connection



Figure 8-12: Displacement around Adit Connection, Stage 1

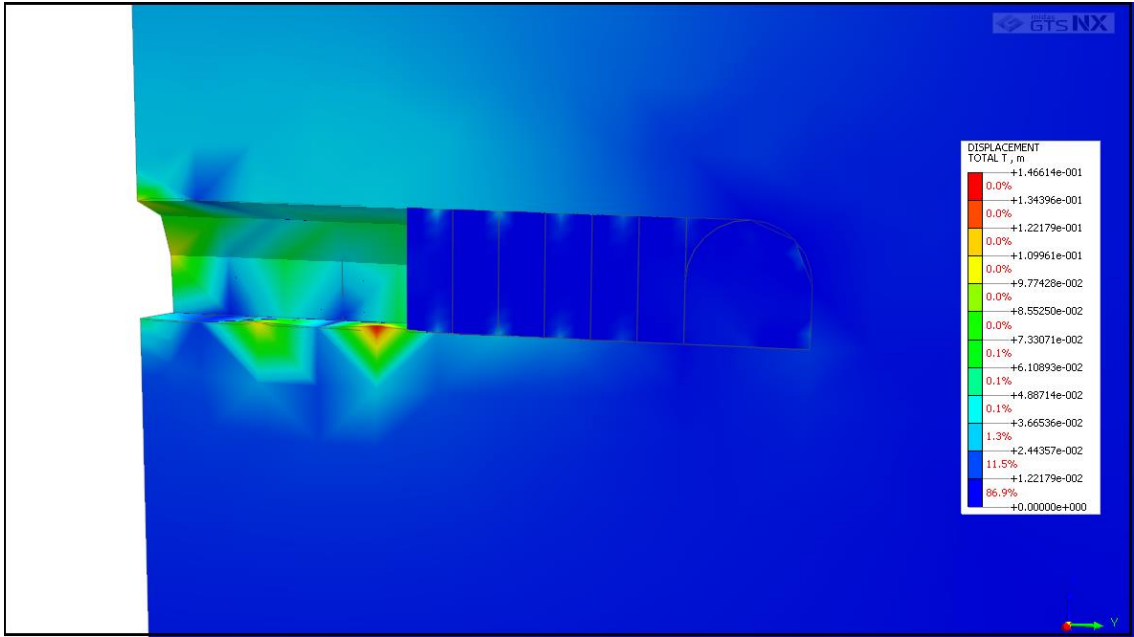


Figure 8-13: Displacement around Adit Connection, Stage 6

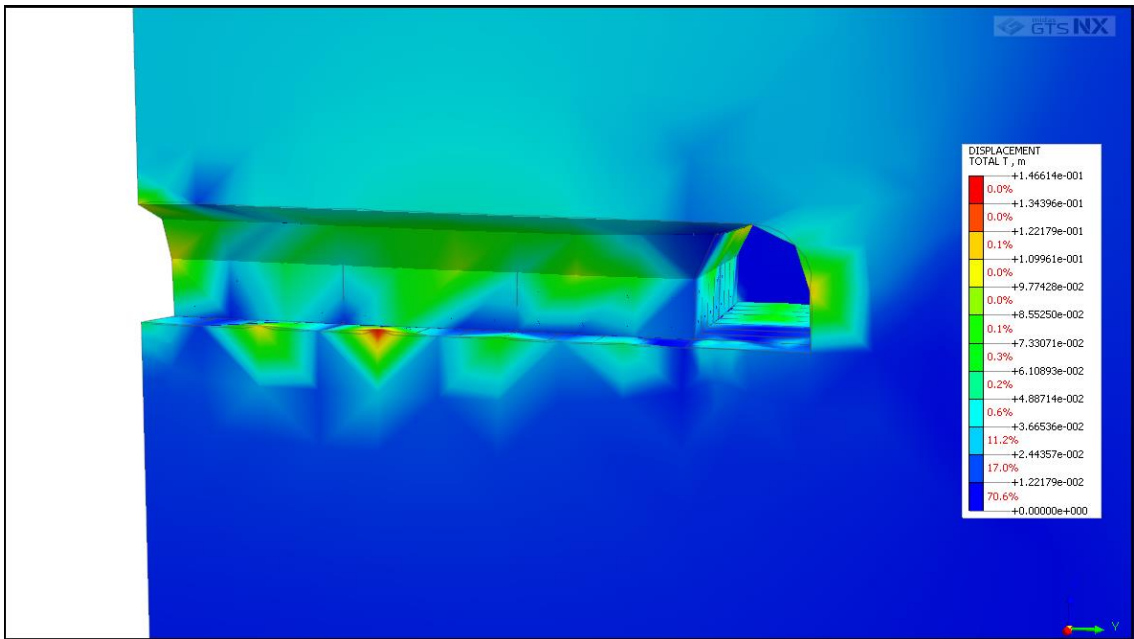


Figure 8-14: Displacement around Adit Connection, Stage 23

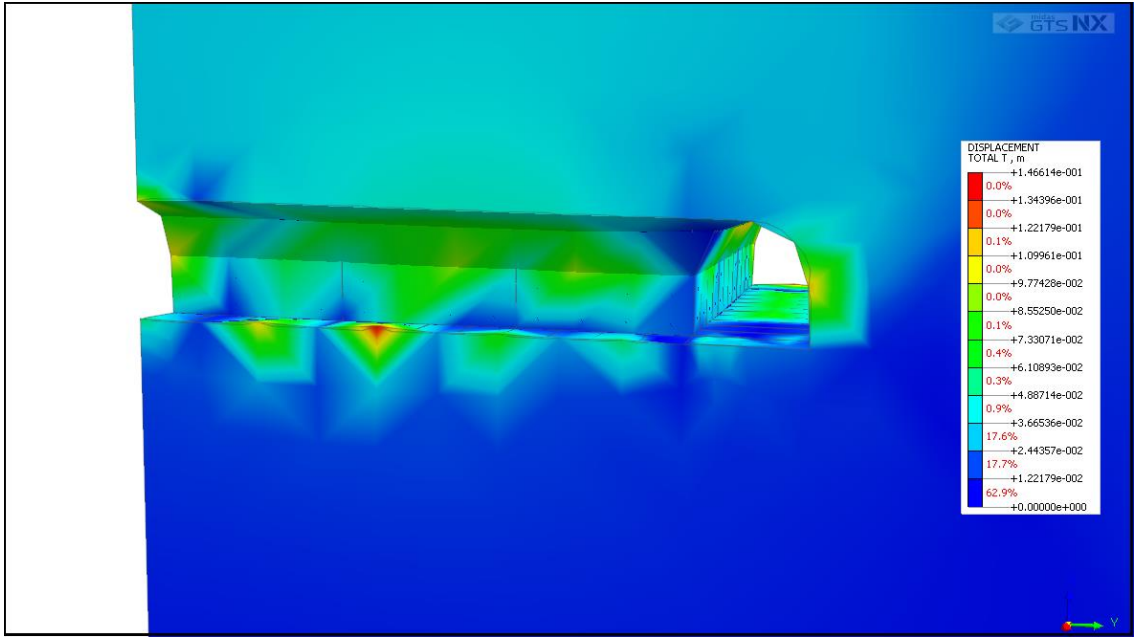


Figure 8-15: Displacement around Adit Connection, Stage 28

3D Surge Shaft

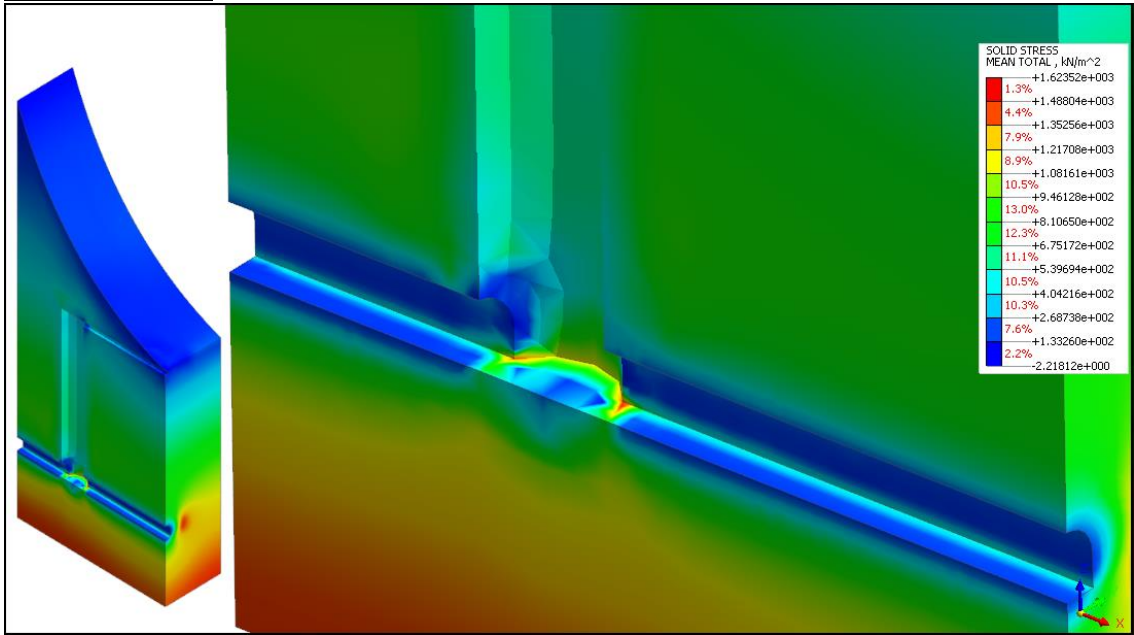


Figure 8-16: Mean stress around Surge Shaft

3D Tunnel Bend

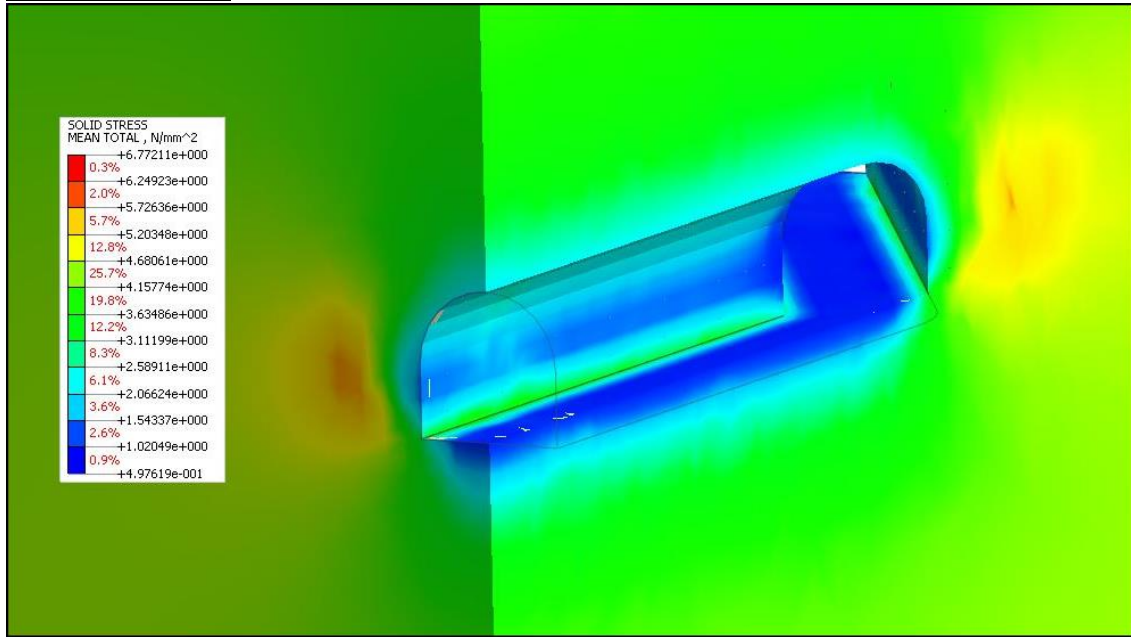


Figure 8-17: Mean stress around Tunnel bend

9 ANNEX C: STANDARD CHARTS AND FIGURES

Table 9-1: Guidelines for excavation support by RMR system (After Bienawski, 1989)

Rock mass class	Rock bolts (20mm diameter, fully grouted)	Shotcrete	Steel sets
I- Very good rock RMR: 81 - 100	Generally, no support required except spot bolting		
II - Good rock RMR: 61 - 80	Locally, bolts in crown 3m long, spaced 2.5m with occasional wire mesh.	50 in crown where required.	None.
III- Fair rock RMR: 41-60	Systematic bolts 4 m long, spaced 1.5 - 2 m in crown and walls with wire mesh in crown.	50-100 mm in crown and 30 mm in sides.	None.
IV - Poor rock RMR: 21 - 40	Systematic bolts 4-5 m long, spaced 1-1.5 m in crown and walls with wire mesh.	100-150 mm in crown and 100 mm in sides.	Light to medium ribs spaced 1.5 m where required.

V - Very poor rock RMR: < 20	Systematic bolts 5-6 m long, spaced 1-1.5 m in crown and walls with wire mesh. Bolt invert.	150-200 mm in crown and 150 mm in sides, and 50mm on face.	Medium to heavy ribs spaced 0.75m with steel lagging and forepoling if required. Close invert.
-------------------------------------	---	--	--

Table 9-2: Rock Mass Classification using Q value

Q-Value	Rock mass Description	Class number
> 40	Very Good Rock	I
10 - 40	Good Rock	II
4 - 9	Fair Rock	III
1 - 3	Poor Rock	IV
< 1	Very Poor Rock	V

Table 9-3: Table for ESR

S. N	Type of excavation	ESR
A	Temporary mine openings, etc.	c.a. 3-5
B	Vertical shafts*: i) circular sections ii) rectangular/square section * Dependent of purpose. May be lower than given values.	c.a. 2.5 c.a. 2.0
C	Permanent mine openings, water tunnels for hydro power (exclude high pressure Penstocks), water supply tunnels, pilot tunnels, drifts and headings for large openings.	1.6
D	Minor road and railway tunnels, surge chambers, access tunnels, sewage tunnels, etc.	1.3
E	Power houses, storage rooms, water treatment plants, major road and railway tunnels, civil defense chambers, portals, intersections, etc.	1.0
F	Underground nuclear power stations, railways stations, sports and public facilities, factories, etc.	0.8
G	Very important caverns and underground openings with a long lifetime, ~ 100 years, or without access for maintenance.	0.5

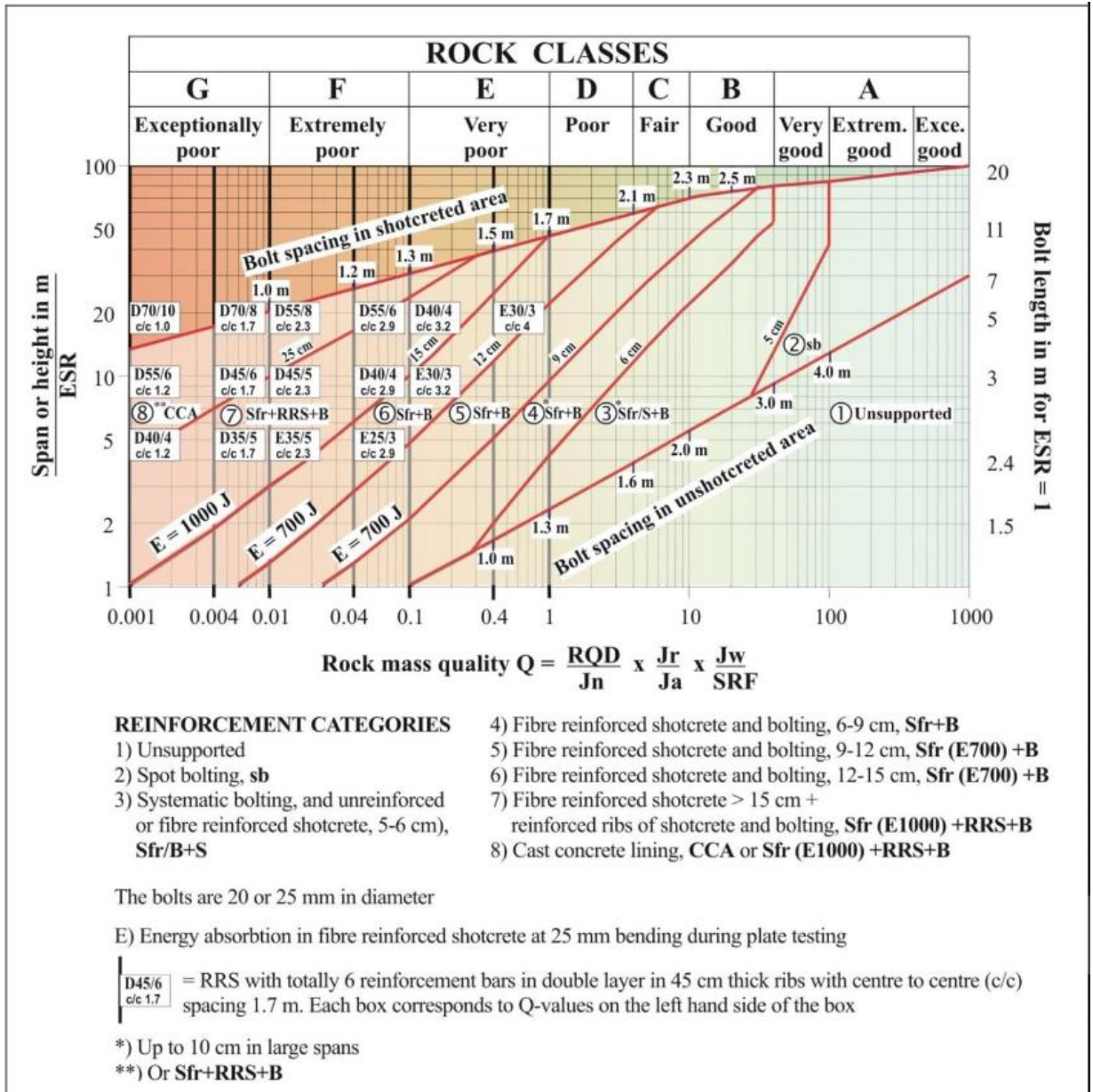








Figure 9-1: Q-support chart published by Grimstad in 2007 (Barton & Grimstad, 2014)

Table 9-4: Values of constant m_i given by intact rock (Hoek & Brown, 1997)

Rock type	Class	Group	Texture			
			Coarse	Medium	Fine	Very Fine
SEDIMENTARY	Clastic		Conglomerate (22) Breccias (10)	Sandston 19	Siltstones 9 Greywackes (18)	Claystones 4
	Non-Clastic	Organic	Chalk 7			
		Carbonates		Sparitic Limesone 8	Micritic Limestone 20	
		Evaporites		Gypstone 16	Anhydrite 13	
METAMORPHIC	Non-Foliated		Marble 9	Hornfels (19)	Quartzites (24)	
	Slightly foliated		Migmatite (30)	Amphobolites 31		
	Foliated*		Gneiss 33	Schist (10)	Phyllites (10)	Slate 9
IGNEOUS	Plutonic	Light	Granite 33 Granodiorite (30)	Diorite (28)		
		Dark	Gabbro 27 Norite 22	Dolerite (19)		
	Volcanic	Lava		Rhyolite (16) Andesite 19	Dacite (17) Basalt (17)	Obsidian (19)
		Pyroclastic	Agglomerate (20)	Breccia (18)	Tuff (15)	

Table 9-5 : General chart for GSI estimates from the geological observations

Rock Type: GSI Selection:	SURFACE CONDITIONS				
	VERY GOOD	GOOD	FAIR	POOR	VERY POOR
STRUCTURE	DECREASING SURFACE QUALITY →				
 INTACT OR MASSIVE - intact rock specimens or massive in situ rock with few widely spaced discontinuities	90			N/A	N/A
 BLOCKY - well interlocked undisturbed rock mass consisting of cubical blocks formed by three intersecting discontinuity sets	80	70			
 VERY BLOCKY - interlocked, partially disturbed mass with multi-faceted angular blocks formed by 4 or more joint sets		60	50		
 BLOCKY/DISTURBED/SEAMY - folded with angular blocks formed by many intersecting discontinuity sets. Persistence of bedding planes or schistosity			40	30	
 DISINTEGRATED - poorly interlocked, heavily broken rock mass with mixture of angular and rounded rock pieces				20	
 LAMINATED/SHEARED - Lack of blockiness due to close spacing of weak schistosity or shear planes	N/A	N/A			10






Appearance of rock mass	Description of rock mass	Suggested value of D
	Excellent quality controlled blasting or excavation by Tunnel Boring Machine results in minimal disturbance to the confined rock mass surrounding a tunnel.	$D = 0$
	Mechanical or hand excavation in poor quality rock masses (no blasting) results in minimal disturbance to the surrounding rock mass. Where squeezing problems result in significant floor heave, disturbance can be severe unless a temporary invert, as shown in the photograph, is placed.	$D = 0$ $D = 0.5$ No invert
	Very poor quality blasting in a hard rock tunnel results in severe local damage, extending 2 or 3 m, in the surrounding rock mass.	$D = 0.8$
	Small scale blasting in civil engineering slopes results in modest rock mass damage, particularly if controlled blasting is used as shown on the left hand side of the photograph. However, stress relief results in some disturbance.	$D = 0.7$ Good blasting $D = 1.0$ Poor blasting
	Very large open pit mine slopes suffer significant disturbance due to heavy production blasting and also due to stress relief from overburden removal. In some softer rocks excavation can be carried out by ripping and dozing and the degree of damage to the slopes is less.	$D = 1.0$ Production blasting $D = 0.7$ Mechanical excavation

Figure 9-2: Guidelines for estimating disturbance factor D

10 ANNEX D: PROJECT RELATED DATA AND DOCUMENTS

Table 10-1: Summary of geological classification of the rock mass along the tunnel alignment based on Q-chart published by Barton in 2007 (Barton & Grimstad, 2014) taken from (Report on Rock Support Analysis of Underground Excavation, 2017)

Chainage (m)	Q Index	Rock Mass Quality	Rock Type Description
0 to 200	0.02 to 0.2	Extremely poor to very poor rock mass (Class III-IV)	The rock mass consists of three sets of joint plus random. The foliation plane is rough to smooth. The foliation plane is tight where as other joint set is slightly open to tight in nature. The filling material consist of mica to clay. The rock mass is dry.
200 to 900	4 to 15	Fair to Good Rock Mass (Class I)	Jointed thin to medium foliated (0.3 to 3 m band width) slight to moderately weathered garnet schist intercalated with 1 to 3 m band width of banded gneiss. Three prominent joint sets and random joint exist in the banded gneiss.
900 to 1100	0.1 to 0.5	Very Poor to Poor Rock Mass (Class III-II)	Weakness zone at Maiyun khola. Water bearing zone with a water leakage up to 10 litres/sec with pressure at about 10 bars. Predominantly jointed and weathered garnet schist and banded gneiss.
1100 to 1600	2 to 6	Poor to Fair Rock Mass (Class II-I)	Thinly foliated, deformed garnet schist in intercalation with moderately weathered and thickly bedded (band width 1 to 3 m) schistose gneiss.

1600 to 2300	0.6 to 7	Poor to Fair Rock Mass (Class II-I)	Thinly foliated, deformed garnet schist in intercalation with moderately weathered and thickly bedded (band width 1 to 3 m) schistose gneiss.
2300 to 2600	0.5 to 6	Poor to Fair Rock Mass (Class IV-III)	Thinly foliated, deformed garnet schist in intercalation with moderately weathered and thickly bedded schistose gneiss. Minor water dampening expected.
2600 to 2700	0.5 to 1	Poor Rock Mass (Class IV)	Thinly foliated and deformed garnet schist with thin layer of jointed mica gneiss. Minor leakage to the tunnel is expected.
2700 to 3000	0.3 to 3	Poor to Fair Rock (Class IV-III)	Thinly foliated and deformed garnet schist alternated with bands of jointed mica gneiss. Water dampening is expected in the tunnel.
3000 to 3100	0.01 to 0.7	Very Poor to Poor Rock Mass (Class V-IV)	Thinly foliated and deformed garnet schist with thin bands of highly fractured mica gneiss. Minor water leakage is expected.
3100 to 3700	0.2 to 5	Poor to Fair Rock Mass (Class IV-III)	Thinly foliated and deformed garnet schist with bands of jointed mica gneiss. Water dampening is expected in the tunnel.
3700 to 3800	0.26 to 1	Poor Rock Mass (Class IV)	Thinly foliated and deformed garnet schist with thin bands of highly fractured mica gneiss. Minor water leakage is expected.

3800 to 4100	0.2 to 3	Poor to fair Rock Mass (Class IV-III)	Thinly foliated and deformed garnet schist with thin bands of fractured mica gneiss.
4100 to 4447	0.02 to 0.2	Extremely Poor to Very Poor Rock Mass (Class III-IV)	The rock mass consists of three sets of joint plus random. The foliation plane is undulating, rough. The foliation plane is tight where as other joint set is slightly open to tight in nature. The filling material consist of clay to silty material. The rock mass is dry. Few weakness zones is present which is parallel to perpendicular to foliation plane.

Salient features of Upper Balephi 'A' hydropower project:

1 Project location

Sindhupalchowk, Bagmati State, Nepal

Intake site: Golche/Gumba VDC Powerhouse site: Baikunthe village

Geographical coordinates: Latitude: 27° 53' 45" N to 27°57'00" N Longitude: 85° 45' 30" E to 85° 47' 40" E

2 General Name of River

Balephi Khola

Nearest town: Kartike Bazaar

Type of scheme: Run of river

Gross head: 203.00 m (208.00-5.00)m Net head: 197.24 m (202.24-5.00)m

Installed capacity: 36 MW

3 Hydrology

Catchment Area at intake 434.27 km²

Mean Annual discharge: 38.37 m³/s

Design discharge (at Q40PoE) 21.30m³/s Riparian release: 0.764 m³/sec

Design flood discharge: 1606 m³/s (100 Yr. Flood)

Average Annual Precipitation: 1700-2700 mm

4 Diversion Weir

Type of Weir: Gravity Free Flow

Concrete Length of Weir 45.00 m

Crest Elevation EL. 1257.00 m

5 Intake Structure

Type: Side Intake

Size: 4.00 m x 2.40 m (W x H)

Nos. 4 (Four)

Elevation of intake invert EL.1253.50 m amsl

6 Under sluice

Size:3.00 m x 3.00 m (W x H)

Nos. 2 (Two)

Elevation of bottom sill EL.1251.00 m amsl

7 Gravel Trap

Size 12.40 m x 9.10 m x 11.70 m (L x B x H)

Number of basins 2 (two)

8 Gravel Flushing structure

Type RCC Box culvert Size 1.00 m x 1.40 m (W x H)

Number 2 (two)

9 Spillway in Gravel Trap

Type Ogee shaped Length 12.40 m

Crest level 1257.00 m

10 Approach Culvert (Pressurized)

Size 4.20 / 4.40 m x 3.0 m (W x H)

Average Length 36.82 m

11 Settling Basin

Type Conventional, Surface

No of Basin 2 (Two)

Size 75.00 (L) x 18.00 (W) x 7.80 m (H)

Particle Size to be settled 0.20 mm at 87 % trap efficiency

Flushing type RCC Box culvert, 4 Nos.

Flushing culvert size 1.00 m x 1.40 m (W x H)

12 Inverted Siphon

Diameter 3.20 m

Length 191.50 m

Type: Steel pipe (12.00 mm) encased in 0.80m thick RCC

13 Headrace Tunnel

Section Type Inverted D

Length 4235.00 m

Finish Diameter (Concrete/Shotcrete) 4.00 m

Support Shotcrete Lining: 3811.5 m

Concrete Lining: 423.5 m

14 Surge Shaft

Type: Underground

Circular Finish

Diameter 8.00 m

Height 50.5 m

Upstream surge water level (m)

EL: 1265.47 m amsl

Down surge water level (m) EL: 1235.90 m amsl

15 Penstock

Pipe Material: Steel

Length 372.48 m, Diameter 3.00 m & 81.95m, Dia. 1.75 m Material/Thickness 12.00-32.00 mm

16 Powerhouse

Type Semi-Surface Size (L x W x H) 58.00 m x 21.00 m x 18.50 m

Turbine axis level =1054.49m (1049.49+5.00)m amsl

17 Tailrace

Type: Free-flow box culvert

Section type Rectangular

Total Length 94 m Size 6.00 m x 3.00 m (W X H)

Tail Water Level EL. 1054.00 m (1049.00+5.00)m

18 Turbine

Type Horizontal Axis Francis Number of Units Three (3)

Rated Output Capacity per unit 12.5 MW

Average Efficiency 93 %

19 Generator

Type Synchronous, 3 Phase No of Units Three (3) Rated output Capacity per unit 15 MVA Power Factor 0.85 Voltage 11 kV Frequency 50 Hz Excitation System Brushless Efficiency 97 %

20 Transformer

Type Three Phase, Oil Immersed, Outdoor No of Units 3 (Three) Rated Capacity per Unit 15 MVA Voltage Ratio 132/11 kV Average Efficiency 99%

21 Transmission

Line Voltage Level 132 kV, S/C Length 22.00 km Conductor “Wolf” From Powerhouse to Proposed NEA sub-station at Lamosangu